Chapter 7: Physical and Geophysical Environment

URS-EIA-REP-204635

Table of Contents

7 Physical and Geophysical Environment 7-1

7.1 Introduction 7-1

7.2 Spatial and Temporal Boundaries 7-2
7.2.1 Project Area 7-2
7.2.2 Study Areas 7-2
7.2.3 Survey Areas 7-2

7.3 Baseline Data 7-2
7.3.1 Methodology and Data 7-2
7.3.2 Secondary Data 7-2
7.3.3 Baseline Surveys 7-3
7.3.3.1 Terrestrial Surveys 7-6
7.3.3.2 Marine Surveys 7-7
7.3.4 Applicable Standards 7-17

7.4 Physical Environment 7-18
7.4.1 Meteorological Conditions 7-18
7.4.2 Electromagnetic Fields 7-23
7.4.3 Radiation 7-24
7.4.3.1 Gamma Radiation Levels 7-24
7.4.3.2 Equivalent Dose of Gamma Radiation 7-25
7.4.3.3 Radioactive Isotopes 7-25
7.4.3.4 Summary 7-26
7.4.4 Oceanography 7-26
7.4.4.1 Bathymetry 7-26
7.4.4.2 Sea Level Variation 7-27
7.4.4.3 Wave Climate 7-32
7.4.4.4 Storm Surges 7-34
7.4.4.5 Currents 7-34
7.4.4.6 Ice Period 7-37
7.4.4.7 Water Temperature 7-38
7.4.4.8 Water Salinity 7-40
7.4.4.9 Water Density 7-43
7.4.5 Marine Water Quality 7-46
7.4.5.1 Oxygen 7-47
7.4.5.2 Hydrogen Sulphide 7-49
7.4.5.3 pH 7-49
7.4.5.4 Alkalinity 7-49
7.4.5.5 Silica 7-50
7.4.5.6 Organic Matter 7-50
7.4.5.7 Turbidity and Suspended Sediments 7-51
7.4.5.8 Phosphorus Compounds 7-51
7.4.5.9 Nitrogen Compounds 7-54
7.4.5.10 Sea Water Contamination 7-57

7.5 Geophysical Environment 7-62
7.5.1 Tectonic Setting and Geology 7-62
7.5.1.1 Tectonic Setting 7-62
7.5.1.2 Terrestrial Geology 7-65
7.5.1.3 Marine Geology 7-69
7.5.2 Seismicity and Geohazards 7-69
7.5.3 Terrestrial Geomorphology 7-71
7.5.3.1 Fluvial Geomorphology 7-77
7.5.3.2 Coastal Morphology 7-79
7.5.4 Marine Geomorphology 7-80
7.5.4.1 Continental Shelf 7-81
7.5.4.2 Continental Slope 7-82
7.5.4.3 Abyssal Plain 7-94
7.5.5 Marine Sediments 7-95
7.5.5.1 Sediment Transport 7-95
7.5.5.2 Sediment Composition 7-97
7.5.5.3 Sediment Quality 7-103

7.6 Conclusion 7-109

Tables

Table 7.1 Onshore, Nearshore and Offshore Surveys, 2009 to 2013 7-3

Table 7.2 Marine Water Quality Samples (Ref 7.1)...7-12

Table 7.3 Average Monthly Air Temperature (°C)...7-18

Table 7.4 Maximum Number of Days with Fog, by month 7-19

Table 7.5 Average Wind Statistics by Geographic Direction at Anapa (Ref. 7.19)..................7-19

Table 7.6 Predicted Normal Marine Wind Conditions (Ref. 7.6) 7-21

Table 7.7 Predicted Extreme Marine Wind Conditions (in m/s) (Ref. 7.6) 7-22

Table 7.8 Electric and Magnetic Field Intensity Measurements, at 50 Hz 7-24

Table 7.9 Long-Term Average Sea Levels in the Black Sea at Sochi (Ref. 7.1) 7-31

Table 7.10 Measured Range of Sea Level Values in Marine Survey Area (Ref. 7.4) 7-31

Table 7.11 Typical Maximum Wave Geometry (Ref. 7.1, 7.2)...7-33

Table 7.12 Correlation of Wave Heights and Directions (Ref. 7.1) 7-33

Table 7.13 Summary of Estimated Wave Heights (Ref. 7.6) 7-34

Table 7.14 Surge Level Fluctuations (m) Compared with Average Black Sea Level (Ref. 7.1) .7-34

Table 7.15 Summary of Surface Currents (Ref. 7.6) 7-36

Table 7.16 Summary of Nearbed Currents (Ref. 7.6)..7-36

Table 7.17 Summary of the Ice Period in Kerch Strait from 1991–2005 (Ref. 7.1) 7-37

Table 7.18 Measured Salinity with Depth for 2010-2011 (Ref. 7.1)......................................7-42

Table 7.19 Measured Water Density with Depth in 2010-2011 (Ref. 7.1) 7-45

Table 7.20 Summary of Contaminants in Sea Water for Autumn (Ref. 7.1) 7-58

Table 7.21 Summary of Contaminants in Sea Water for Spring 2011 (Ref. 7.1).....................7-59

Table 7.22 Sediment Type Groupings of 2013 Marine Survey Sediment Type Data (Ref. 7.8) .7-99

Table 7.23 Typical Composition of Clay Sediments on Continental Shelf (Ref. 7.1) 7-100

Table 7.24 Typical Composition of Silt Sediments on Continental Slope (Ref. 7.1) 7-102

Table 7.25 Summary of Contaminants in Marine Sediments for 2010-2011 (Ref. 7.1, 7.18) . 7-105

Table 7.26 Summary of Contaminants in Marine Sediments from 2013 Grab Samples (Ref. 7.8, 7.18)..7-106

Table 7.27 Summary of Contaminants in Marine Sediments from 2013 Core Samples (Ref. 7.8, 7.18)....7-108

Figures

Figure 7.1 Terrestrial Survey Locations (Ref. 7.1, 7.7)....7-9

Figure 7.2 Metocean Survey Locations for 2011 to 2012 (Ref. 7.4)....7-11

Figure 7.3 Marine Water Quality Survey Locations for 2010 and 2011 (Ref. 7.1)....7-13

Figure 7.4 Marine Sediment Quality Survey Locations for 2010, 2011 and 2013 (Ref. 7.1, Ref. 7.8)....7-15

Figure 7.5 Average Monthly Rainfall at Anapa Meteorological Station (Ref. 7.19)....7-19

Figure 7.6 Wind Rose, Anapa Meteorological Station (Ref. 7.1)....7-20

Figure 7.7 Seasonal Patterns in Offshore Winds, Ref. 7.6....7-23

Figure 7.8 Changes in Sea Level in the Black Sea from 1917 to 2005 (Ref. 7.1)....7-27

Figure 7.9 Bathymetry of the Russian Sector of the Black Sea....7-29

Figure 7.10 Deviation in Average Sea Level from 1917 to 2005 (Ref. 7.1)....7-31

Figure 7.11 Main Black Sea Current (Ref. 7.1)....7-35

Figure 7.12 Long-term Average Annual Profiles of Temperature with Depth (Ref. 7.1)....7-39

Figure 7.13 Sea Water Temperatures (°C) in the Surface Waters in April 2011 (Ref. 7.1)....7-40

Figure 7.14 Long-term Average Annual Profiles of Salinity with Depth (Ref. 7.1)....7-41

Figure 7.15 Sea Water Salinity (‰) in the Surface Waters in April 2011 (Ref. 7.1)....7-42

Figure 7.16 Distribution of Sea Water Salinity (‰) with Depth and Distance from Shore in April 2011 (Ref 7.1)....7-43

Figure 7.17 Long-term Average Annual Profiles of Conventional Density with Depth (Ref. 7.1, 7.2)....7-44

Figure 7.18 Comparison of Distribution Profiles of Temperature, Salinity and Density with Depth (Ref 7.1)....7-45

Figure 7.19 Vertical Stratification in Hydrogeochemistry (Ref. 7.36)....7-47

Figure 7.20 Distribution of Oxygen (Green) and Hydrogen Sulphide (Brown) Concentrations (µM) from Archival Data (Ref. 7.1)....7-48

Figure 7.21 Distribution of Phosphate Concentrations (µM) with Depth and Distance from Shore based on Archival Data (Ref. 7.1)....7-52

Figure 7.22 Spatial Distribution of Phosphate Concentrations in Surface Waters (Ref. 7.1) 7-53

Figure 7.23 Spatial Distribution of Total Phosphorus Concentrations in Surface Waters (Ref. 7.1) 7-54

Figure 7.24 Distribution of Nitrate Concentrations (µM) with Depth and Distance from Shore based on Archival Data (Ref. 7.1) 7-55

Figure 7.25 Spatial Distribution of Nitrate Concentrations in Surface Waters (Ref. 7.1) 7-56

Figure 7.26 Spatial Distribution of Oil Product Concentrations in Surface Waters (Ref. 7.1) ... 7-60

Figure 7.27 Spatial Distribution of Lead Concentrations in Surface Waters (Ref. 7.1) 7-61

Figure 7.28 Spatial Distribution of Copper Concentrations in Surface Waters (Ref. 7.1) 7-61

Figure 7.29 Tectonic Setting of the Eastern Black Sea Region (Ref. 7.24) 7-63

Figure 7.30 Geological Map of the Terrestrial Landfall Section (Ref. 7.25) 7-67

Figure 7.31 Mapped Faults in Terrestrial Landfall Section (Ref. 7.5, 7.22) 7-73

Figure 7.32 Geomorphological Map of the Terrestrial Survey Area (Ref. 7.1) 7-75

Figure 7.33 Typical Undulating Landscape of Terrestrial Landfall Section (Ref. 7.1) 7-77

Figure 7.34 Erosion Features Associated with the Watercourse in the Graphova Gap (Ref 7.1) 7-78

Figure 7.35 Examples of Typical Coastal Abrasion Features Associated with Coastal Cliff Landsliding and Erosion of Softer Sediments on the Cliff Face (Ref. 7.1) 7-80

Figure 7.36 Geomorphological Zones of Russian Sector of the Black Sea (Ref. 7.5) 7-81

Figure 7.37 Schematic Diagram of Anapa Submarine Canyon (Ref. 7.28) 7-84

Figure 7.38 Summary Interpretation of Geomorphological Features on Upper Russian Slope (Ref. 7.36) 7-85

Figure 7.39 3D Representation of the Upper Russian Slope (Location A) (Ref. 7.36) 7-86

Figure 7.40 Sidescan Sonar Image of Dendritic Gully Systems on Upper Russian Slope (Location B) (Ref. 7.36) 7-86

Figure 7.41 Sidescan Sonar Image of Upslope Part of Dendritic Gully System (Location C) (Ref. 7.36) 7-87

Figure 7.42 Sidescan Sonar Image of Outcropping Bedrock on Gully Walls (Location D) (Ref. 7.36) 7-88

Figure 7.43 ROV Survey Images of Boulders on Upper Russian Slope (Ref. 7.36) 7-89

Figure 7.44 Sidescan Sonar Image of Small Carbonate Mounds near Shelf Break (Location E) (Ref. 7.36) 7-90

Figure 7.45 Overview of Sidescan Sonar Data for Lower Russian Slope (Location F) (Ref. 7.36) 7-90

Figure 7.46 Sidescan Sonar Image of Landslide Scarp on Lower Russian Slope (Ref. 7.36)....7-91

Figure 7.47 Sidescan Sonar Image of Debris Lobes on Lower Russian Slope (Ref. 7.36)........7-92

Figure 7.48 Anapa Canyon Crossing 7-93

Figure 7.49 Continental Slope Crossing...7-93

Figure 7.50 Sidescan Sonar Image of Abyssal Plain Showing Lineations and Tool Marks (Ref. 7.36)...7-94

Figure 7.51 Sediment Transport Processes within the Black Sea (Ref. 7.42) 7-95

Figure 7.52 Photographs of Seabed Sediments in Coastal Waters (Ref. 7.8) 7-98

7 Physical and Geophysical Environment

7.1 Introduction

This chapter provides a description of the physical and geophysical environment associated with the South Stream Offshore Pipeline – Russian Sector (the Project). The chapter provides context and background to the detailed baseline studies contained within the environmental and social assessment chapters which follow.

Attributes discussed in this chapter comprise:

- Physical Environment:
  - Meteorological conditions;
  - Electromagnetic fields;
  - Radiation;
  - Oceanography; and
  - Marine Water Quality.
- Geophysical Environment:
  - Tectonic setting and geology;
  - Seismicity (including terrestrial and marine geohazards);
  - Terrestrial and Marine Geomorphology; and
  - Marine Sediments.

Where possible, the physical characteristics described in this chapter apply to the overall Project. However, where specific characteristics were observed to be variable across the landfall section, nearshore section and offshore sections of the Project, this is specified.

Receptors sensitive to the terrestrial environment include soil, groundwater, surface water and landscape. These receptors are discussed in detail in **Chapter 8 Soils, Groundwater and Surface Water** and **Chapter 13 Landscape and Visual**. The terrestrial physical environment may also influence ecological receptors; these receptors are discussed in **Chapter 11 Terrestrial Ecology.**

The receptors sensitive to the changes in the marine environment are, for the most part ecological ones, and the significance of any such changes are discussed in detail in **Chapter 12 Marine Ecology**.

Potential environmental issues associated with geohazards and seismicity are discussed further in **Chapter 19 Unplanned Events**.

7.2 Spatial and Temporal Boundaries

7.2.1 Project Area

The Project Area (as described in **Chapter 1 Introduction**) is subdivided into three sections: the landfall, nearshore and offshore sections. This chapter considers all three sections.

7.2.2 Study Areas

The Terrestrial Study Area is a zone extending up to approximately 1.5 km either side of the centreline of the pipeline route and landfall facilities boundary. The Terrestrial Study Area has been assessed within a regional context with respect to the geology. The Terrestrial Study Area is bounded to the southwest by the coast.

The Marine Study Area is a zone of variable extent either side of the centreline of the pipeline route. The Marine Study Area is wider in the coastal waters and on the continental shelf and slope than it is in the deep waters of the abyssal plain. The Marine Study Area is bounded to the northeast by the coast and to the west by the edge of the Russian EEZ.

7.2.3 Survey Areas

The Terrestrial Survey Area for the physical environment is the same as the Terrestrial Study Area. The Marine Survey Area is typically the same as the Marine Study Area. The Marine Survey Area has varied over time as the pipeline routing has been refined.

7.3 Baseline Data

7.3.1 Methodology and Data

In order to provide context for the assessment of environmental impacts (discussed in subsequent chapters), baseline information on the physical environment, geology and oceanography of the region has been collected.

Secondary (i.e. existing data based on desk-based research) and primary data regarding the relevant baseline characteristics have been identified and assessed. Primary data was then collected during field surveys.

7.3.2 Secondary Data

Contextual information on the regional setting was obtained through literature review. Meteorological data for the region was sourced from published datasets.

Published geological, seismological and topographical maps were reviewed to characterise the regional tectonic setting, geology and geomorphology.

Background information on the oceanography and hydrography of the Black Sea has been based (Ref. 7.1) on the hydro-environmental database of the Southern Branch of the Institute of

Ocean Sciences of RAS (Gelendzhik City) (Ref. 7.2). This dataset includes results from 82 survey voyages (1756 stations) undertaken between 1924 and 2012 in the area from 43° to 44.5°N and from 38° to 39.5°E. Background information is available on contamination of marine waters and sediments based on previous surveys (Ref. 7.1).

Additionally, the Black Sea Commission State of the Environment report (Ref. 7.3) was used to provide additional baseline data on the region.

7.3.3 Baseline Surveys

A number of onshore and offshore engineering and environmental surveys have been undertaken to aid the engineering design and the ESIA process. These surveys are detailed in Table 7.1. The surveys were undertaken between 2009 and 2013 and covered the following aspects of relevance to this chapter:

- Meteorological conditions;
- Electromagnetic fields and radiation;
- Seismicity;
- Geology;
- Geomorphology;
- Marine oceanography and setting; and
- Marine sediment and water quality.

The baseline data presented in this chapter is predominantly based on published literature and the information gathered during these surveys (Refs. 7.1, 7.4, 7.5, 7.6, 7.7, and 7.8).

Table 7.1 Onshore, Nearshore and Offshore Surveys, 2009 to 2013

Survey Date(s)	Survey Extent	Title of Survey / Information reviewed
April to July 2009	Russian Territorial and EEZ Waters (offshore section)	Geotechnical, hydrographical and geophysical surveys. Reconnaisance survey – multi-beam echosounder and sub-bottom profiler (slope and abyssal plain)
April 2009 to May 2012	Russian Territorial and EEZ Waters (landfall, nearshore and offshore sections)	Metocean survey. Measured waves, currents and water levels near the Russian coast
July 2009	Russian Territorial Waters (landfall and nearshore sections)	Geotechnical and geophysical surveys

Continued...

Survey Date(s)	Survey Extent	Title of Survey / Information reviewed
July 2009 to April 2011	Russian Territorial Waters (landfall and nearshore sections)	Metocean survey. Measured waves, currents and water levels near the Russian coast.
November to December 2010	Russian Territorial and EEZ Waters (offshore section)	2DHR seismic survey – streamer (slope)
December 2010	Terrestrial Survey Area	Geomorphology, geohazards, radiation survey
April 2011	Russian Territorial Waters (nearshore and offshore sections)	Metocean survey
April to May 2011	Russian Territorial Waters (nearshore and offshore sections)	High resolution geophysical survey – multi-beam echosounder, sub-bottom profiler and side-scan sonar (nearshore and shelf)
May 2011 to May 2012	Russian Territorial and EEZ Waters (nearshore and offshore sections)	Metocean Survey using a variety of instruments to measure parameters including waves, water levels, current velocities, temperature, and salinity
June to July 2011	Russian EEZ (offshore section)	Validation survey – multi-beam echosounder and sub-bottom profiler (abyssal plain)
June to July 2011	Russian Territorial and EEZ Waters (offshore section)	Geochemical sampling – gravity corer (slope and abyssal plain)
July to August 2011	Russian Territorial and EEZ Waters (nearshore and offshore sections)	Geotechnical survey – gravity cores and laboratory testing (abyssal plain, slope and shelf). Geomorphology surveys
September to November 2011	Russian Territorial and EEZ Waters (offshore section)	High resolution geophysical survey – AUV with multi-beam echosounder, sub-bottom profiler and side-scan sonar (slope and abyssal plain)

Continued...

Survey Date(s)	Survey Extent	Title of Survey / Information reviewed
October 2011 to June 2012	Terrestrial Survey Area (landfall section)	Geophysical and geotechnical surveys – geodetic, topographic, electric tomography, seismic refraction, geotechnical and hydrological (onshore microtunnel area)
October 2011	Russian Territorial Waters (nearshore and offshore sections)	High resolution geophysical survey – multi-beam echosounder, sub-bottom profiler and side-scan sonar (shelf)
November 2011 to January 2012	Russian Territorial and EEZ Waters (nearshore and offshore sections)	Geotechnical survey – CPT (abyssal plain, slope and shelf)
May to August 2012	Russian Territorial Waters (nearshore and offshore sections)	Geotechnical survey - boreholes and laboratory testing (nearshore) Geotechnical survey – jumbo piston cores and laboratory testing (slope and abyssal plain)
September to November 2012	Russian Territorial and EEZ Waters (offshore section)	ROV inspection and cable tracking survey Geotechnical survey – box cores and laboratory testing (slope and abyssal plain)
November 2012 to January 2013	Russian Territorial and EEZ Waters (nearshore and offshore sections)	Geotechnical and visual survey – CPT and ROV video (shelf and slope) Geotechnical survey – piston gravity cores and laboratory testing (shelf, slope and abyssal plain)
April to June 2013	Terrestrial Survey Area (landfall section)	Geotechnical survey – boreholes and laboratory testing (onshore route and facility area) Geophysical survey – geodetic, topographic, electric tomography, seismic refraction (onshore route and facility area)

Continued...

Survey Date(s)	Survey Extent	Title of Survey / Information reviewed
May 2013	Russian Territorial Waters (landfall and nearshore sections)	Geophysical survey – seismic refraction (nearshore)
June to July 2013	Terrestrial Survey Area (landfall section)	Radiation survey
July 2013	Russian Territorial and EEZ Waters (landfall, nearshore and offshore sections)	Marine sediment quality and sediment type
September 2013	Terrestrial Survey Area (landfall section)	Topographic survey – geodetic, topographic, (access roads)
September to November 2013	Terrestrial Survey Area (landfall section)	Geotechnical survey – boreholes and laboratory testing (access roads)

Complete.

7.3.3.1 Terrestrial Surveys

Field surveys were undertaken to assess electromagnetic fields and radiation levels (Ref. 7.1, 7.7). The majority of the field measurements and samples were located within or near the terrestrial Project Area.

The electromagnetic survey comprised measurements of the background electric and magnetic field intensity at five locations across the Terrestrial Survey Area (Figure 7.1). The measurements were recorded at an industrial frequency of 50 Hz. The locations sampled all represented potentially high emitting electromagnetic sources across the Terrestrial Survey Area, such as high voltage power lines, outdoor switchgears and transformer units.

Background radiation levels were measured across the Terrestrial Survey Area:

- Measurements of gamma radiation were recorded at a total of 134 control points across the Terrestrial Survey Area with 81 measurements taken during the 2010 survey, and a further 53 measurements taken during the 2011 survey (Figure 7.1);
- The equivalent dose rate[1] for external gamma radiation was then determined for a total of 1144 points in the Terrestrial Survey Area (Figure 7.1). Measurements were undertaken at

[1] The equivalent absorbed radiation dose (equivalent dose), measured in sievert per hour (Sv/h) is a measure for assessing the health risk of radiation exposure. It is a calculated average measure of the radiation absorbed by a fixed mass of biological tissue that attempts to account for the different biological damage potential of different types of ionizing radiation.

175 points during the 2010 survey, 555 points during the 2011 survey, and 414 points during the 2013 survey; and

- In addition, a total of 42 soil and stream bed sediment samples (Figure 7.1) were collected within the Terrestrial Survey Area. The samples were analysed in order to assess the levels of various radioactive isotopes. In total, 20 samples were collected during the 2010 survey, seven samples were collected during the 2011 survey, and 15 samples were collected during the 2013 survey.

The same Terrestrial Survey Area (Figure 7.1) was used for the geomorphological mapping. Additionally, soil and water samples were collected for analysis; this is discussed in **Chapter 8 Soils, Groundwater and Surface Water**.

Geotechnical and geophysical surveys were undertaken along the Pipeline route within the same Terrestrial Survey Area. The geotechnical surveys have included drilling boreholes up to 180 m deep to confirm the ground conditions. Soil and rock samples were collected from the boreholes for geotechnical testing. The geophysical surveys included seismic refraction and electrical tomography profiling to aid interpolation of the ground conditions between boreholes.

7.3.3.2 Marine Surveys

To complement the data obtained from desk studies, several marine surveys specific to the Project have been undertaken (Table 7.1).

A metocean survey of the pipeline route across the Black Sea was undertaken between 2010 and 2012 (Ref. 7.4). The survey locations are shown in Figure 7.2.

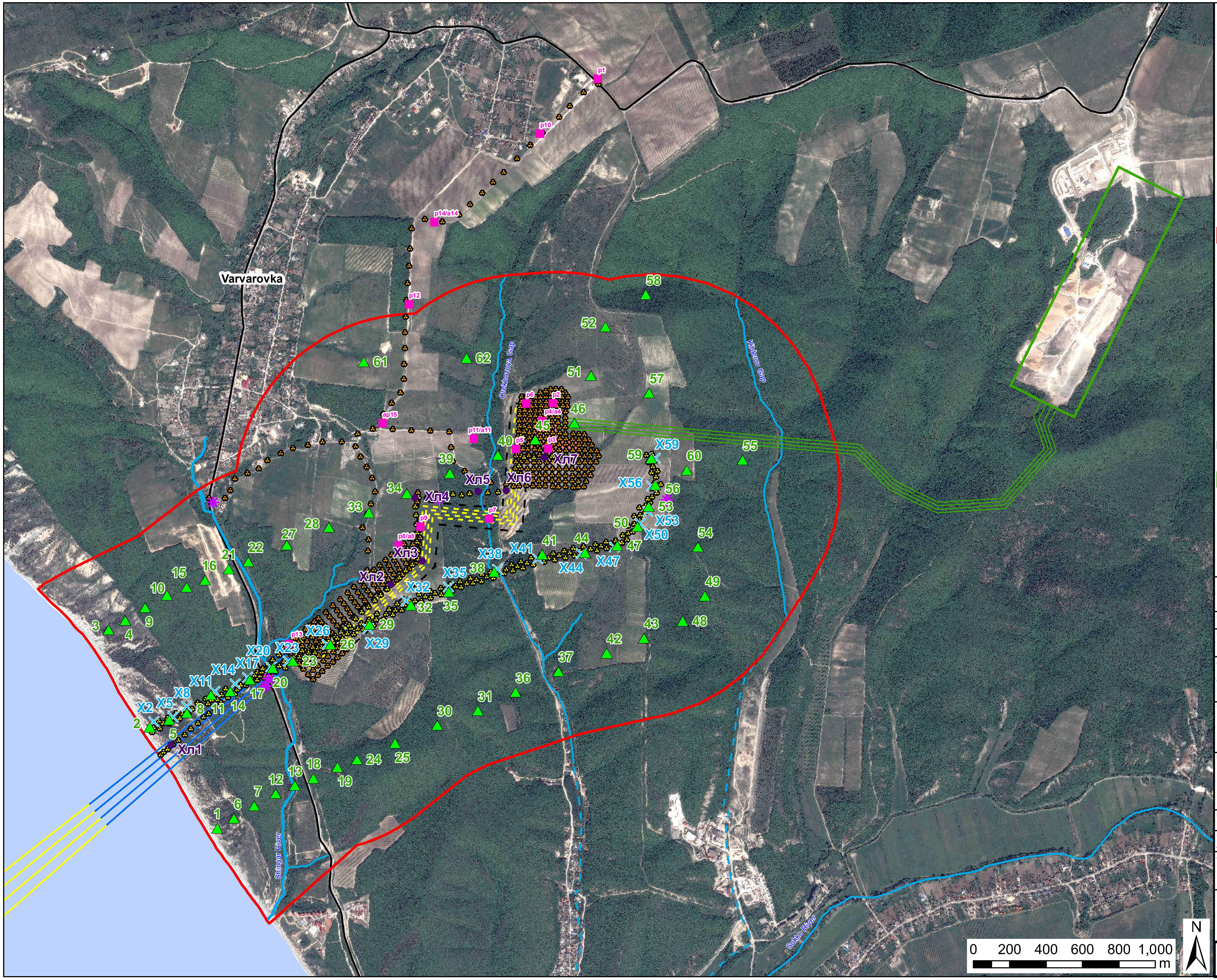

LEGEND

- Geomorphology survey point

Gamma radiation survey

- 2010 Survey
- 2011 Survey
- 2013 Survey

Soil and Sediment Samples Tested for Radioactive Isotopes

- 2010 Survey
- 2011 Survey
- 2013 Survey
- Study Area and PeterGaz Survey Area
- Inferred watercourses
- Rivers
- Main roads

Russian Sector of South Stream Offshore Pipeline

- Proposed landfall section pipelines
- Landfall facilities
- Proposed microtunnels
- Proposed offshore pipelines
- Construction corridor

United Gas Supply System

- Russkaya compressor station
- United Gas Supply System Pipelines

Projection: Lambert Conformal Conic

Revision Details	By	Check	Check Date	Suffix

Purpose of Issue
For Information

Client
South Stream Offshore Pipeline ENERGISING EUROPE

Project Title
SOUTH STREAM OFFSHORE PIPELINE

Drawing Title
LOCATION OF ELECTOMAGNETIC AND RADIATION SAMPLING POINTS

Drawn	Checked	Approved	Date
DH	IS	IS	04 Mar 2014

URS Internal Project No.	Scale @ A3
46369082	1:20,000

URS Infrastructure & Environment UK Limited
Scott House
Alencon Link, Basingstoke
Hampshire, RG21 7PP
Telephone (01256) 310200
Fax (01256) 310201
www.ursglobal.com

URS

Drawing Number	Rev
Figure 7.1	

Plot Date: 04 Mar 2014
File Name:I:\5004 - Information Systems\46369082_South_Stream\MXDs\Report Maps - Russia\Russian ESIA\Chapter 7 Physical and Geophysical Environment\Figure 7.1 Location of electromagnetic and Radiation Sampling Points.mxd

Figure 7.2 Metocean Survey Locations for 2011 to 2012 (Ref. 7.4)

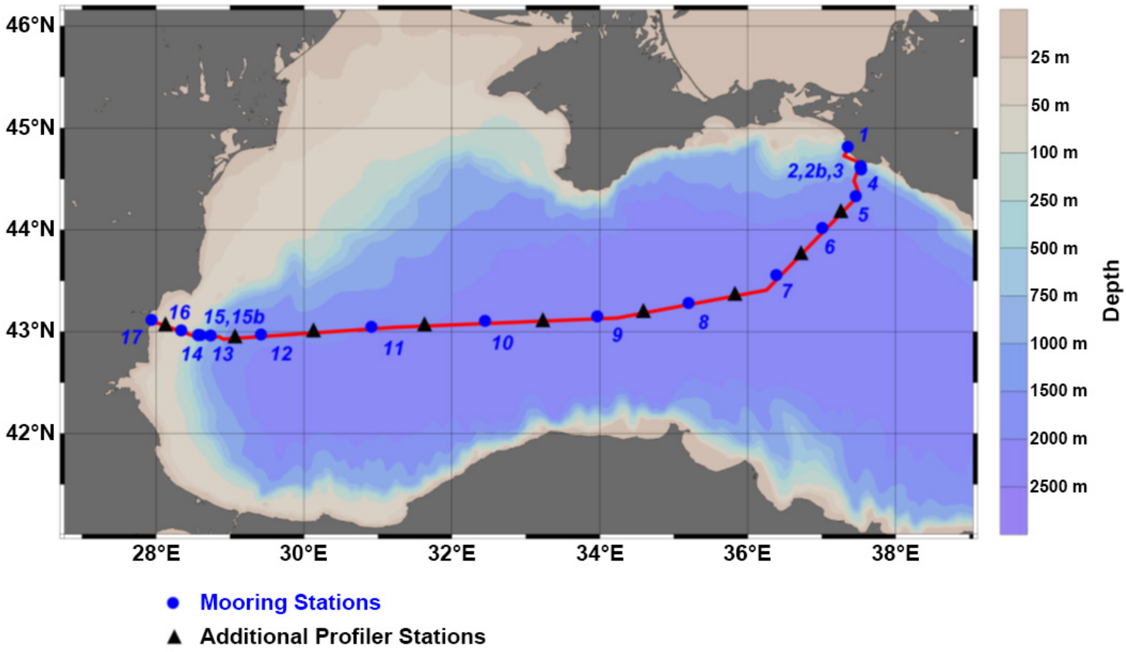

Marine water quality surveys were undertaken (Ref. 7.1) in autumn 2010 and spring 2011. Water quality analysis for general hydrochemistry and potential pollutants was undertaken. Water sampling for laboratory analysis was undertaken in accordance with GOST 17.1.5.05-85 'General requirements for sampling of surface and sea waters'. (Ref. 7.9) Measurements of water temperature, salinity and density were undertaken in situ through the water column using a winched probe. Meteorological and oceanographic measurements were also obtained during these surveys.

In November 2010, a total of 23 water samples were collected at eight survey locations (known as stations). In April 2011, a total of 45 water samples were collected at 14 stations. The spring 2011 survey extended further from the coast and thus covered a larger area than the autumn 2010 survey. In addition, in summer 2011 chemical and bacteriological testing was undertaken at two additional locations: Station 4C near the coast line and 5C in shallow waters (Ref. 7.1). The locations of the marine water survey location stations are presented in Figure 7.3. The depths at which the water samples were collected are presented in Table 7.2.

Marine sediment sampling from the seabed was undertaken between 2010 and 2011 and in July 2013 (Ref. 7.1, 7.8). The 2013 survey included coring within the area to be dredged and areas of seabed intervention to establish levels of potential contamination within the sediment in these areas in line with the requirements of the London Convention for disposal of dredged material. The sampling locations are shown on Figure 7.4.

Table 7.2 Marine Water Quality Samples (Ref 7.1)

Autumn 2010 Survey		Spring 2011 Survey	
Survey Location Station No.	**Sample Depths (m)**	**Survey Location Station No.**	**Sample Depths (m)**
1	0; 30	1	0; 30
2	0; 32	2	0; 15
3	0; 55; 86	3	0; 10; 80
6	0; 30; 120	6	0; 35; 160
8	0; 40; 100	8	0; 50; 136
17	0; 30; 110; 1,000; 1,900	9	0; 40; 105
18	0; 35; 89	10	0; 40; 105
19	0; 26	13	0; 45; 94
-	-	14	0; 40; 115; 1,000; 2,157
-	-	15	0; 45; 102
-	-	16	0; 45; 103; 1,000; 2,124
-	-	17	0; 35; 160; 1,000; 1,888
-	-	18	0; 10; 88
-	-	19	0; 21.5
Stations	*Total Number of Samples*	*Stations*	*Total Number of Samples*
8	23	14	45

In total, 28 samples were collected during the 2010 and 2011 surveys (Ref. 7.1): 6 in autumn 2010, 8 in spring 2011 and 14 in summer 2011. During the 2013 survey (Ref. 7.8), 57 sediment samples for analysis of contaminants were collected from 42 locations: 43 grab samples from 35 grab locations and 14 core samples at 7 core locations. The sediment samples were visually described before undergoing chemical analysis and grain size distribution analysis. Data on sediment type at sample locations were also collected by analysis of grain size in sediment samples or ROV footage where sediment samples could not be collected. Further interpretation of the bathymetric surveys and ROV footage was undertaken a report summarising the results is contained in Appendix 7.1 Abyssal Plain Report.

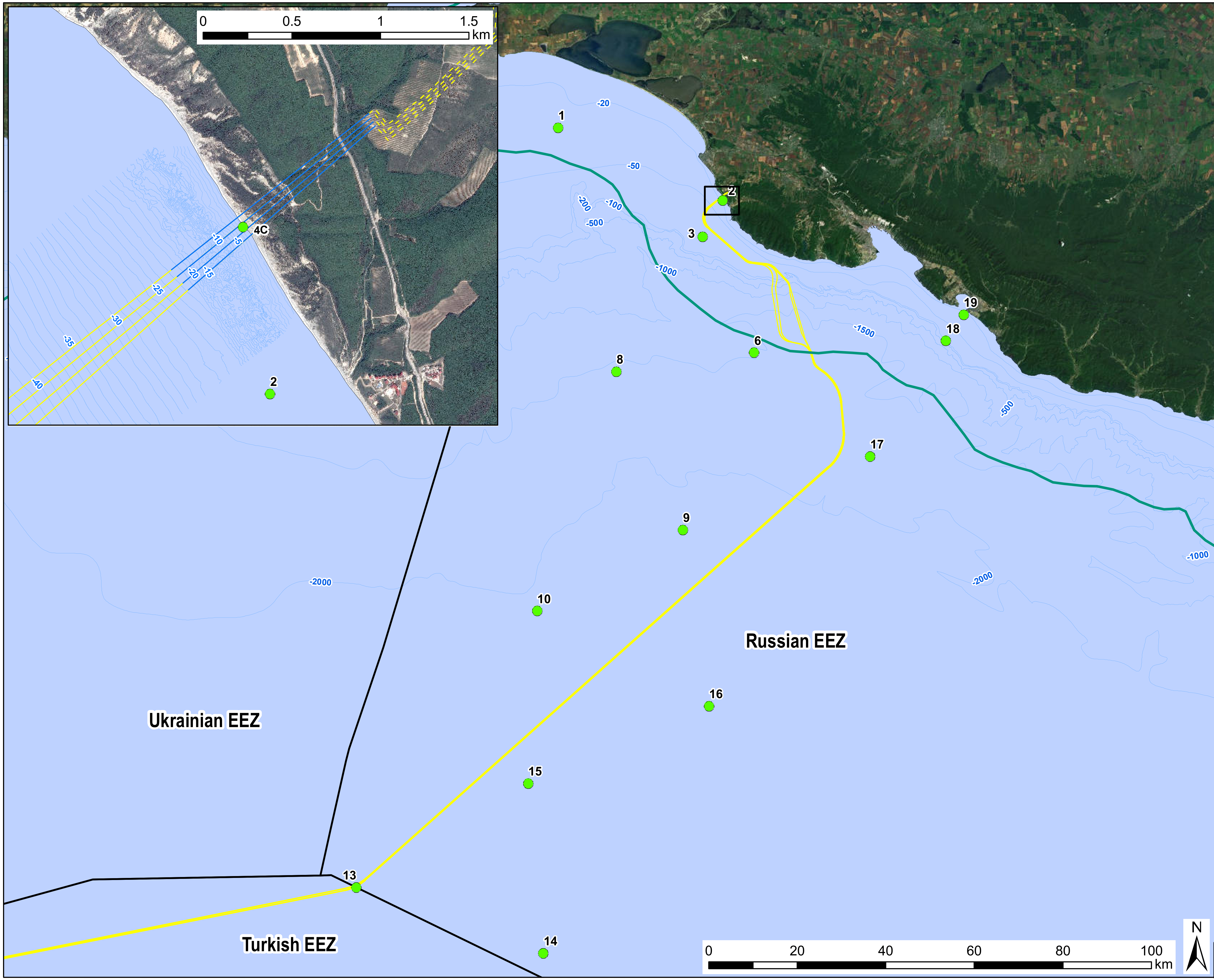

LEGEND

- Marine water quality survey locations

Russian Sector of South Stream Offshore Pipeline

- Proposed landfall section pipelines
- Proposed microtunnels
- Proposed offshore pipelines
- Russia territorial waters boundary
- Exclusive Economic Zone boundary
- Isobaths

Projection: Lambert Conformal Conic

Revision Details	By / Check	Check Date	Suffix

Purpose of Issue
For Information

Client
South Stream Offshore Pipeline ENERGISING EUROPE

Project Title
SOUTH STREAM
OFFSHORE PIPELINE

Drawing Title
MARINE WATER QUALITY
SURVEY LOCATIONS
(2010 & 2011)

Drawn	Checked	Approved	Date
DH	RW	MW	04 Mar 2014

URS Internal Project No.	Scale @ A3
46369082	1:800,000

URS Infrastructure & Environment UK Limited
Scott House
Alencon Link, Basingstoke
Hampshire, RG21 7PP
Telephone (01256) 310200
Fax (01256) 310201
www.ursglobal.com

Drawing Number
Figure 7.3

Rev

Plot Date: 04 Mar 2014
File Name:I:\5004 - Information Systems\46369082_South_Stream\MXDs\Report Maps - Russia\Russian ESIA\Chapter 7 Physical and Geophysical Environment\Figure 7.3 Marine Water Quality Survey Locations (2010 & 2011).mxd

This page has been left intentionally blank

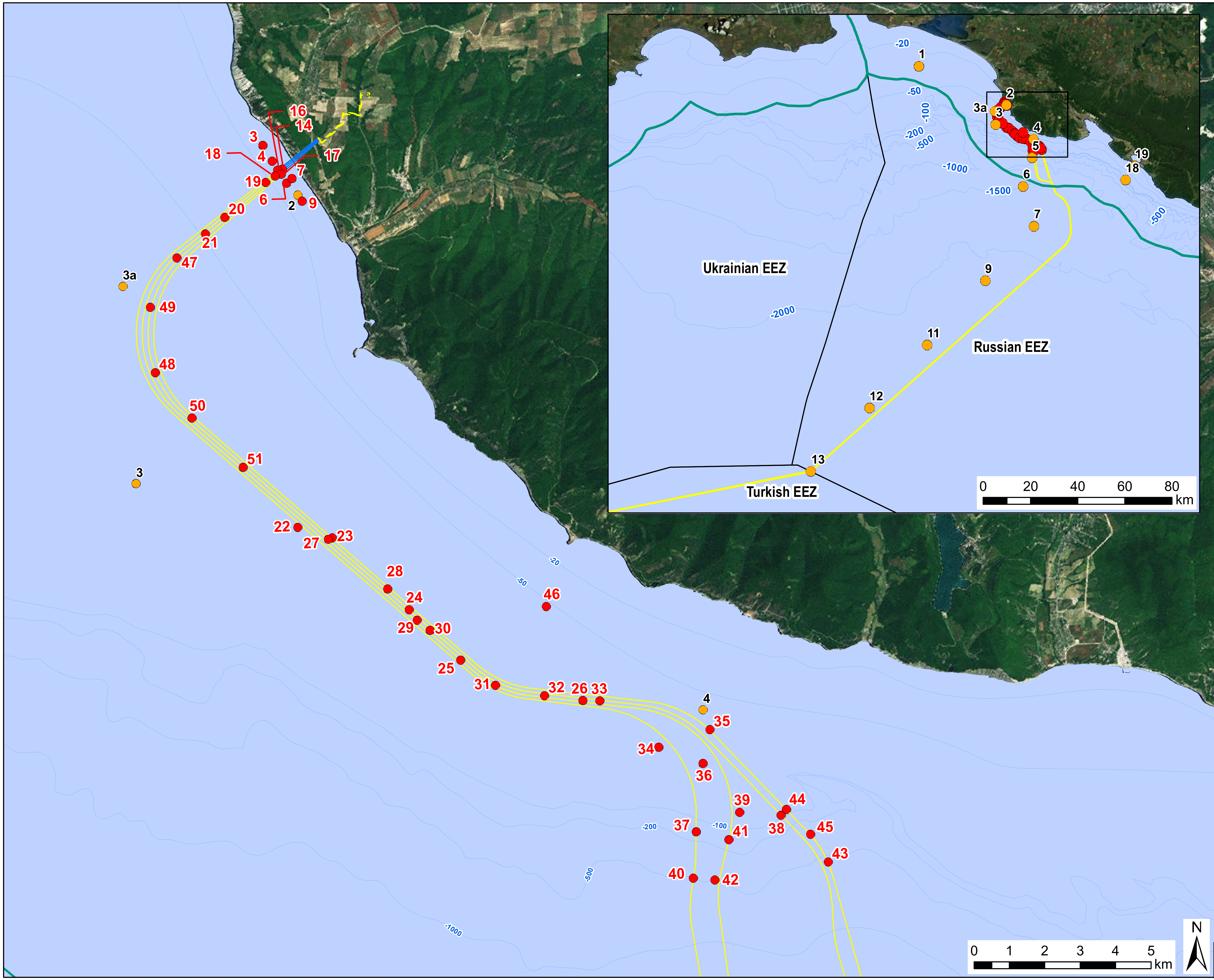

LEGEND

- Marine Sediment Quality Survey Locations 2010/2011
- Marine Sediment Quality Survey Locations 2013

Russian Sector of South Stream Offshore Pipeline

- Proposed landfall section pipelines
- Proposed microtunnels
- Proposed offshore pipelines
- Russia territorial waters boundary
- Exclusive Economic Zones Boundary
- Isobaths

Projection: Lambert Conformal Conic

Revision Details	By / Check	Check Date	Suffix

Purpose of Issue: For Information

Client: South Stream Offshore Pipeline — ENERGISING EUROPE

Project Title: SOUTH STREAM OFFSHORE PIPELINE

Drawing Title: MARINE SEDIMENT QUALITY SURVEY LOCATIONS FOR 2010, 2011 & 2013

Drawn	Checked	Approved	Date
DH	RW	MW	04 Mar 2014

URS Internal Project No.	Scale @ A3
46369082	1:100,000

URS Infrastructure & Environment UK Limited
Scott House
Alencon Link, Basingstoke
Hampshire, RG21 7PP
Telephone (01256) 310200
Fax (01256) 310201
www.ursglobal.com

Drawing Number: Figure 7.4

Rev

Plot Date: 04 Mar 2014
File Name:I:\5004 - Information Systems\46369082_South_Stream\MXDs\Report Maps - Russia\Russian ESIA\Chapter 7 Physical and Geophysical Environment\Figure 7.4 Marine Sediment Quality Survey Locations.mxd

This page has been left intentionally blank

7.3.4 Applicable Standards

The policy, regulatory and administrative frameworks relevant to the Project and ESIA process are outlined in **Chapter 2 Policy, Regulatory and Administrative Framework**. In addition to these, there are a number of standards of specific relevance to this chapter. These comprise:

- International standards on electromagnetic fields:
  - International Finance Corporation (IFC) Environment, Health, and Safety Guidelines Electric Power Transmission and Distribution (Ref. 7.10); and
  - International Commission on Non-Ionizing Radiation Protection (ICNIRP) guidelines for Limiting Exposure to Time-varying Electric, Magnetic, and Electromagnetic Fields (Ref. 7.11).
- Russian national standards on electromagnetic fields:
  - Russian Standard SanPiN 2971-84 on Regulations for Public Protection Against the Impact of an Electrical Field Created by Overhead Power Lines with an Alternating Power of Industrial Frequency (Ref. 7.12); and
  - Russian standard GN 2.1.8/2.2.4.2262-07 on Maximum Permissible Levels of Magnetic Fields with a Frequency of 50 Hz in Residential Premises, Public Buildings and on Residential Territories (Ref. 7.13).
- Russian national standards on radiation:
  - Russian Standard MU 2.6.1.2398-08 on Radiation Monitoring and Sanitary Epidemiological Assessment of Land Plots for Construction of Houses, Buildings and Public Facilities and Industrial Projects with Regard to Radiation Safety (Ref. 7.14); and
  - Russian Standard SanPiN 2.6.1.2523-09 on Radiation Safety Standards (Ref. 7.15).
- Russian standards on marine water quality:
  - Order of the Federal Fisheries Agency No. 20 dated 18.01.2010, on Approving the Standards for Water Quality in Fishing Water Bodies, including Standards for Maximum Permissible Concentrations of Harmful Substances in the Water of Fishing Water Bodies (Ref. 7.16); and
  - Russian Standard SanPiN 2.1.5.2582-10 on Sanitary and Epidemiological Requirements for Protection of Sea Coastal Waters Against Pollution in Areas of Water Use of the Population (Ref. 7.17).
- Dutch standards on marine sediment quality (adopted in absence of equivalent Russian standards):
  - Circular on target values and intervention values for soil remediation, 2000. Ministry of Infrastructure and Environment of the Netherlands (Ref. 7.18). Recommended for use as a methodological guide by Russian Standard SP 11-102-97 'Environmental science surveys for construction'.

7.4 Physical Environment

7.4.1 Meteorological Conditions

The Krasnodar Regional Centre for Hydrometeorology and Environmental Monitoring has monitored long-term climatic characteristics for the period from 1977 to 2009 (Ref. 7.1) at the nearest weather station to the Project, which is located in Anapa, 5 km north of the proposed pipeline route (Anapa WMO, Station ID 37001, Ref. 7.19).

The Study Area is characterized by a Mediterranean-type climate, with a sunny, hot and dry summer and a relatively mild and humid winter.

The average air temperature data is summarised in Table 7.3. The annual average air temperature in Anapa is 12.1 ºC. On average, the warmest months are June to September with a maximum monthly average temperature of 21.0 °C. The coolest are November to March, with a minimum average temperature of 4.4 °C. The average maximum daily temperature is 29.0 °C and the average minimum daily temperature is -2.2 °C (Ref. 7.19). The absolute maximum and minimum air temperature during the period 1977 to 2009 is 38°C and -26°C, respectively.

Table 7.3 Average Monthly Air Temperature (°C)

Jan	Feb	Mar	Apr	May	June	July	Aug	Sep	Oct	Nov	Dec	Annual Average.
1.8	2.4	5.4	11.0	15.2	20.1	23.1	22.7	18.2	12.8	7.7	4.2	12.1

The annual average precipitation is 539 mm (an average of 45 mm per month), mainly in the form of rain (Figure 7.5). The maximum recorded daily precipitation is 85.9 mm. There is relatively limited seasonal variation in precipitation, with the greatest amount occurring during the months of November, December and January.

The deepest snowfall on record is 33 cm, though snowfall is generally sparse in comparison with the rest of the region and the Russian Federation. Snowfalls usually occur between November and March. Blizzard conditions can occur during winter storms. Frosts occur between October and April.

Figure 7.5 Average Monthly Rainfall at Anapa Meteorological Station (Ref. 7.19)

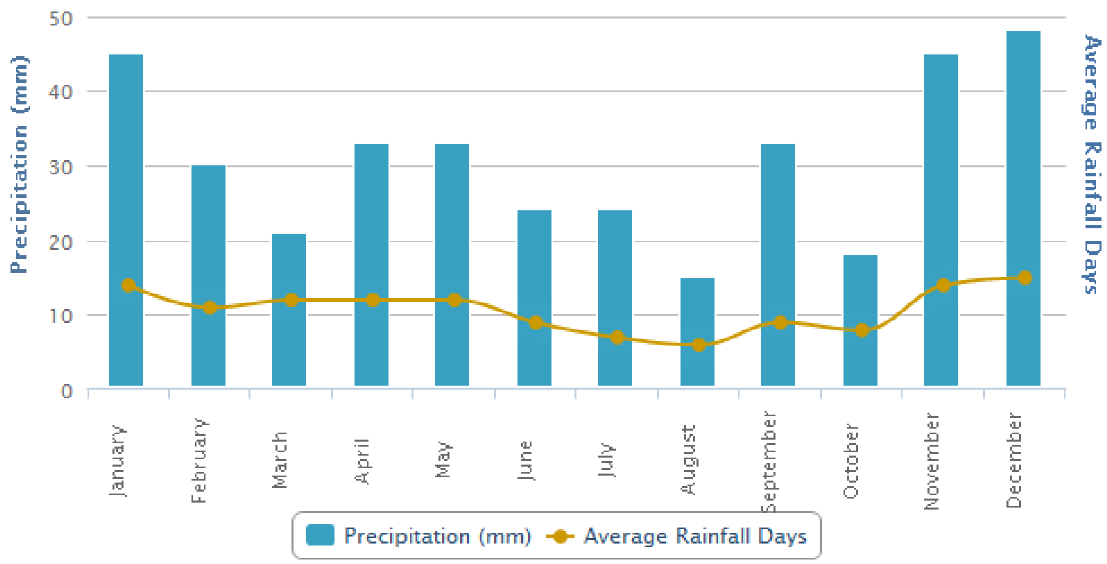

Table 7.4 presents the maximum number of recorded days with fog by month. It shows that May has the maximum number of fog days with nine fog events. August has the least number of fog days, with an average of one day with fog.

Table 7.4 Maximum Number of Days with Fog, by month

Jan	Feb	Mar	Apr	May	June	July	Aug	Sep	Oct	Nov	Dec
3	5	6	5	9	4	2	1	4	4	3	4

Wind conditions vary seasonally. The summer is characterised by light breezes whereas squally winds are characteristic in winter. The average annual wind speed in Anapa is 4.8 m/s. The wind speed is over 13 m /s less than 5% of the time. Wind speeds of up to 40 m/s have been recorded at Anapa. Table 7.5 presents the wind statistics by geographic direction for Anapa.

Table 7.5 Average Wind Statistics by Geographic Direction at Anapa (Ref. 7.19)

Parameter	N	NE	E	SE	S	SW	W	NW
Average wind speed (m/s)	3.6	4.4	3.7	4.8	6.7	5.7	4.7	4.3
Frequency of wind direction (%)	11	25	17	5	21	9	8	4

Hourly sequential meteorological data has been sourced from the nearest available meteorological station, Anapa WMO (Station ID 37001), for the period 2008 to 2012 inclusive.

Anapa is located on the coastline of the Black Sea and is, therefore, sufficiently similar to conditions at the Terrestrial Study Area (Figure 7.6).

Figure 7.6 Wind Rose, Anapa Meteorological Station (Ref. 7.1)[2]

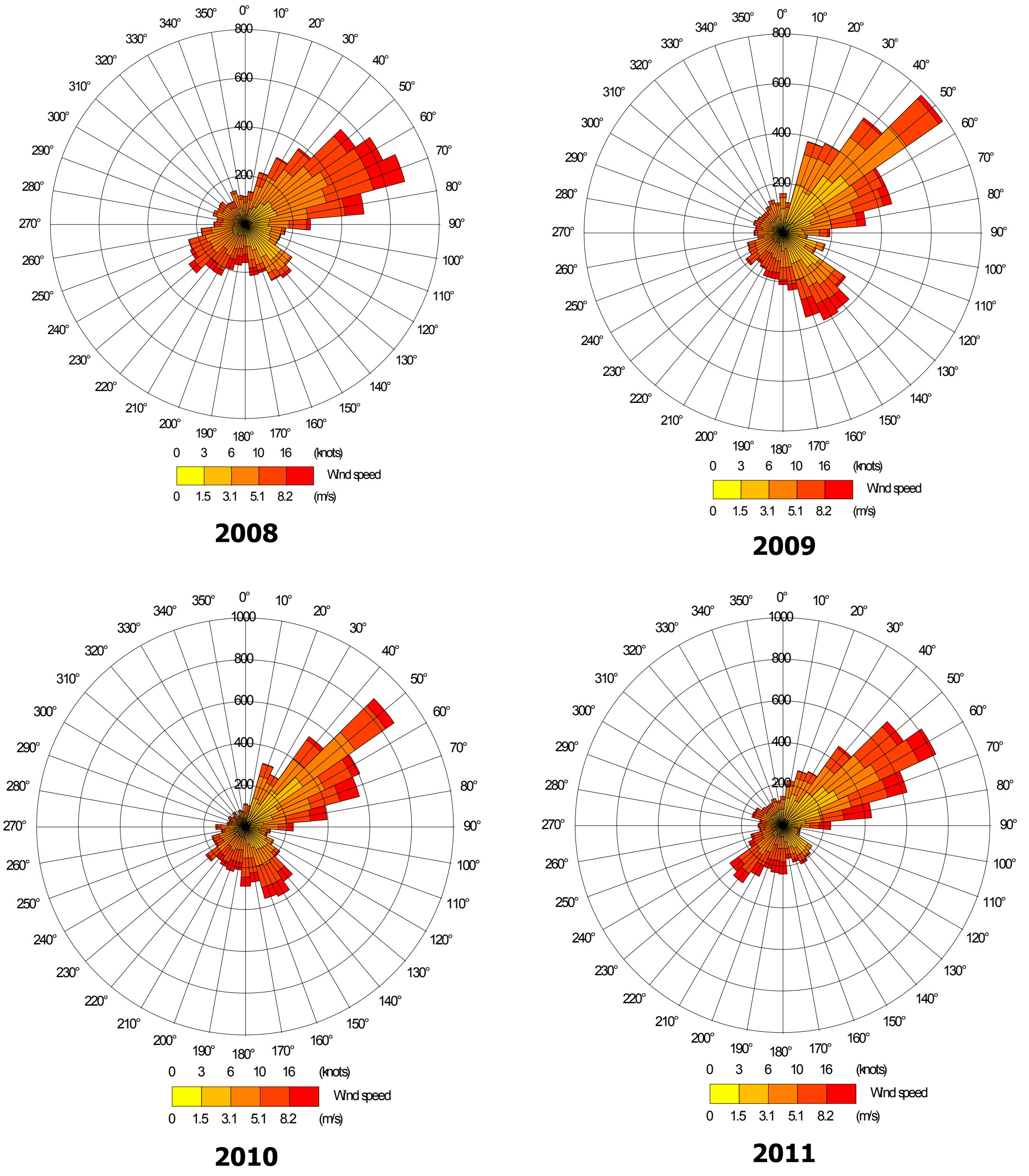

[2] The vertical axis on each wind rose represents the frequency (number) of measurements that are in a given sector.

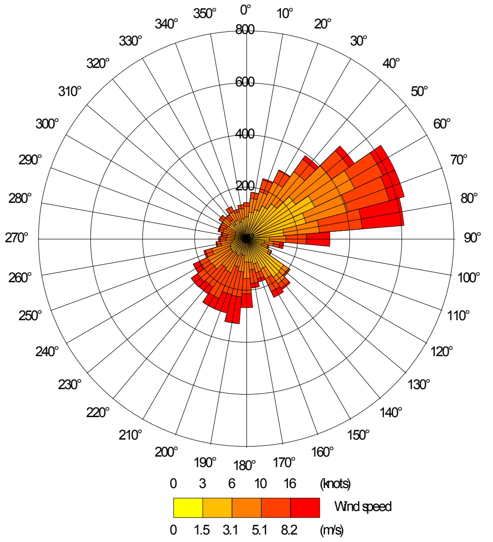

2012

The wind direction is predominantly from the northeast onshore with secondary winds from the south and southwest offshore (Figure 7.6). On average wind speed is slightly stronger from the south than from the northeast.

Wind monitoring has also been undertaken at sea in 2011 in the Marine Survey Area (Figure 7.2) as part of the metocean surveys (Ref. 7.6). The measured wind speeds were typically between 2 and 7 m/s with maximum wind speeds of up to 21 m/s during the survey period. The measured data were compared with hindcast and satellite data for the period 1992 to 2011 (Ref. 7.4, 7.6). The wind data was then modelled to predict wind statistics for the Marine Study Area (Ref. 7.6). The data shows that the wind speeds in the Marine Study Area during the survey period are approximately the same as the long-term wind speeds (Ref. 7.6).

The wind regime varies seasonally (Figure 7.7). Winds are stronger in winter with greater variability in wind direction. The seasonal variation in the wind regime is illustrated by Figure 7.7. The predicted normal and extreme wind conditions are presented in Tables 7.6 and 7.7.

Table 7.6 Predicted Normal Marine Wind Conditions (Ref. 7.6)

Parameter	Deep Water	Continental Slope	Coastal Waters
Monitoring Station (Figure 7.2)	6	3	1
% Time with Normal Wind Speed > 14 m/s (Beaufort Force 7 – High Wind)	0.480 (equivalent to 2 days per year)	0.892 (equivalent to 3 days per year)	0.892 (equivalent to 3 days per year)

Continued…

Parameter	Deep Water	Continental Slope	Coastal Waters
% Time with Normal Wind Speed > 17 m/s (Beaufort Force 8 – Gale)	0.049 (equivalent to <1 day per year)	0.110 (equivalent to <1 day per year)	0.110 (equivalent to <1 day per year)
Maximum Normal Wind Speed (m/s)	21	24	24

Complete.

Table 7.7 Predicted Extreme Marine Wind Conditions (in m/s) (Ref. 7.6)[3]

Extreme Wind Duration	**Deep Water** **Monitoring Station 6 (Figure 7.2)**					**Continental Slope** **Monitoring Station 3 (Figure 7.2)**				
Return Period (years)	***1***	***5***	***10***	***50***	***100***	***1***	***5***	***10***	***50***	***100***
1 hour	15.26	16.53	17.04	18.17	18.63	15.99	17.30	17.83	18.99	19.47
10 minutes	16.03	17.36	17.90	19.08	19.57	16.79	18.17	18.72	19.94	20.44
1 minute	18.99	20.57	21.20	22.61	23.18	19.90	21.52	22.18	23.62	24.22
10 seconds	21.87	23.69	24.42	26.04	26.70	22.92	24.79	25.55	27.21	27.90
3 seconds	23.03	24.95	25.72	27.42	28.12	24.13	26.11	26.90	28.66	29.38

[3] Extreme wind predictions were not made for coastal waters.

Figure 7.7 Seasonal Patterns in Offshore Winds, Ref. 7.6

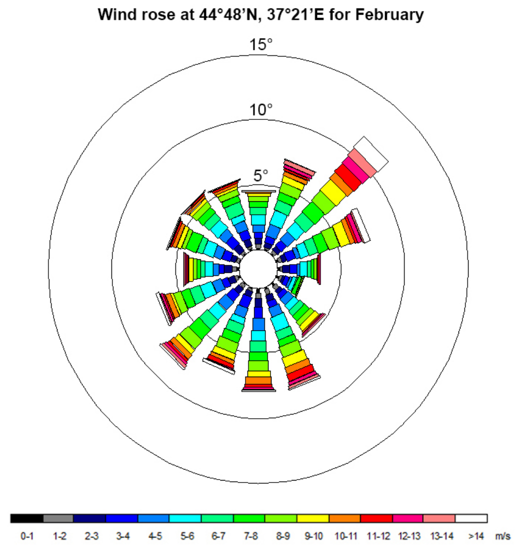

a) Coastal Mooring Station (1) - Winter

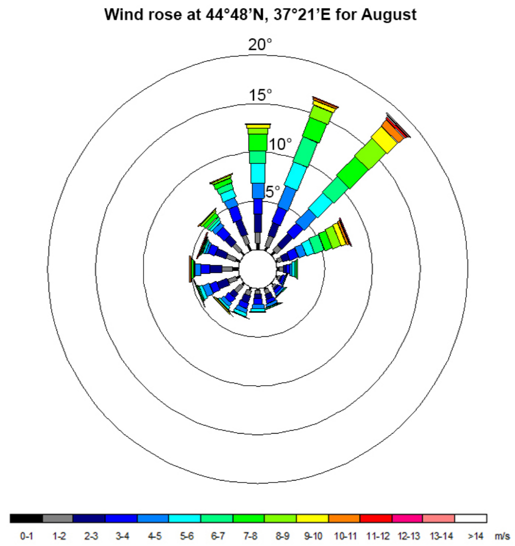

b) Coastal Mooring Station (1) - Summer

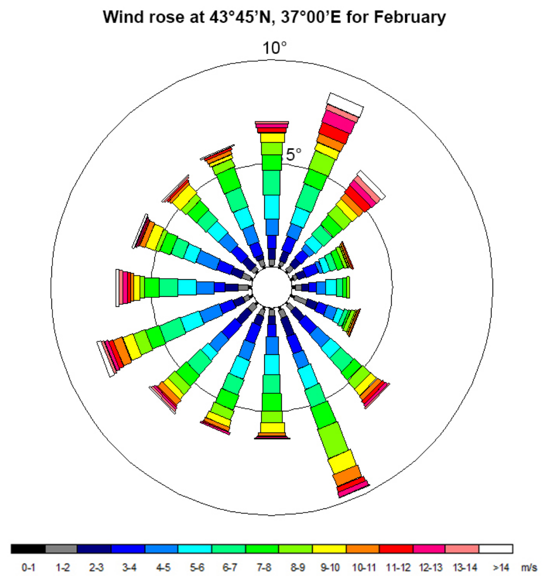

c) Deep Water Mooring Station (6) - Winter

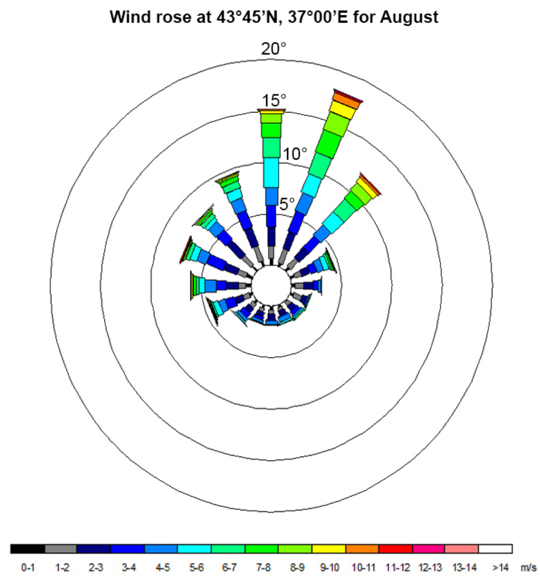

d) Deep Water Mooring Station (6) – Summer

Note: Mooring stations are shown on Figure 7.2

7.4.2 Electromagnetic Fields

Electric and magnetic fields (EMF) are invisible lines of force produced by electrical devices, such as power lines and electrical equipment. Electric fields are produced by voltage and increase in strength as the voltage increases. Magnetic fields result from the flow of electric current and increase in strength as the current increases (Ref. 7.10).

Table 7.8 presents the results of the electric and magnetic field survey compared against both ICNIRP and Russian recommended exposure limits (Ref. 7.11 and 7.13, respectively). The results of the electromagnetic survey indicate that the background electric and magnetic field measurements recorded were within both the ICNIRP and Russian peak exposure limits for the prevention of adverse indirect effects for more than 90% of exposed individuals of the general public (Ref. 7.1).

Table 7.8 Electric and Magnetic Field Intensity Measurements, at 50 Hz

Limits		**Intensity of Electric Field, E (kV/m)**	**Magnetic Flux Density, B (μT)**
ICNIRP peak exposure limit (Ref. 7.11)		5	200
Russian Standard maximum permissible limits (for non-residential areas) (Ref. 7.13)		5	20
ID no.	*Location*	-	-
1	Close to the residential territory (Varvarovka)	0.01	0.00
2	Close to the Greater Utrish – Varvarovka road	0.02	0.01
3	Close to the Greater Utrish – Varvarovka road	0.03	0.00
4	Under 150 kV power line	0.21	0.05
5	Under 150 kV power line	0.15	0.02

7.4.3 Radiation

Background radiation levels associated with the Terrestrial Survey Area were assessed during surveys carried out in 2010, 2011 and 2013 (Ref. 7.1, 7.7).

7.4.3.1 Gamma Radiation Levels

Results of the surveys across the Terrestrial Survey Area recorded the following background gamma radiation levels:

- 2010 survey: background gamma radiation levels ranged from 0.10 to 0.15 microSieverts per hour (μSv/h), with an average of 0.11 μSv/h;
- 2011 survey: background gamma radiation levels ranged from 0.04 to 0.15 μSv/h, with an average of 0.09 μSv/h; and
- 2013 survey: background gamma radiation levels ranged from 0.08 to 0.15 μSv/h, with an average of 0.1 μSv/h.

All measurements taken were assessed to be normal for gamma background levels, and did not exceed the Russian limits for anomalous levels (defined as readings of greater than twice the average background gamma radiation levels or 0.3 µSv/h) (Ref. 7.14).

7.4.3.2 Equivalent Dose of Gamma Radiation

The average equivalent dose[4] of gamma radiation levels in the area were calculated to range from 0.09 to 0.13 µSv/h across the Terrestrial Survey Area, as follows:

- 2010 survey: calculated equivalent dose of gamma radiation ranged from 0.08 to 0.15 µSv/h;
- 2011 survey: calculated equivalent dose of gamma radiation ranged from 0.06 to 0.14 µSv/h; and
- 2013 survey: calculated equivalent dose of gamma radiation ranged from 0.07 to 0.13 µSv/h, with an average of 0.1 µSv/h.

These levels were within acceptable background levels, and met the requirements of the Russian guidelines for assessing radiation safety (Ref. 7.14).

7.4.3.3 Radioactive Isotopes

Samples of soils and stream bed sediments were analysed using gamma spectroscopy methods to assess the levels of radioactive isotopes including: Radium-226 (^{226}Ra), Thorium-232 (^{232}Th), Potassium-40 (^{40}K), Caesium-137 (^{137}Cs) and Strontium-90 (^{90}Sr).

Elevated levels of ^{137}Cs in the environment are associated with nuclear testing in the atmosphere (during the last century) and emissions from nuclear accidents at nuclear power facilities. The behaviour of the ^{137}Cs isotope in the soil is controlled largely by the processes of particle absorption, migration of isotope carrying particles and erosion processes.

In general, ^{137}Cs levels measured in the soils within the Terrestrial Survey Area were predominantly within the range expected for background soil levels (Ref. 7.1):

- Of the 42 samples taken, the measured specific activity of isotope ^{137}Cs recorded in 26 samples was below detection limits of five Becquerels per kilogram (Bq/kg). In a further 14 samples the measured specific activity of isotope ^{137}Cs recorded was within anticipated background levels associated with radiation falling to the ground, i.e. within 5 to 15 Bq/kg (Ref. 7.1);
- Two samples recorded isotope ^{137}Cs activity above background levels (15 Bq/kg). The maximum recorded ^{137}Cs activity value of 22 Bq/kg was recorded during the 2010 survey. However, these values were still within acceptable limits (Ref. 7.14) and

---

[4] The equivalent dose (or equivalent absorbed radiation dose) is a computed average measure of the radiation absorbed by a fixed mass of biological tissue that attempts to account for the different biological damage potential of different types of ionizing radiation.

- Isotope activity levels for ^{90}Sr were measured in 20 soil samples taken from the 2010 survey only (Ref. 7.1). The activity levels measured for isotope ^{90}Sr ranged from 0 to 47 Bq/kg (with an average measured value of 24 Bq/kg recorded) within the Terrestrial Survey Area and were within normal background levels.

Isotope activity levels recorded for natural radionuclides ^{226}Ra and ^{232}Th and ^{40}K in soils within the Terrestrial Survey Area were found to be within normal background levels (Ref. 7.15):

- Isotope activity levels for ^{226}Ra were typically well below normal natural background levels of 20 to 50 Bq/kg. Measurements of isotope activity levels for all 42 samples were at or below natural background levels, with measurements ranging from 8 to 27 Bq/kg for ^{226}Ra;
- Isotope activity levels for ^{232}Th measured in the soils ranged from 9 to 32 Bq/kg and were within normal natural background levels for ^{232}Th (20 to 50 Bq/kg);
- Isotope activity levels for ^{40}K measured in the soils ranged from 88 to 513 Bq/kg and were within or below normal natural background levels for ^{40}K (200 to 800 Bq/kg); and
- Effective specific NRN activity in the soils ranged from 32 to 114 Bq/kg. These values are well below the Russian threshold intervention level of 370 Bq/kg permitted for building materials at public buildings and facilities (Ref. 7.15).

7.4.3.4 Summary

Results of the radiation survey indicate background radiation levels within the Terrestrial Survey Area meet the requirements of the Russian Standards on radiation protection. Radiation levels measured in the soils do not pose a risk to human health in terms of radiation exposure.

7.4.4 Oceanography

7.4.4.1 Bathymetry

The bathymetry of the Russian Sector of the Black Sea is shown in Figure 7.9.

The Black Sea is a semi-enclosed sea connected to the shallow (10 to 20 m deep) Azov Sea through the Kerch Straits and to the Mediterranean Sea through the Bosporus Straits, the Marmara Sea and the Dardanelles Straits. The flat abyssal plain (at a depth of 2,000 m) rises to the continental shelves. The north western shelf, with a mean depth 50 m, has a shelf break at about 100 m depth between the Crimean peninsula and Varna in the south.

The Russian continental shelf is gently inclined towards the west and extends to a water depth of 100 m (Ref. 7.1). Beyond 100 m depth, the continental slope starts dipping steeply to the west; it is characterised by patterns of ridges and canyons. The slope angle decreases towards the base (at 1,900 m depth) and typically varies from 27° at the top to 5° at the bottom.

The oceanography of the Black Sea has been assessed based on published datasets (Refs. 7.3, 7.35, 7.36, 7.37) and using Project survey data (Refs. 7.1, 7.4, 7.6).

7.4.4.2 Sea Level Variation

The Black Sea is practically non-tidal with a maximum range of no more than 0.1 m. Changes in water levels in the Black Sea are thus primarily caused by one or more of the following factors:

- Inter-annual fluctuations in the sea level;
- Seasonal fluctuation as a result of seasonal atmospheric dynamics (e.g. temperature, wind, rainfall and storms);
- River flows;
- Spatial changes in the atmospheric pressure; and
- Natural temporal and spatial variability in dynamics of the water column.

Long-term data collected (for approximately the last 90 years) along the Caucasian coast shows a slight yearly increase in mean sea level of about 0.23 cm per year (Figure 7.8), while the water level of the Black Sea is subject to seasonal fluctuations of about 20 cm (Figure 7.10). Long-term average seal level data is presented in Table 7.9.

Figure 7.8 Changes in Sea Level in the Black Sea from 1917 to 2005 (Ref. 7.1)

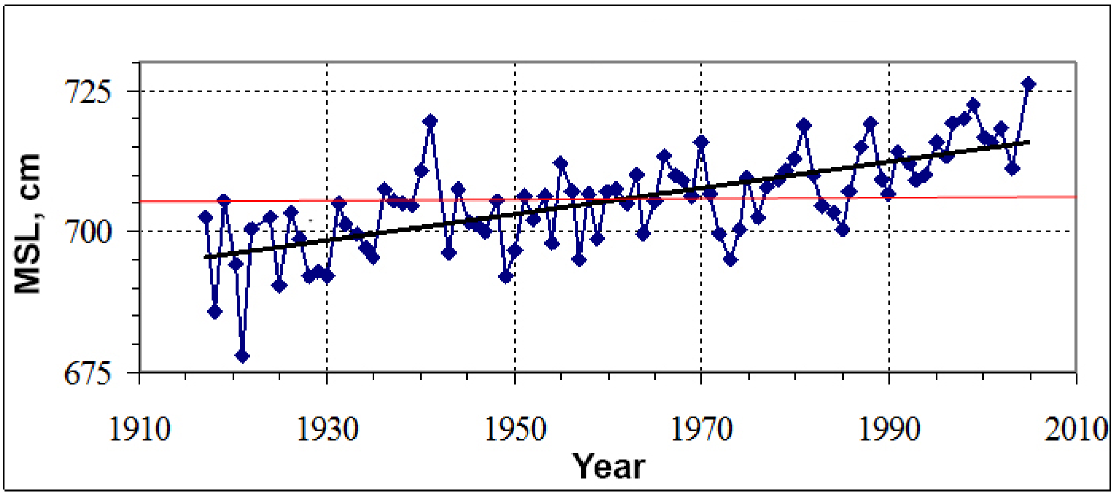

LEGEND

Russian Sector of South Stream Offshore Pipeline

- Proposed offshore pipelines
- Exclusive Economic Zone boundary
- Isobaths
- Regional Boundaries
- Country Boundaries

Projection: Lambert Conformal Conic

Purpose of Issue: For Information

Client: South Stream Offshore Pipeline – Stream Energising Europe

Project Title: SOUTH STREAM OFFSHORE PIPELINE

Drawing Title: BATHYMETRY OF RUSSIAN SECTOR OF BLACK SEA

Drawn	Checked	Approved	Date
AH	IS	IS	21 Mar 2014

URS Internal Project No.	Scale @ A3
46369082	1:2,250,000

URS Infrastructure & Environment UK Limited
Scott House
Alençon Link, Basingstoke
Hampshire, RG21 7PP
Telephone (01256) 310200
Fax (01256) 310201
www.ursglobal.com

Drawing Number: Figure 7.9

Rev

Plot Date: 21 Mar 2014
File Name:I:\5004 - Information Systems\46369082_South_Stream\MXDs\Report Maps - Russia\Russian ESIA v2\Chapter 7 Geology\Figure 7-8 Bathymetry of Russian Sector of Black Sea.mxd

This page has been left intentionally blank

Figure 7.10 Deviation in Average Sea Level from 1917 to 2005 (Ref. 7.1)

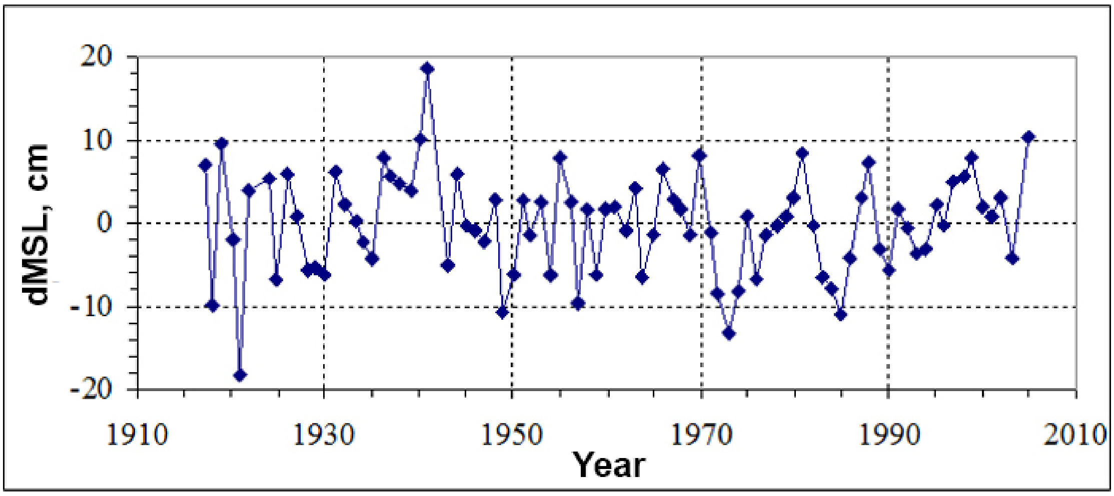

Table 7.9 Long-Term Average Sea Levels in the Black Sea at Sochi (Ref. 7.1)

Sea level	Average annual sea level	Maximum annual sea level		Minimum annual sea level	
	m+BS	m+BS	year	m+BS	year
Annual maximum	-0.01	+0.17	1953	-0.23	1949
Average annual	-0.34	-0.22	1981	-0.48	1949
Annual minimum	-0.62	-0.46	1955	-0.88	1928

In addition to the long-term dataset, sea levels were measured in the Marine Survey Area during the 2011 to 2012 metocean surveys (Ref. 7.4); the results are presented in Table 7.10.

Table 7.10 Measured Range of Sea Level Values in Marine Survey Area (Ref. 7.4)

Monitoring Station	Water Depth (m)	Observed Maximum (m+BS)	Observed Minimum (m+BS)
1	25	0.13	-0.14
1b	73	0.83	-0.26
2	381	0.22	-0.19
5	1790	0.20	-0.18

Much more significant sea level variations have, however, occurred during the Quaternary Period, which are associated with global climatic variations, ice sheet collapse and the regional tectonic events that led to the opening of the Bosphorus Strait. There has been considerable scientific debate about the timing and process of the transition from the Black Sea lake at the end of the last ice age to its present mode. Over the past 30,000 years sea levels have varied due to periods of low river input during cold periods and major river inflow during periods of ice melt (Ref. 7.36). The timing of the most recent reconnection of the Black Sea with the Mediterranean is estimated to be 9,000 years BP[5] (Ref. 7.36). This caused a transition from freshwater to marine conditions and resulted in the inundation of coastal landscapes. These transgressions caused wide spread shoreline regression in some locations and led to significant wave based shoreline erosion. The refilling of the Black Sea once the reconnection with the Mediterranean was established is estimated to have occurred over about 100 years but the transition from freshwater to marine conditions is estimated to have taken about 900 years beginning with the deepest water (Ref. 7.36). The transition was completed by about 7,700 years BP at mid water depths and by about 7,200 years BP on the shelves (Ref. 7.36).

Inundation of prehistoric habitations and reworking of cultural materials within the sediments is discussed further in **Chapter 16 Cultural Heritage**.

7.4.4.3 Wave Climate

The wind regime in the Russian part of the Black Sea is defined by the air mass transfer with a south-southwest to north-northeast direction, which is typical for the moderate zone of the Northern hemisphere. The winter is characterized by squally northerly, north-eastern and easterly winds, as a result of the increased Mediterranean cyclone activity and the existing anticyclone activity above Eastern Europe.

The prevailing winds in the Russian part of Black Sea are from the southwest. The highest wind speeds usually are registered during November to March when the hurricane north-eastern wind (bora) winds may bring gusty winds and cold temperatures to the coastline. The Russian coastline experiences approximately 15 to 20 storm days each winter, with wind speeds reaching up to 20 m/s approximately once a year.

The wave climate adjacent to the Russian coastline of the Black Sea is heavily influenced by the shallow continental shelf. The limited fetch lengths result in smaller primarily wind driven waves. The relatively shallow continental slope affects entering waves by transforming their 2-dimensional (2D) spectrum due to bottom friction and wave breaking.

Estimation of wave characteristics based on archival data held by the Institute of Ocean Sciences has been undertaken (Ref. 7.1, 7.2). A typical yearly maximum wave height in the Marine Study Area has been estimated as 2.9 m, with a 1 in 100 year return period wave reaching 4.8 m. A summary of the wave characteristics based on archival data (Ref. 7.1, 7.2) is presented in Table 7.11 and Table 7.12.

---

[5] Before Present

Table 7.11 Typical Maximum Wave Geometry (Ref. 7.1, 7.2)

Return Period (years)	1	5	10	25	50	100
Wave Height, Hs (m)	2.9	3.6	3.9	4.3	4.6	4.8
Wave Length (m)	105	129	139	153	164	174
Wave Period (s)	8.2	9.1	9.5	9.9	10.2	10.6

Table 7.12 Correlation of Wave Heights and Directions (Ref. 7.1)

Wave Height (m)	N	NE	E	SE	S	SW	W	NW	Frequency (%)
0-1	4.7	9.0	4.2	2.7	2.8	7.5	11.1	3.7	45.6
1-2	3.4	7.2	2.9	1.5	2.1	6.5	8.1	3.1	34.9
2-3	1.1	3.1	0.9	0.3	0.7	3.1	3.0	1.3	13.5
3-4	0.2	1.1	0.2	0.02	0.2	1.1	0.9	0.4	4.1
4-5	0.03	0.4	0.07	-	0.03	0.4	0.3	0.08	1.3
5-6	+	0.13	0.02	-	+	0.13	0.11	0.02	0.4
6-7	-	0.04	+	-	+	0.04	0.03	+	0.12
>7	-	0.01	-	-	+	0.01	+	-	0.03
Frequency of Wave Direction	9.5	21.0	8.3	4.5	5.8	18.8	23.5	8.6	100
Regression	1.2	1.4	1.2	1.0	1.2	1.5	1.3	1.3	

Wave measurements were undertaken during the 2011 to 2013 metocean survey (Ref. 7.4); the station locations are shown on Figure 7.2. The results were correlated with a long-term satellite data (26 year dataset) (Ref. 7.6). The significant wave height[6] predictions are presented in Table 7.13. The average significant wave height increases with distance from the shore to about 1 m offshore. Near the coast, waves are predominantly from the west and southwest. Offshore, there is additionally a north-northeast wave component due to the increased fetch.

[6] Significant wave height is the average wave height of the 1/3 highest waves.

Table 7.13 Summary of Estimated Wave Heights (Ref. 7.6)

Location	Deep Water	Continental Shelf	Nearshore Waters
Water Depth	>150 m	50 m	23 m
Significant Wave Height (50% Probability)	1 m	0.5 m	0.5 m
Significant Wave Height (90% Probability)	2 m	1.5 m	1.5 m
Maximum Significant Wave Height	8 m	6.75 m	6.25 m

7.4.4.4 Storm Surges

Short-term sea level variations are also associated with varying meteorological conditions and can result in localised sea level surges of up to 1 m. However, storm surge levels along the Caucasus coast are typically less than 40 cm.

Surge predictions based on published data (Ref. 7.1) are presented in Table 7.14.

Table 7.14 Surge Level Fluctuations (m) Compared with Average Black Sea Level (Ref. 7.1)

Surge Level	Maximum (positive surge)				Minimum (negative surge)			
Return Period (years)	10	25	50	100	10	25	50	100
Anapa	0.52	0.58	0.62	0.67	-0.46	-0.51	-0.54	-0.58

The frequency of storm surges in the Black Sea is lower than that in other regions of the world's oceans (Ref. 7.38). The gently sloping continental slope open to winds and waves is subject to storm surges. It is estimated that typical storm durations vary between 56 and 151 hours with an average duration of 95 hours (Ref. 7.39). Extreme storms have quite a short growth phase with an average duration of 61 hours. Hence, the typical storm pattern is characterised with fast growth, a rather durable energetic development phase and relatively prolonged decay.

7.4.4.5 Currents

The Main Black Sea Current (MBSC) affects the whole basin in one cyclonic (counter clockwise in the northern hemisphere) circular motion. A prominent feature in the upper layer circulation in the Black Sea is the so-called "Rim Current", a cyclonic current that follows the abrupt continental slope and encompasses a cyclonic cell that occupies the basin. A diagram of the MBSC is shown in Figure 7.11.

The MBSC is directed counter-clockwise forming the two rings over the basin apron in the western and eastern parts of the Sea (referred to as the 'Knipovich spectacles' after the name of one of the Russian oceanographers who described the phenomenon). The MBSC is associated with a series of cyclonic and anti-cyclonic eddies in the cyclonic meanders. Outside the Rim Current, numerous quasi-permanent coastal eddies are formed as a result of 'wind curl' mechanisms and upwelling around the coastal apron (Ref. 7.36).

The MBSC is a 50 to 80 km wide flow within the upper 300 m of the water column and remains present during the entire year. The current is more distinct during summer and winter. On average, the current passes some 15 to 50 km from the Russian coast.

Figure 7.11 Main Black Sea Current (Ref. 7.1)

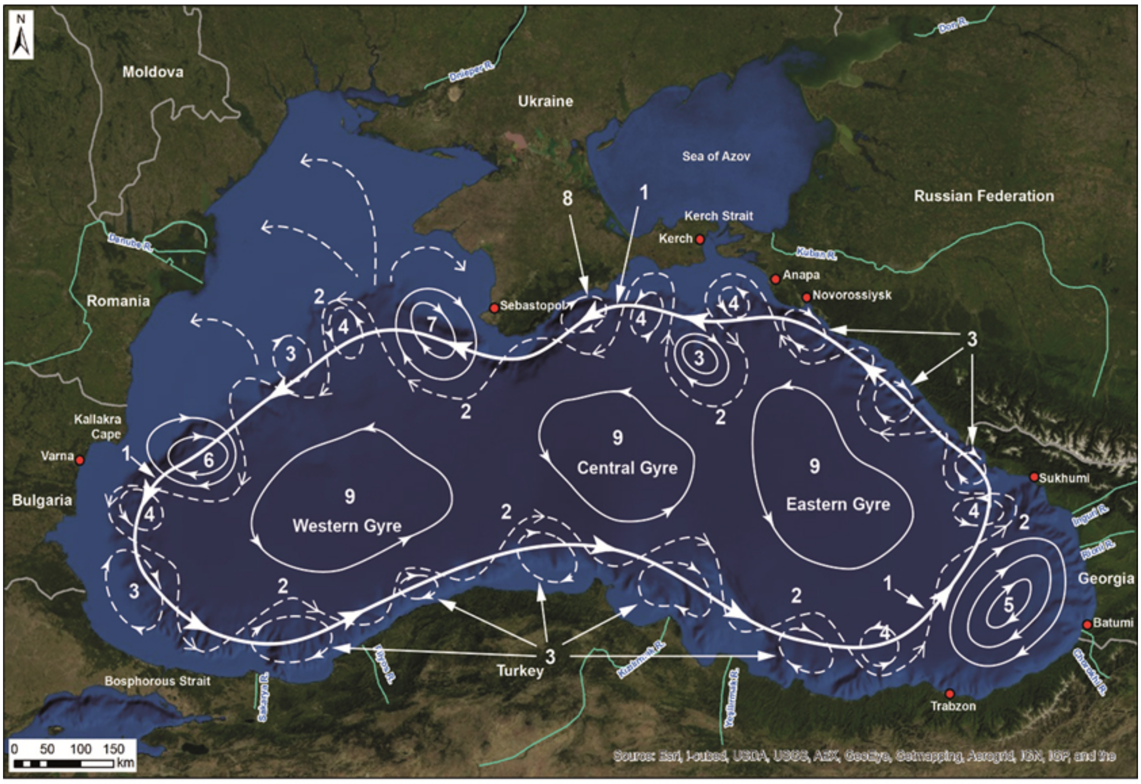

Key:
1: mean position of the cyclonic Rim Current jet current
2: Rim Current meanders
3: anticyclonic coastal eddies
4: cyclonic eddies
5: Batumi anticyclonic eddy
6: Kaliakra anticyclonic eddy
7: Sebastopol anticyclonic eddy
8: Crimea anticyclonic eddy
9: quasi-stationary cyclonic gyres

As shown in Figure 7.11, coastal currents in the Caucasus region are characterised by two diametrically opposite directions of water movement: north-western and south-eastern. The north-western flow direction is dominant over the south-eastern flow (approximate ratio is 85% and 15% respectively). The maximum velocity of the north-western current is between 0.3 to

0.5 m/s and between 0.5 to 0.8 m/s in the summer and winter respectively; in comparison, the maximum velocity of the south-eastern current is 30 to 50% less (Ref. 7.1).

Current speeds in the core of the MBSC typically flow at 0.3 to 0.6 m/s depending on synoptic, seasonal and inter-annual variability.

Based on the results of current data measurements in 1998-1999, the values of extreme current speeds on the shelf, continental slope and abyssal plain were estimated (Ref. 7.1). Current speeds are inversely proportionate to depth. The 1-year return period nearshore current velocity is approximately 0.7 m/s. The maximum velocity (1:100 years return period) is approximately 1 m/s. On the continental slope (depth 100 to 1700 m), the current velocity varies from 0.1 m/s (1:1 year return period) to 0.2 m/s (1:100 years). A similar pattern is observed in the current speeds on the abyssal plain.

Further surveys of marine currents have been undertaken from 2011 to 2012 (Ref. 7.6) with currents measured close to the pipeline route; the station locations are shown in Figure 7.2. This included monitoring of differences in currents with depth. The current measurements have been combined with hindcasting from long-term datasets to estimate potential current speeds (Ref. 7.6). Surface and nearbed current data for the Marine Survey Area are summarised in Table 7.15 and Table 7.16. Yearly variation in nearbed currents is estimated to be about 30% in the nearshore section and 20% in the offshore section of the Marine Study Area (Ref. 7.6). Only minor variations in surface currents, predominantly due to the wind conditions, are anticipated.

Table 7.15 Summary of Surface Currents (Ref. 7.6)

Station	Water Depth (m)	Observed Maximum (m/s)	Return Period (years)				
			1	5	10	50	100
1	25	0.64	0.69	0.76	0.81	0.91	0.95
1b	73	1.38	1.54	1.70	1.77	1.92	1.98
2	381	1.35	1.72	1.91	1.99	2.18	2.26
3	509	1.38	1.55	1.71	1.78	1.94	2.00

Table 7.16 Summary of Nearbed Currents (Ref. 7.6)

Station	Water Depth (m)	Observed Maximum (m/s)	Return Period (years)				
			1	5	10	50	100
1	25	0.40	0.49	0.55	0.58	0.63	0.66
2	381	0.51	0.18	0.20	0.22	0.24	0.26

Continued…

Station	Water Depth (m)	Observed Maximum (m/s)	Return Period (years)				
			1	5	10	50	100
3	509	0.13	0.13	0.15	0.16	0.18	0.19
4	1750	0.06	0.06	0.07	0.07	0.07	0.07
5	1790	0.09	0.10	0.11	0.12	0.13	0.13
6	2088	0.11	0.12	0.13	0.13	0.14	0.15
7	2129	0.06	0.07	0.07	0.07	0.07	0.08

Complete.

7.4.4.6 Ice Period

The northern part of the Black Sea and the Kerch Strait are normally covered by ice during winter (Table 7.17). Shore ice occurs regularly along the eastern and western shores of the strait. The ice normally occurs between December and April.

The ice period of the Anapa-Novorossiysk region is unique. Ice in the form of "shuga" (slush ice) is short-term, forming nearly every year, but it is rare for the sea to freeze over completely. Novorossiysk Bay froze completely twice in the past century: during the winters of 1924-25 and 1933-34. The width of the shore ice exceeded 200 m and the ice was up to 15 m thick.

Table 7.17 Summary of the Ice Period in Kerch Strait from 1991–2005 (Ref. 7.1)

	Winter type	Early	Late
First appearance of early types of ice	mild	12 Dec	24 Jan
	moderate	10 Dec	11 Feb
Maximum distribution to the South	mild	18 Jan	2 Feb
	moderate	19 Dec	28 Mar
Last full clearance	mild	26 Jan	6 Mar
	moderate	1 Mar	5 Apr
Number of clearances a year	mild	1	3
	moderate	3	2

Icing of vessels, hydro-engineering structures, and the near shore area occurs every year. And in this context, the most favourable period for engineering work is from May to October. The key shelter ports are Novorossiysk, Anapa and Gelendzhik. Novorossiysk Port and the adjacent Tsemes Bay are normally ice-free in winter (Ref. 7.40).

Ice scour is caused by erosion of the sea bed where floating sea ice comes into contact with the sea bed. This is not considered to be a significant risk for the Project as the pipelines exit the microtunnels at a water depth 23 m depth and because sea ice is an infrequent occurrence in the Study Area.

7.4.4.7 Water Temperature

The Black Sea exhibits a characteristically layered pattern in the vertical distribution of water temperature (Ref. 7.1, 7.2, 7.3). There are three principal layers: the surface water layer, the low temperature layer and the deep layer (Figure 7.12). This thermal layering is influenced by the salinity stratification described below.

The surface water layer is typically 20 to 40 m deep. The temperature of the surface waters varies seasonally by around 16°C, ranging from about 9°C in February to about 25°C in August. Considerable short term fluctuations (from several hours to several days) are observed against the background of seasonal changes in temperature. In autumn, winter and spring, these fluctuations are only 1 to 2 °C. In summer, short-term changes of water temperature can reach 9 °C. These fluctuations are mainly due to interactions of diurnal (daily) solar radiation and local wind field effects.

Below the surface waters there is a low temperature layer. In this layer, water temperatures reach their minimum values of about 6 to 7°C. The low temperature layer typically extends from the base of the surface water layer at on average 35 m to about 110 to 120 m deep. The thickness of the low temperature layer varies annually in response to the antecedent weather conditions over the preceding winter.

The temperature of the low temperature layer varies seasonally but there is an observable lag of several months compared with the surface layer. Temperatures at the top and the core of the low temperature layer reach their minimums in March and May, respectively, compared with the minimum of the surface layer in February. Similarly, temperatures at the top and the core of the low temperature layer reach their maximums in October and February, respectively, compared with the August maximum in the surface layer.

Below the low temperature zone (>100 to 120 m), water temperatures gradually rise with depth to a nearly constant 8.9°C at 400 m depth. Minimal seasonal variation in water temperatures is observed at depth. The stratification of the Black Sea limits active vertical mixing of surface and deep waters, thus confining seasonal variations to the upper layers.

Figure 7.12 Long-term Average Annual Profiles of Temperature with Depth (Ref. 7.1)

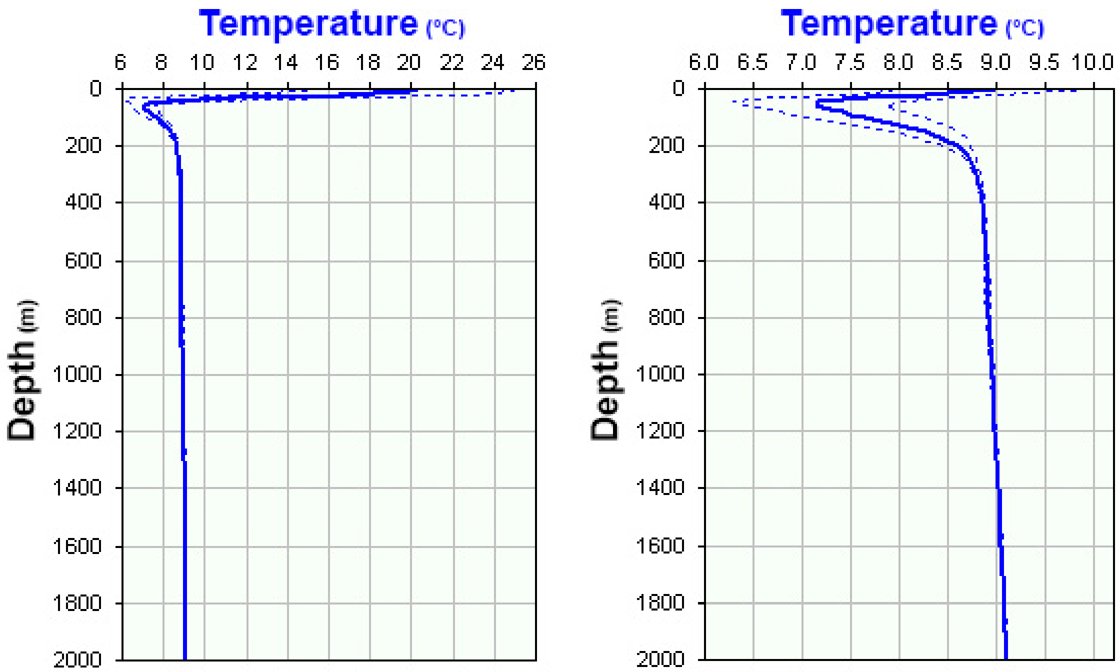

a) Summer Profile

b) Winter Profile

Note: Average square deviations are marked by dotted lines.

The 2011 survey data showed a similar pattern to the literature dataset (Ref. 7.1). Water temperatures varied with depth. In the surface layer, water temperature also decreased with distance from the shore (Figure 7.13). Water temperature in the surface waters ranged from 8.70 to 9.89°C. A thermocline was identified at around 40 to 45 m depth. Water at 100 m and 500 m depth was on average 8.43°C and 8.88°C respectively.

Measured seabed water temperatures ranged from 6.35 to 26.34°C in shallow waters (<20 m) (Ref. 7.6). The seasonal range in seabed water temperature decreases as water depth increases. By water depths of 100 m, the seasonal variation is less than 2°C. There is negligible seasonal variation in seabed water temperatures in water depths over 200 m. Seabed water temperatures in deep water areas are around 9°C (Ref. 7.6).

Figure 7.13 Sea Water Temperatures (°C) in the Surface Waters in April 2011 (Ref. 7.1)

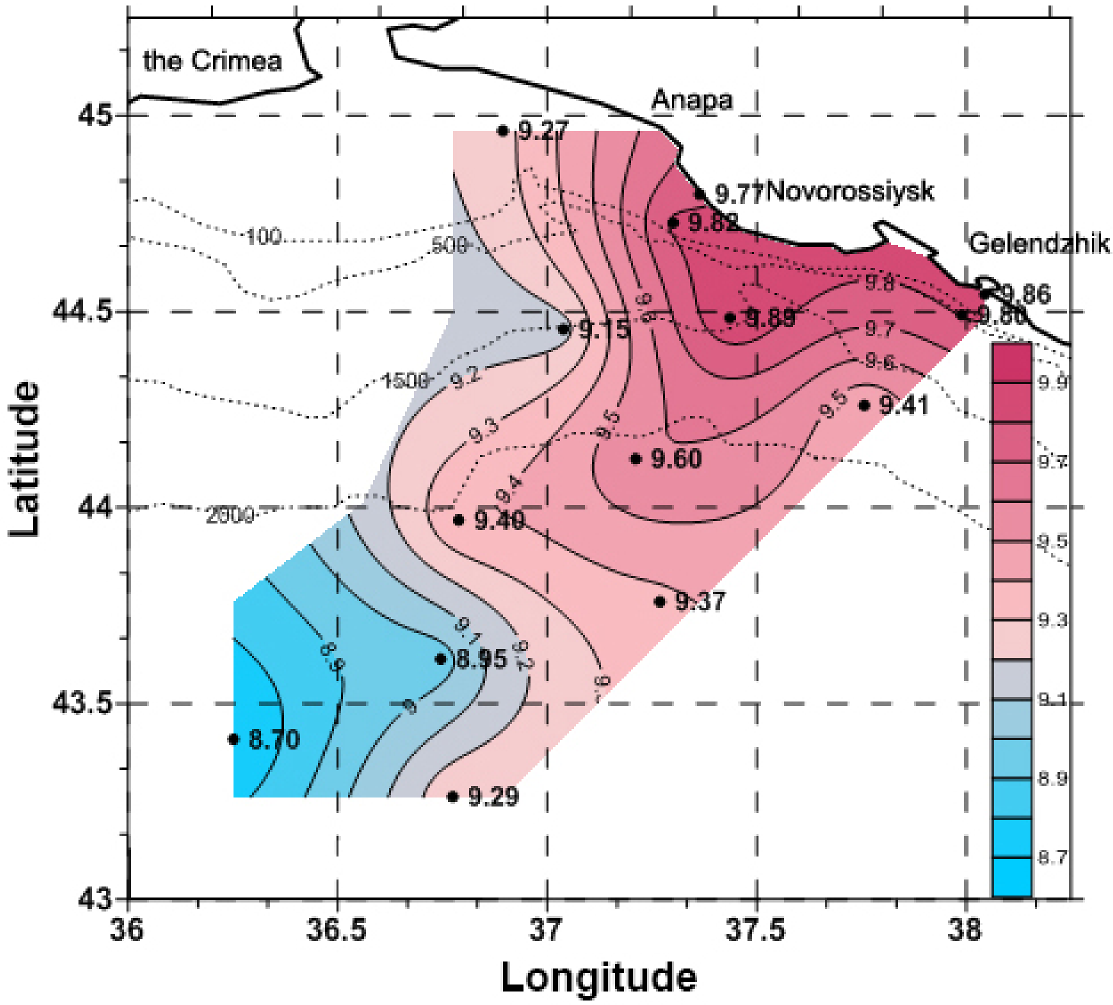

7.4.4.8 Water Salinity

Globally, typical marine salinity is about 35‰. In some inland seas where evaporation exceeds the input of the fresh water, salinity can reach up to 37 to 38‰ (for example, in the eastern part of the Mediterranean Sea) and even 40‰ (in the Red Sea). In comparison, in the Black Sea, salinity is considerably lower at about 22‰ than that of the Mediterranean Sea. This is due to the dominance of fresh water inputs and the limited water exchange with the Mediterranean.

The total volume of river flows and atmospheric precipitation entering the Black Sea exceeds evaporation by more than one third. This forms a surface layer of lower salinity. The deep water is more saline than the surface layer due to the inflow of saline waters into the Black Sea from the Mediterranean through the Bosphorus Strait.

The combination of these factors causes the Black Sea to exhibit strong vertical stratification in salinity. A typical depth profile for salinity based on long-term metocean datasets for the Russian EEZ (Ref. 7.1, 7.2) is shown in Figure 7.14. There is an upper layer of lower salinity water overlying a deep layer of more saline water. The permanent halocline in the Black Sea is located between 120 and 200 m water depth (Ref. 7.1, 7.2, 7.3). Salinity varies in the upper layer varies seasonally.

Figure 7.14 Long-term Average Annual Profiles of Salinity with Depth (Ref. 7.1)

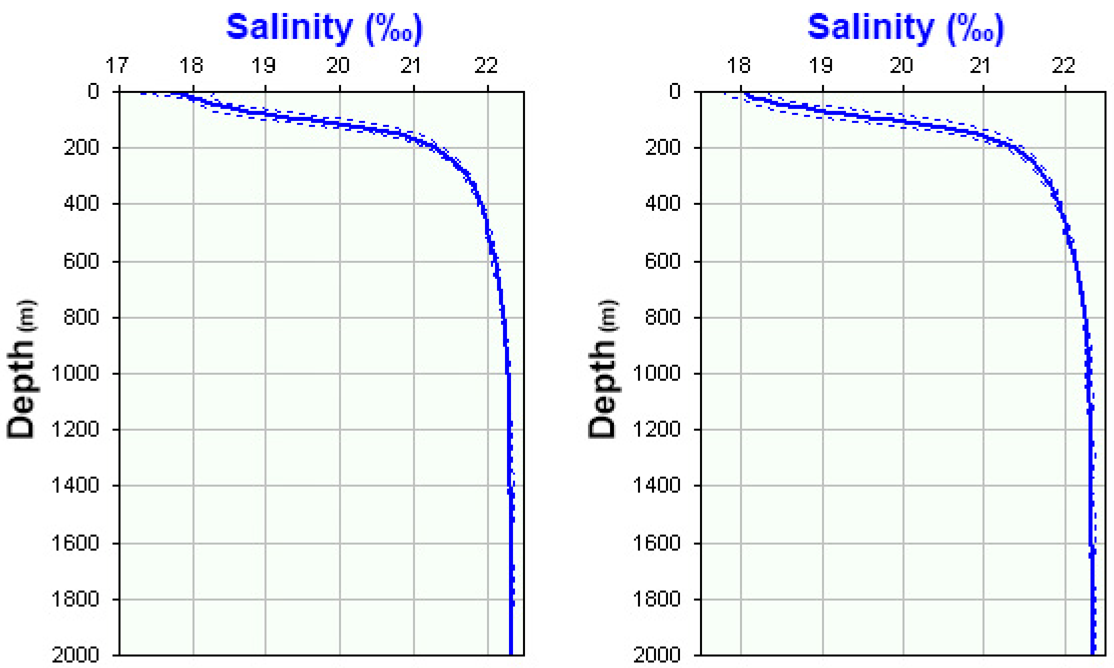

a) Summer Profile

b) Winter Profile

Note: Average square deviations are marked by dotted lines.

Salinity at the sea surface is at a maximum in winter (18.2‰ in December) then reduces to a summer minimum (17.6‰ in August). In the upper layer, water salinity also increases with distance from the shore (Figure 7.15 and Figure 7.16). Salinity varies with depth (Table 7.18). Salinity levels rise rapidly to approximately 21‰ by around 200 m depth. The seasonal pattern in salinity reverses with depth within this zone; from about 25 m downwards salinity is higher in summer than in winter due to the lag time in vertical mixing. By 150 m depth, the salinity minimum is 19.9‰ from December to March and the maximum is 20.6‰ from August to September; the annual range of seasonal salinity change (0.7‰) at this depth is slightly higher that at the sea surface.

Beyond about 200 m depth, salinity levels continue to rise with depth but at a slower rate. Below 500 m, salinity is approximately 22‰ with no significant seasonal variation (Ref. 7.1). Seabed water salinity in the deep water areas is around 22.3 ‰ (Ref. 7.5).

Table 7.18 Measured Salinity with Depth for 2010-2011 (Ref. 7.1)

Depth (m)	Salinity (‰)		
	Minimum	Maximum	Average
Near-Surface	17.16	18.25	17.93
10	17.202	18.250	17.957
25	17.799	18.254	18.059
40-45 (Thermocline)	17.810	18.441	18.139
100	19.355	20.860	20.355
200	21.230	21.578	21.446
500	22.014	22.071	22.044

Figure 7.15 Sea Water Salinity (‰) in the Surface Waters in April 2011 (Ref. 7.1)

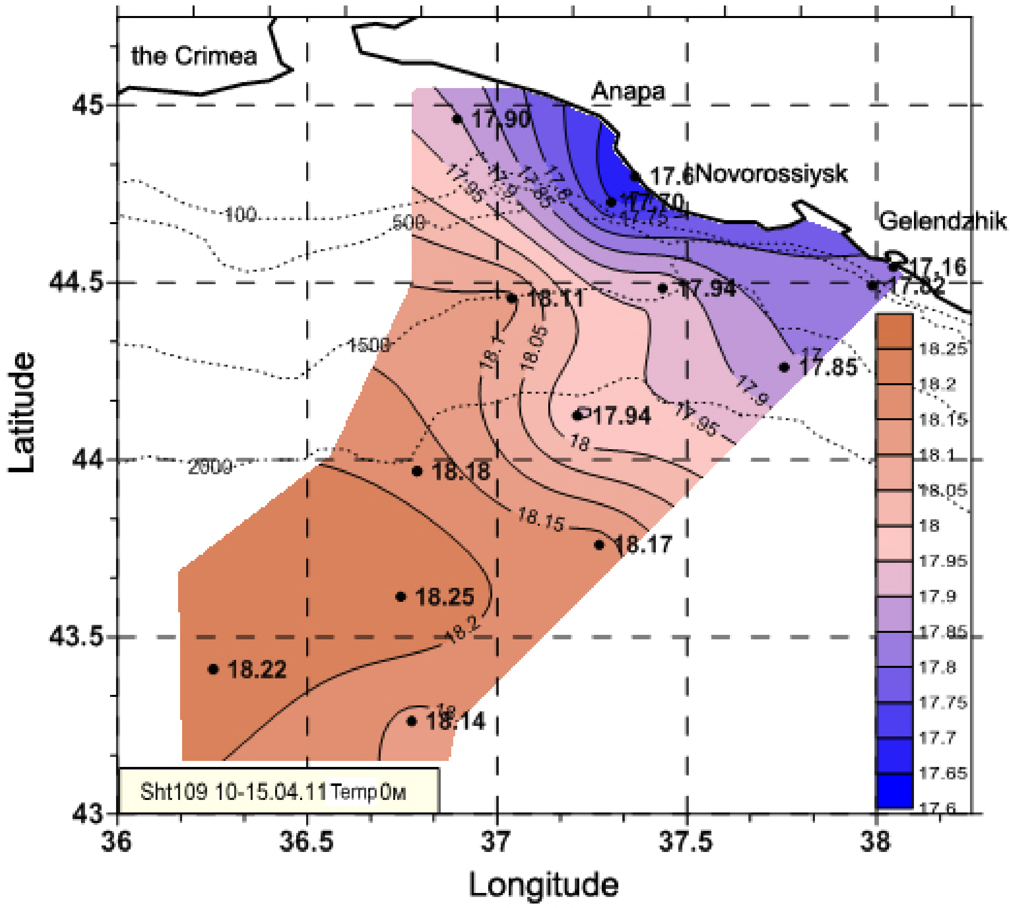

Figure 7.16 Distribution of Sea Water Salinity (‰) with Depth and Distance from Shore in April 2011 (Ref 7.1)

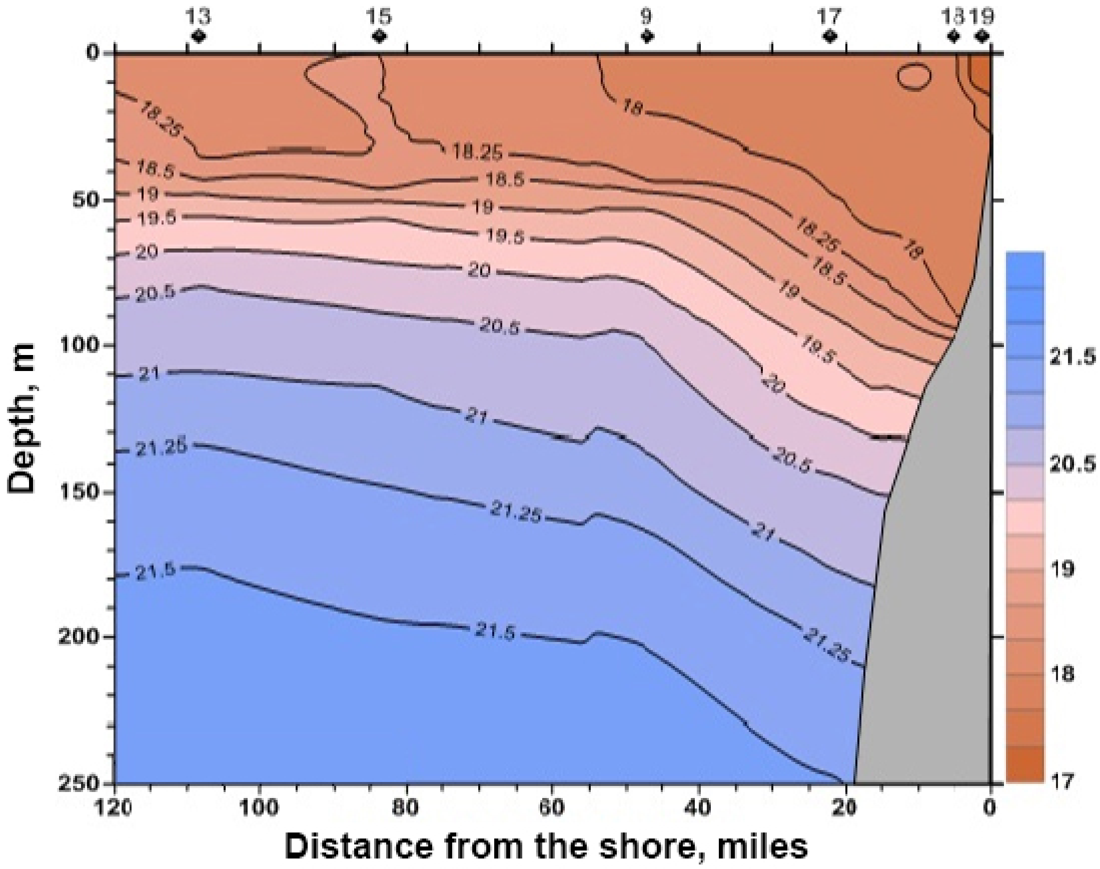

7.4.4.9 Water Density

During the year, water density changes as a function of salinity and temperature.

In the near-surface waters (0 to 10 m), the water density is at a minimum in July and August (10.44 conventional units), when temperatures are highest and salinity is lowest. In comparison, water density is at a maximum in March (14.02 conventional units) (Ref. 7.1, 7.2, 7.3).

Below the surface, density increases rapidly with depth (Figure 7.17) reflecting the increase in salinity and decrease in temperature. The vertical pattern in water density distribution is similar to the salt distribution pattern except that there is an increase in density at around 20 to 60 m relating to the low temperature zone at this depth. The pycnocline is typically higher and more distinct in the central seas as compared with the continental slope.

From 300 to 500 m, density increases slowly with depth. No significant seasonal trends are observed. Below 500 m, density is around 17 conventional units and is relatively constant with depth, mirroring the patterns observed in salinity and temperature.

The 2011 survey data (Ref. 7.1) showed a similar pattern to the literature dataset (Table 7.19). Water density varied with depth. In the upper layer, water density also increased with distance from the shore. As would be expected, the vertical and lateral distribution patterns for density were broadly similar to those for salinity. Density in the surface layer ranged from 13.08 to 14.05 conventional units with an average value of 13.73 conventional units. At 100 m and 500 m, the average density values were 15.75 and 17.02 conventional units respectively.

Figure 7.17 Long-term Average Annual Profiles of Conventional Density with Depth (Ref. 7.1, 7.2)

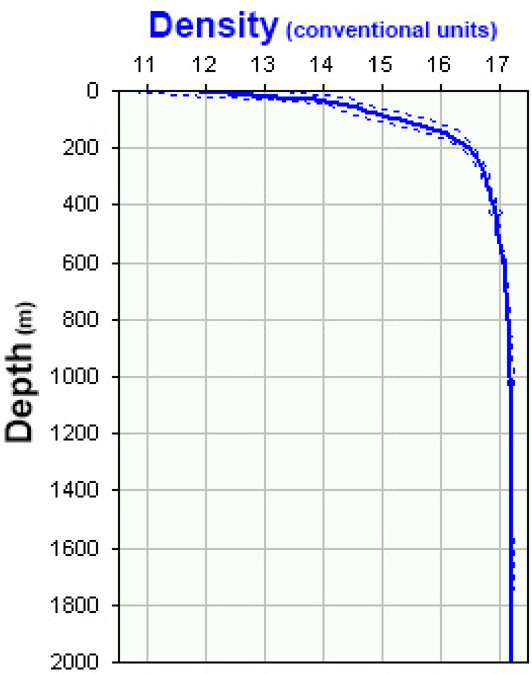

a) Summer Profile

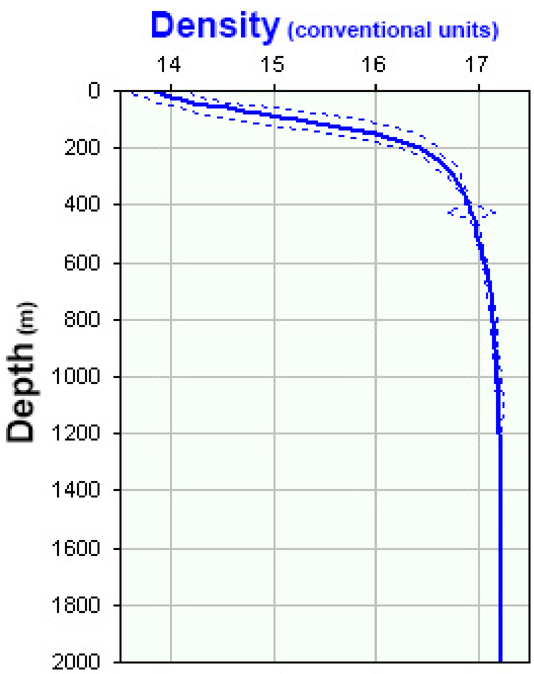

b) Winter Profile

Note: Average square deviations are marked by dotted lines.

The relationship between salinity, temperature and density is key to appreciating the stratification of the Black Sea. This stratification has implications for water quality and for biological activity. Figure 7.18 shows the typical interrelationship.

Table 7.19 Measured Water Density with Depth in 2010-2011 (Ref. 7.1)

Depth (m)	Density (conventional unit)		
	Minimum	Maximum	Average
Near-Surface	13.080	14.050	13.730
10	13.133	14.053	13.766
25	13.599	14.077	13.869
40-45 (Thermocline)	13.609	14.282	13.972
100	14.967	16.136	15.749
200	16.411	16.667	16.570
500	16.992	17.036	17.015

Figure 7.18 Comparison of Distribution Profiles of Temperature, Salinity and Density with Depth (Ref 7.1)

a) Winter Profiles

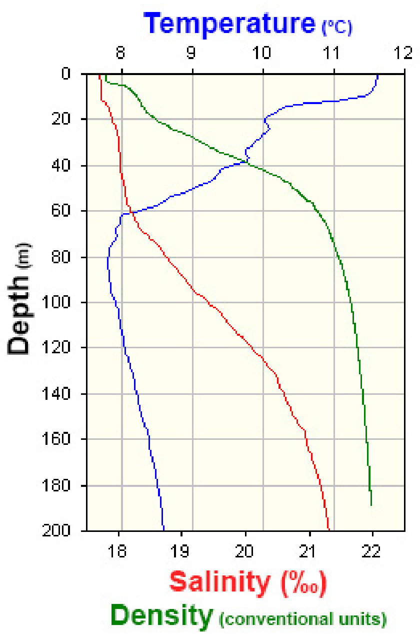

i) Central Black Sea

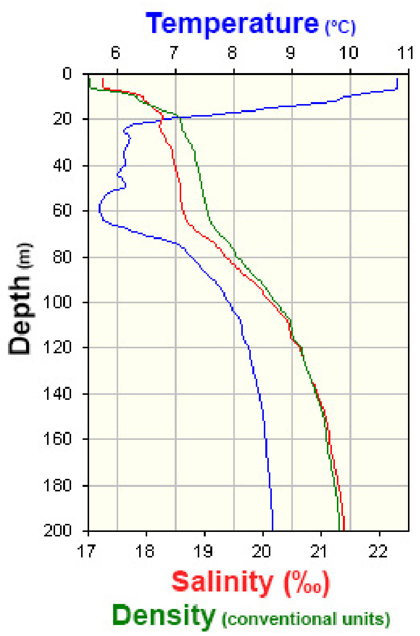

ii) Russian Continental Slope

b) Summer Profiles

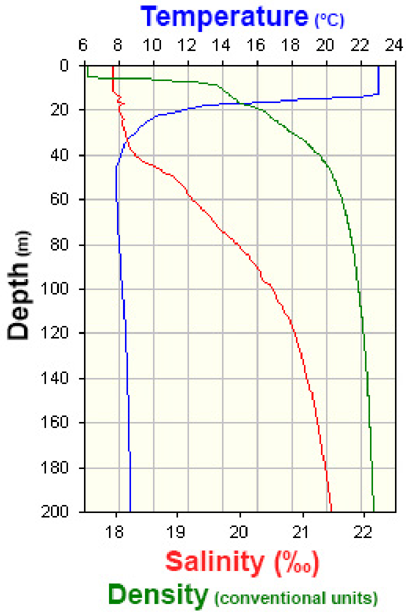

i) Central Black Sea

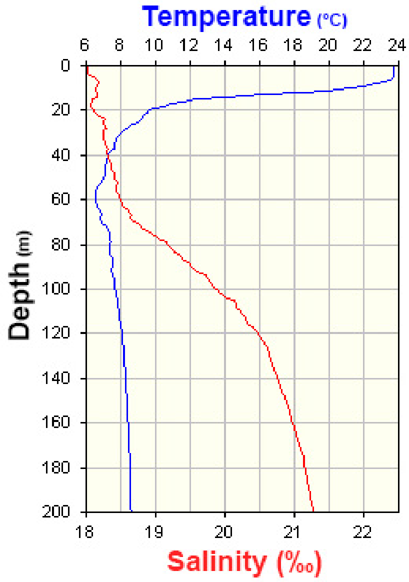

ii) Russian Continental Slope

7.4.5 Marine Water Quality

Understanding of marine water quality in the Black Sea requires an appreciation of the importance of stratification with depth. The upper sea layer experiences seasonal and year to year variation in hydrophysical and hydrochemical characteristics under the influence of external climatic factors. Its lower boundary is a deep pycnocline, below which influence of the external factors does not normally extend and hydrochemical conditions are relatively stable (Ref. 7.1). The upper layer is aerobic whereas anaerobic conditions exist at depth. The vertical zonation in hydrogeochemistry is illustrated in Figure 7.19.

All characteristic features of the depth distribution of hydrochemical parameters (horizons of wedging out of oxygen, hydrogen sulphide, and extreme values of biogenic elements) are usually located lower in the Black Sea coastal zone than in the central areas. This domal structure to the stratification is connected with the cyclonic character of water circulation. However, the hydrochemical horizons are almost always at the same density levels, consistent with the importance of density stratification to hydrochemical processes. Note that the upper boundary of the anaerobic zone exactly corresponds to a specific isopycnic surface (water density).

Figure 7.19 Vertical Stratification in Hydrogeochemistry (Ref. 7.36)

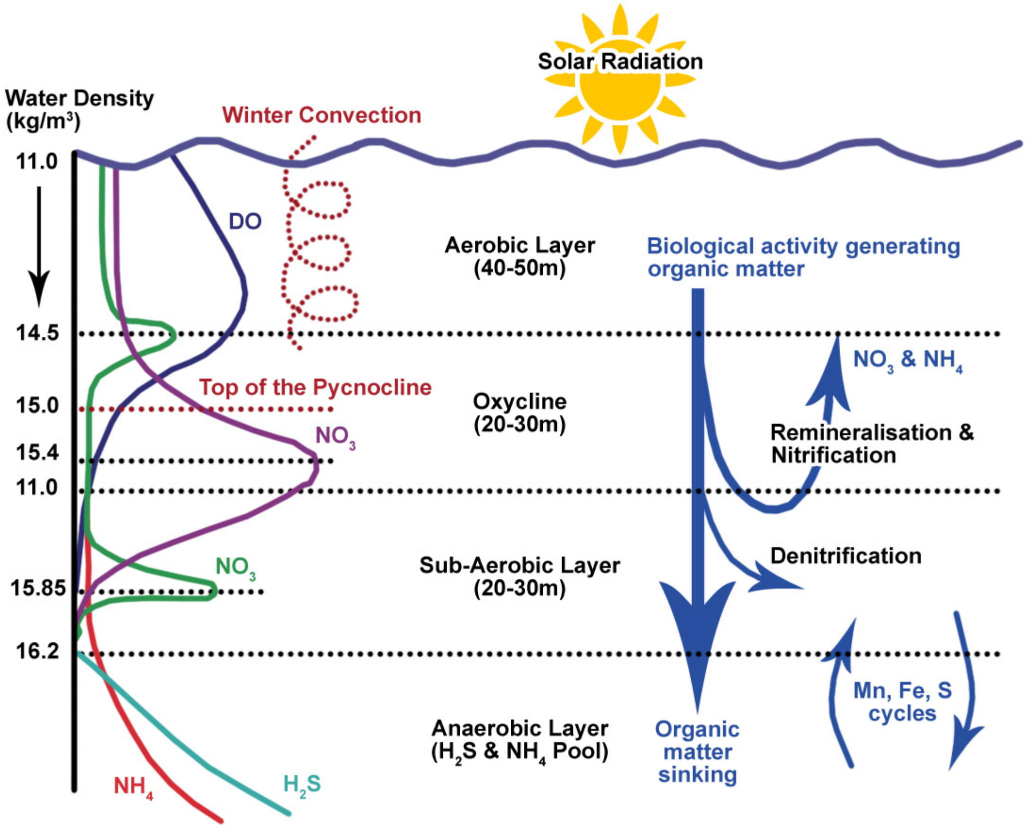

7.4.5.1 Oxygen

Oxygen is present in the surface waters, being at highest in concentration around 10 to 40 m depth. Oxygen concentrations in the surface waters vary seasonally, reflecting biological activity and the inverse relationship between oxygen solubility and water temperature. Oxygen concentrations in the surface waters are highest in March to May, which relates to the spring phytoplankton bloom and when surface water temperatures are relatively low. The minimum oxygen concentrations are in August to September when surface water temperatures are at their maximum.

Oxygen concentrations decrease from around 40 m depth, with oxygen depletion occurring in layers below 80 to 150 m (Figure 7.20). Oxygen disappears at a water density of about 15.9 conventional units. This is due to the salinity stratification limiting the potential for vertical mixing. Oxygen is typically absent from the deeper waters below the pycnocline, creating anoxic conditions; the Black Sea is the world’s largest anoxic basin. Waters with hypoxic or entirely anoxic conditions are typically incapable of sustaining permanent populations of species dependant on aerobic respiration.

Figure 7.20 Distribution of Oxygen (Green) and Hydrogen Sulphide (Brown) Concentrations (µM) from Archival Data (Ref. 7.1)

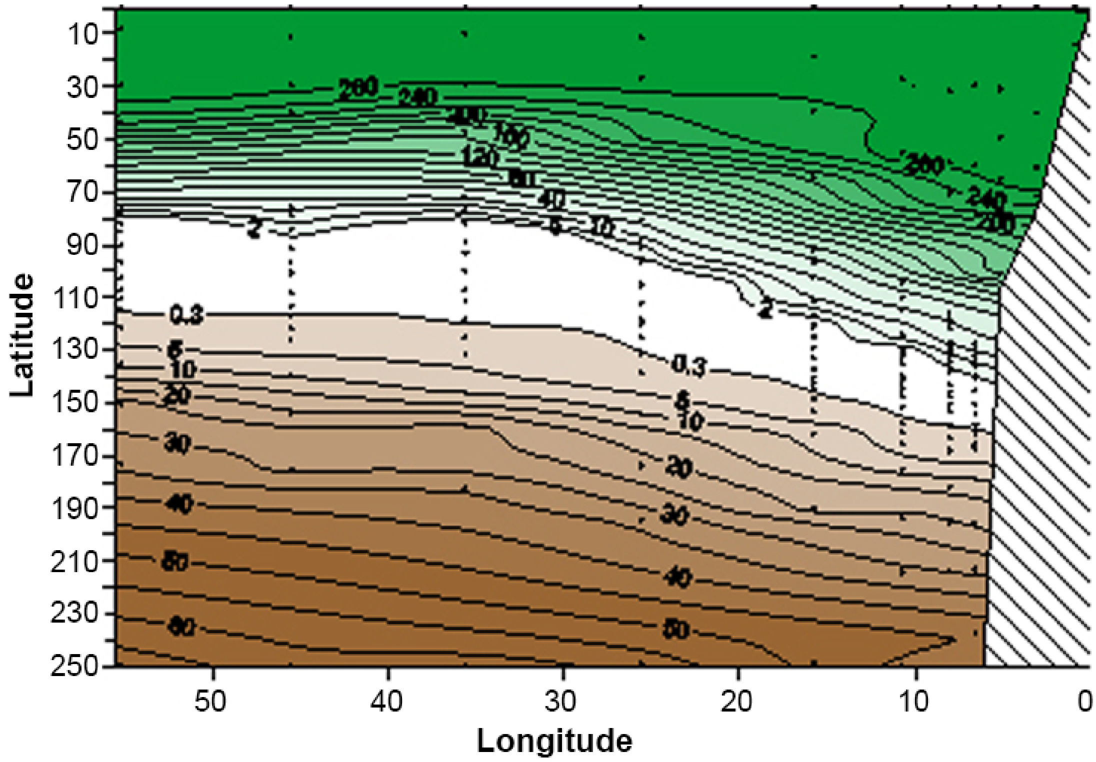

The average oxygen content of the surface waters was 8.91 mg/L in autumn 2010 (Ref. 7.1). Oxygen concentrations decreased below about 25 to 35 m; oxygen was not detected below about 100 to 140 m depth. In spring 2011, the oxygen content of the surface waters ranged from 10.10 to 10.35 mg/L. Oxygen concentrations decreased below about 30 m depth; oxygen was not detected below about 80 m depth.

Both autumn 2010 and spring 2011 surveys had similar spatial patterns in oxygen content (Ref. 7.1). Oxygen concentrations generally increased with distance from the coast. Coastal concentrations were highest near Gelendzhik and lowest near Anapa. The lower oxygen concentrations near the coast are interpreted to be due to warmer water temperatures near the coast, continental run-off and oxygen consumption by the oxidation of terrestrially-sourced organic matter.

In the summer 2011 survey (Ref. 7.1), the dissolved oxygen content in the surface layer of water in the coastal waters (as measured at coastal station "4C"; location on Figure 7.3) was 7.48 mg/L, which satisfies the Maximum Permissible Concentration (MPC) for human health in bathing waters set in SanPiN 2.1.5.2582-10 (Ref. 7.17).

7.4.5.2 Hydrogen Sulphide

The lack of oxygen at depth due to vertical stratification of the water column means that the potential for significant marine life occurring at depths of greater than 200 m within the Black Sea is likely to be limited to those organisms capable of anaerobic respiration (e.g. chemosynthetic life). Chemosynthesis typically produces hydrogen sulphide (H_2S) and methane as by-products, although these molecules are also formed by other biological and non-biological processes.

The widespread presence of hydrogen sulphide at depth is a notable characteristic of the Black Sea. The deep part of the water column throughout the Black Sea is characterised by high concentrations of H_2S. H_2S first appears at a water density of about 16.1 conventional units. From surveys in spring 2011 (Ref. 7.1), the H_2S upper boundary occurred at a depth of between 100 to 160 m in Russian waters (Figure 7.19). H_2S concentrations increased with depth up to a relatively high value of 13.2 mg/L in depths exceeding 2,000 m.

The depth at which H_2S appears varies seasonally, being deeper in winter. This is more pronounced in the shore areas compared with the deeper sea. This reflects seasonal changes in density as there is a close correlation between the conditional density and the appearance of H_2S. There is typically minimal seasonal variation in H_2S concentrations at depth.

7.4.5.3 pH

The surface waters of the Marine Survey Area are alkaline with a pH of around 8.2 to 8.3. Slightly lower pH levels have been recorded in the surface waters in and near river estuaries. Below 25 m, the pH decreases reaching 7.6 to 7.9 at the depth of H_2S appearance (c.80 to 160 m). Thereafter, pH slowly decreases with depth to about 7.5 at 2,000 m.

Slight seasonal variation in pH occurs (<0.5 pH units) in the surface waters, with summer values typically being slightly higher than winter values in coastal areas but the inverse in open seas.

In autumn 2010, the pH of the surface waters ranged from 8.2 to 8.4. In spring 2011, the pH of the surface waters were slightly lower, typically about 8.2. The pH values decreased with depth, dropping sharply below 80 m to 7.6. In the deep waters (>2,000 m) the pH is about 7.4, which corresponds to the long-term average pH for the deep waters of the Black Sea (Ref. 7.1).

7.4.5.4 Alkalinity

The total alkalinity of the surface waters is on average 3.196 mg/L. Alkalinity increases with depth, being 4.100 to 4.787 mg/L at 2,000 m.

Alkalinity in the surface waters varies spatially and seasonally, reflecting variations in river flows and quality and in precipitation inputs.

Alkalinity values measured in the autumn 2010 and spring 2011 surveys were within typical ranges for the Black Sea (Ref. 7.1). Coastal concentrations in the surface waters increased northwards along the coast. Concentrations were lower in the vicinity of the MBSC and then increased in the central part of the Eastern Black Sea. Alkalinity concentrations increased with depth.

7.4.5.5 Silica

Silica concentrations in surface waters are low at 0.1 mg/L. Low silica concentrations in surface waters reflect its intensive use in biochemical processes in the photosynthesis zone. Below 50 m, silica concentrations rise gradually to 8.5 to 11.2 mg/L at 2,000 m.

Silica concentrations vary seasonally and spatially. Concentrations are typically higher in coastal waters than in the open seas and are higher in winter than in summer.

In autumn 2010, silica concentrations in the surface waters ranged from 0.03 to 0.06 mg/L with an average value of 0.03 mg/L (Ref. 7.1). Concentrations were higher in the southern part of the Marine Survey Area. The silica concentrations increased with depth. Silica concentrations below 60 to 80 m exceeded 1 mg/L, with the maximum concentration of 6.51 mg/L being recorded at a depth of 1900 m.

In spring 2011, the silica concentrations in the surface waters were up to 0.2 mg/L (Ref. 7.1). Again, higher concentrations were observed in the south around Gelendzhik, reflecting river inputs in this area. Silica increases with depth, being on average about 6 mg/L at 1,000 m depth.

7.4.5.6 Organic Matter

Measurements of the biochemical consumption of oxygen (BOD5) have been undertaken to provide indirect measurement of organic matter in the water.

BOD5 is highest in the surface waters. Maximum concentrations in the surface waters in coastal areas are higher than in the open sea. Concentrations in coastal areas are relatively variable but have been measured up to 2.92 mg/L. BOD5 concentrations in the open seas are 0.1 to 0.6 mg/L. Organic matter decreases with depth. Beneath the pycnocline, BOD5 levels are typically 0.3 mg/L.

In autumn 2010, the BOD5 concentrations in the surface waters ranged from 0.09 to 0.47 mg/L with an average value of 0.31 mg/L (Ref. 7.1). In spring 2011, the BOD5 concentrations in the surface waters ranged were up to 1.03 mg/L. The measured BOD5 values are relatively low (compared with Maximum Allowable Concentrations (MAC) of 3 mg/L) and are consistent with background values in the Black Sea and a relative lack of significant water pollution by organic compounds.

Chemical Oxygen Demand (COD) measurements were also obtained in autumn 2010 and spring 2011 (Ref. 7.1). COD values reflect the total organic matter content of the sea water. Measured COD values ranged from 1.2 to 1.5 mg/L with an average of 1.37 mg/L in autumn 2010. Measured COD values in spring 2011 ranged from 0.7 to 4.5 mg/L with an average of 1.3 mg/L in the whole water column but from 0.9 to 1.5 mg/L with an average of 1.2 mg/L in the surface waters. COD concentrations were highest near the coast and lowest in the MBSC. The measured COD values typically fell within the range (1 to 2 mg/L) considered representative of “clean” water (Ref. 7.1).

No BOD5 or COD was detected in measureable concentrations in coastal waters during the summer 2011 survey.

7.4.5.7 Turbidity and Suspended Sediments

The optical properties (transparency and colour) of the Black Sea waters vary seasonally. In interpreting the seasonal patterns it should be noted that there is limited data available on typical optical properties in the sea water over winter. Spatial variations are also observed, with transparency typically being lower near the coast especially near river mouths.

Transparency in the eastern and central parts of the Black Sea is typically highest during summer when the volume of water discharged by rivers is lowest. Correspondingly, colour values are at their lowest at this time. Transparency is lowest and colour values are highest in spring due to phytoplankton blooms and snow melt flows. From autumn to spring, storm activity in shallow waters mobilises seabed sediments causing an increase in turbidity in coastal areas.

In April 2011 (Ref. 7.1), turbidity values at 10 m depth ranged from 0.11 to 15.47 relative units with an average value of 1.90 relative units. Turbidity declined with depth, with average values of 0.50, 0.25 and 0.08 relative units at 25, 50 and 100 m respectively. The depth profiles show a clear distinction between the more turbid, upper active layer and the less turbid deep layer.

The main source of suspended solids is from river waters, wave induced disturbance of seabed sediments, and airborne particles. At the Caucasus shores where there is little in the way of shallow waters, the river flows entering the sea are rapidly mixed into the deep water column. Up to the depth of 100 m, the vertical distribution of suspended solids is characterised by gradual decrease in their concentration.

In the autumn 2010 survey (Ref. 7.1) the measured suspended sediment concentration varied from 2.0 to 6.7 mg/L with the greatest concentrations within the water column occurring in the southern part of the Marine Survey Area.

In the spring 2011 survey (Ref. 7.1) the suspended sediment concentration varied across the Marine Survey Area from 2.0 to 41.3 mg/L. However the peak concentration of 41.3 mg/L was only recorded at one station, with all other concentrations being below 10 mg/L.

7.4.5.8 Phosphorus Compounds

Phosphorus compounds play a key environmental role, influencing biological productivity.

Phosphates

The vertical distribution of phosphates is controlled by density and redox conditions, reflecting the stratification of the sea (Figure 7.21).

Figure 7.21 Distribution of Phosphate Concentrations (µM) with Depth and Distance from Shore based on Archival Data (Ref. 7.1)

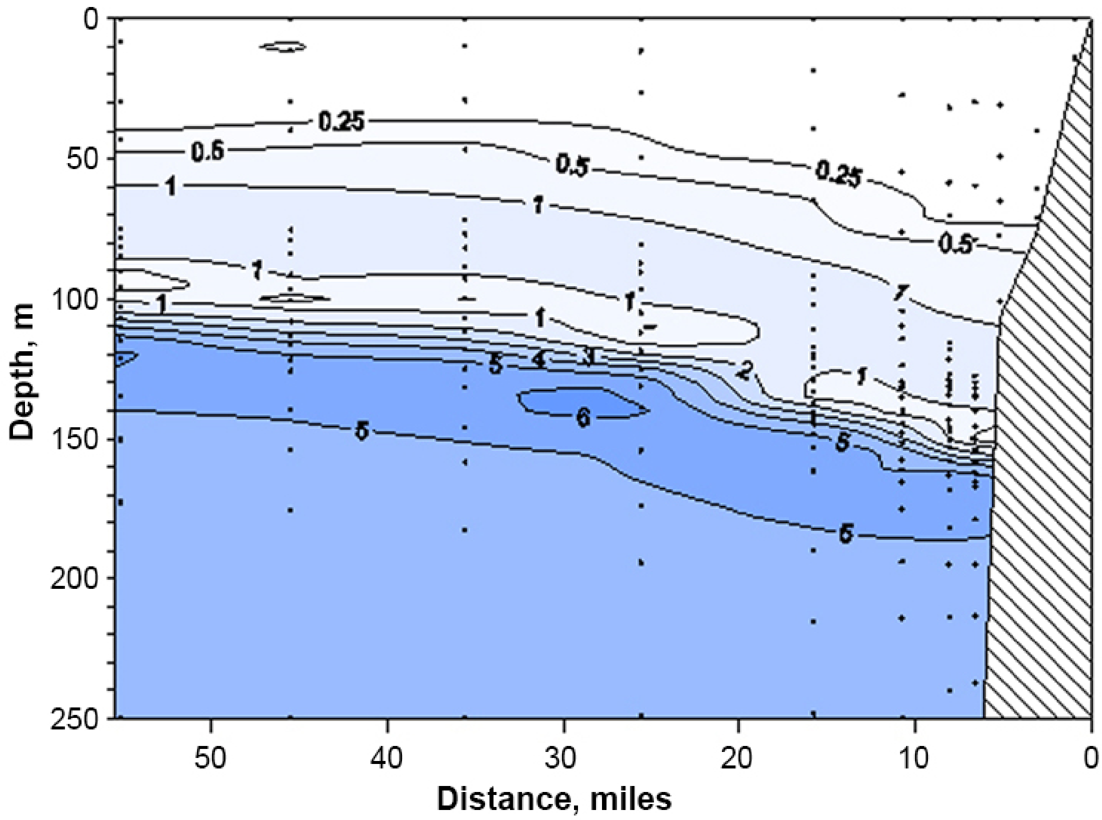

Concentrations are lowest in the surface waters, particularly during active photosynthesis. Phosphate concentrations are typically higher in coastal areas than in the open seas, reflecting the influence of continental runoff. Surface concentrations in nearshore areas are typically 0.013 mg/L in winter and 0.028 mg/L in summer, compared with 0.009 mg/L in winter and 0.017 mg/L in summer in the open sea.

Phosphate concentrations increase below around 40 m, with a secondary maximum around 100 to 150 m depth, then decreasing slightly before rising again to around 0.45 to 0.48 mg/L when the density is around 16.2 conventional units. Concentrations at 2,000 m depth are of the order of 0.5 to 0.7 mg/L.

Phosphate concentrations vary seasonally. Concentrations are higher in summer than in winter. An increase in phosphate concentrations in both summer and winter has been observed in recent years.

In autumn 2010, phosphate in the surface waters ranged up to 0.004 mg/L with an average value of 0.001 mg/L (Ref. 7.1). Concentrations were highest near Gelendzhik (Figure 7.22). Maximum phosphate concentrations of about 0.2 mg/L were observed at the depth where hydrogen sulphide begins to appear.

In spring 2011, phosphate concentrations in the surface waters ranged from 0.002 to 0.005 mg/L, being highest in the northwest of the Marine Survey Area (Figure 7.22). Phosphate concentrations increase with depth, reaching 0.25 to 0.27 mg/L at 2,000 m.

In summer 2011, the measured phosphate concentration in the coastal waters was 8 mg/L (Ref. 7.1).

Phosphate content in the surface waters of the nearshore and offshore sections of the Marine Survey Area do not typically exceed the MAC for fisheries (0.15 mg/L) (Ref. 7.16).

Figure 7.22 Spatial Distribution of Phosphate Concentrations in Surface Waters (Ref. 7.1)

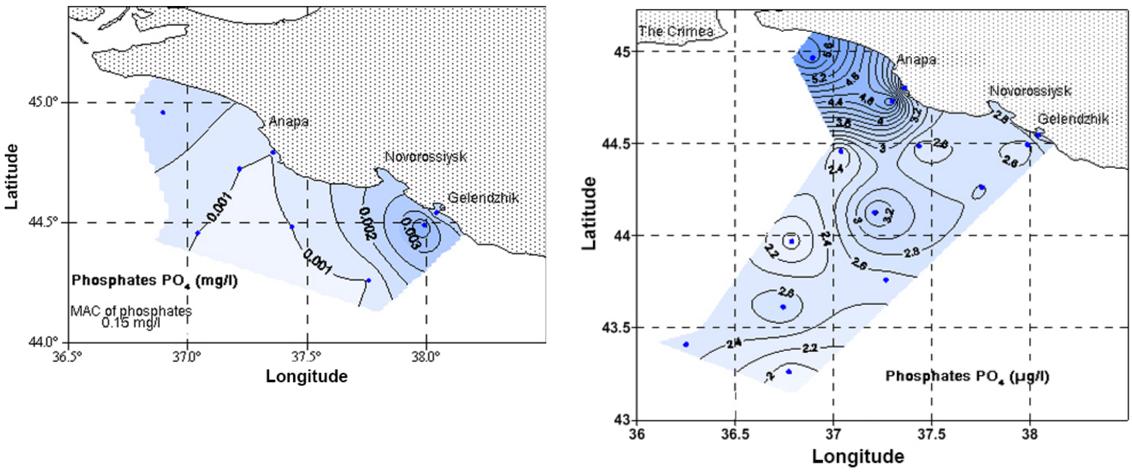

a) Autumn 2010

b) Spring 2011

Total and Organic Phosphorus

There is limited information available regarding total and organic phosphorus concentrations in the Black Sea.

Concentrations of total phosphorus in the surface waters of the Black Sea are typically 8 to 10 µg/L. Concentrations are usually highest near the coast as the main source of total phosphorus in the surface waters are coastal flows. Concentrations rise at the pycnocline to around 200 µg/L. Organic phosphorus concentrations are also relatively low in the surface waters. The spatial patterns in organic phosphorus concentrations are typically generally similar to those observed for total phosphorus.

In autumn 2010, total phosphorus concentrations in the surface waters ranged from 2 to 6 µg/L being 3 µg/L on average. Concentrations were higher near Gelendzhik and in the seaward part of the surface area (Figure 7.23).

In Spring 2011, total phosphorus concentrations in the surface waters varied from 8 to 10 µg/L in the MBSC to around 20 µg/L near the coast (Figure 7.23).

Figure 7.23 Spatial Distribution of Total Phosphorus Concentrations in Surface Waters (Ref. 7.1)

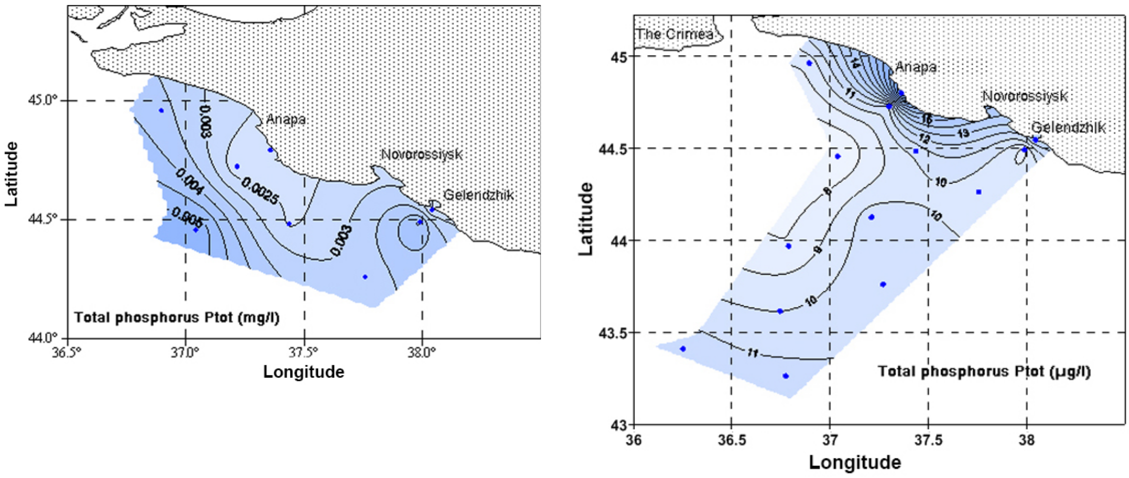

a) Autumn 2010 b) Spring 2011

7.4.5.9 Nitrogen Compounds

In sea water, nitrogen is represented by inorganic (nitrate, nitrite, ammonium salts) and organic (humic and fulvic acids, proteins, amino acids, amines etc.) compounds. Nitrogen distribution is an important controlling factor in biological productivity.

Nitrate

Nitrates are predominantly present at around 50 to 150 m depth within the transition zone between aerobic and anaerobic conditions (Figure 7.24). Typical concentrations in this zone are around 0.1 to 0.2 mg/L. Nitrate concentrations are very low in the surface waters above 50 m, being typically 0.028 to 0.12 mg/L. Nitrate is absent at depth in the deeper anaerobic (H_2S) zone.

Nitrate concentrations vary seasonally, reflecting variations in biological activity. Nitrate concentrations are highest in winter, dropping markedly with the spring phytoplankton bloom before rising slightly in summer. There is a secondary drop in autumn reflecting increased phytoplankton activity. The seasonal variation is more marked at shallow depths.

Figure 7.24 Distribution of Nitrate Concentrations (µM) with Depth and Distance from Shore based on Archival Data (Ref. 7.1)

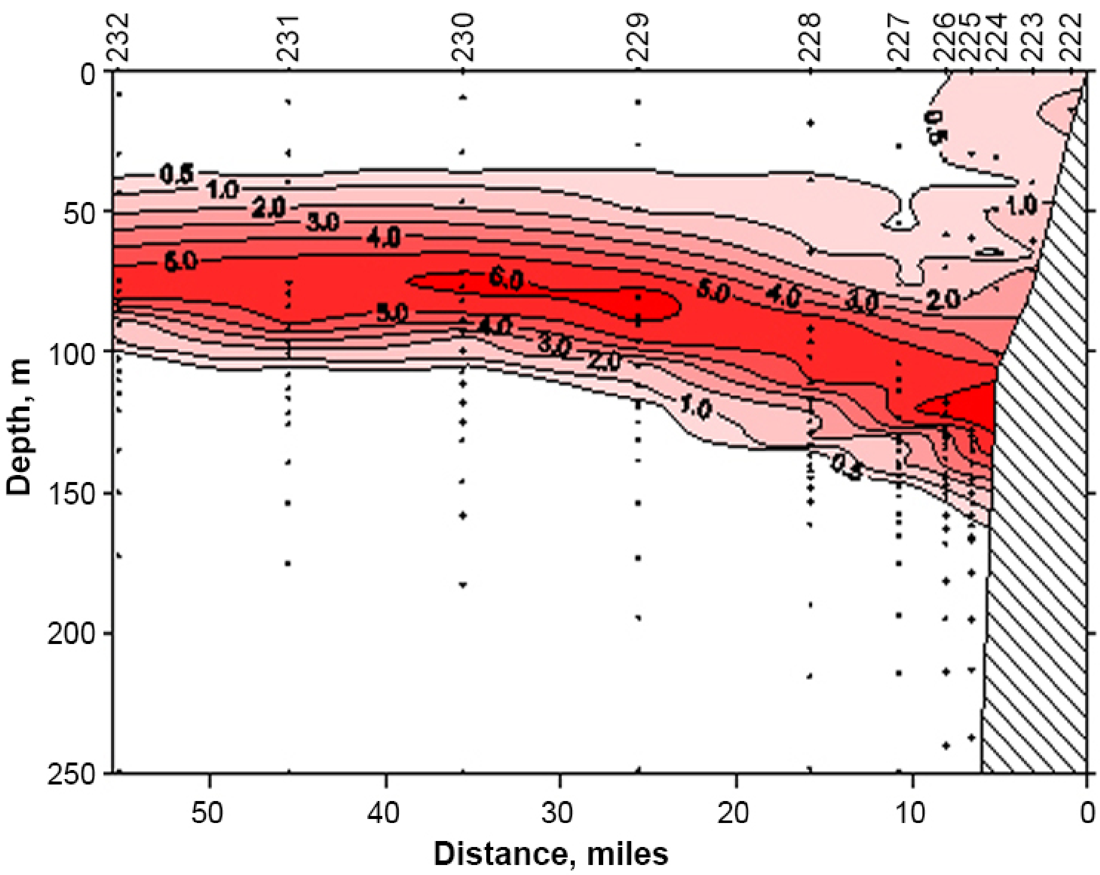

In autumn 2010, nitrate concentrations in the surface waters ranged from 0.003 to 0.014 mg/L. Concentrations were highest in the north-west part of the Marine Survey Area (Figure 7.25). Concentrations rose to between 0.035 and 0.045 mg/L at 60 to 70 m depth.

In spring 2011, nitrate concentrations in the surface waters were highest near the coast, typically around 0.01 to 0.02 mg/L, but were very low (below 0.002 mg/L) further out to sea (Figure 7.25). Concentrations rose to between 0.05 and 0.06 mg/L at 50 to 60 m.

Nitrate content in the surface waters of the nearshore and offshore sections of the Marine Survey Area did not usually exceed the MAC for fisheries (Ref. 7.16).

Nitrite

Nitrite is present in the marine surface waters, being relatively evenly distributed to the thermocline in summer and winter but depleted at the surface during the spring and autumn phytoplankton blooms. Nitrite concentrations in the surface waters typically range from 1.5 to 4.5 µg/L but are 6 to 8 µg/L at around 50 to 75 m depth. Nitrites are absent in the deeper anaerobic (H_2S) zone.

In autumn 2010, nitrite concentrations in the surface waters were up to 6 µg/L. In spring 2011, nitrate concentrations in the surface waters were up to 5 µg/L, being higher near the coast. The maximum concentration was observed in the Anapa area. Nitrite content in the nearshore and offshore sections of the Marine Survey Area did not exceed the MAC of 80 µg/L for fisheries (Ref. 7.16).

Figure 7.25 Spatial Distribution of Nitrate Concentrations in Surface Waters (Ref. 7.1)

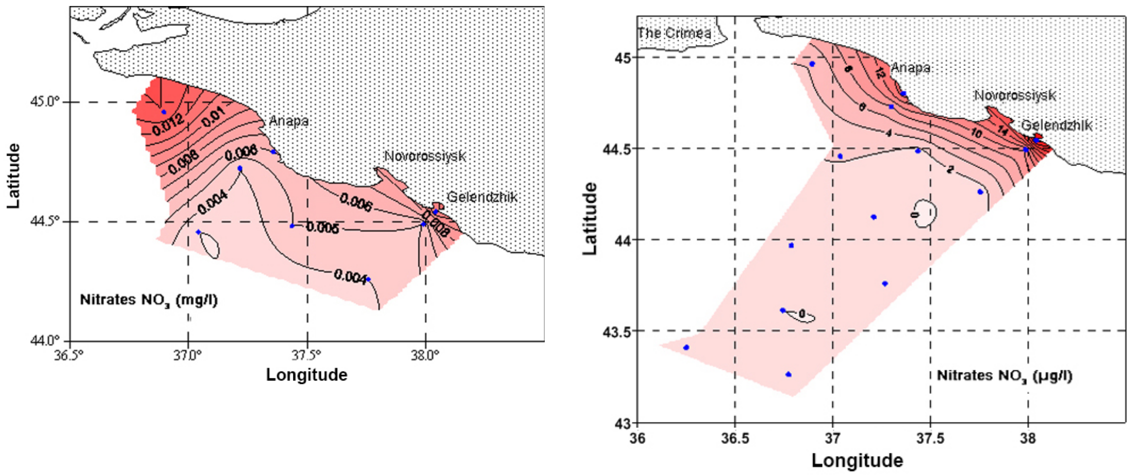

a) Autumn 2010 b) Spring 2011

Ammonium Nitrogen

Ammonium nitrogen concentrations are low in the aerobic surface waters, with concentrations of 0.002 to 0.036 mg/L. In the anaerobic zone, concentrations rise with depth up to 1.8 mg/L at 2,000 m. The seasonal patterns in ammonium nitrogen mirror those of nitrate, reflecting the influence of phytoplankton activity.

In autumn 2010, ammonium nitrogen concentrations in the surface waters ranged from 0.009 to 0.025 mg/L with an average value of 0.011 mg/L. The maximum concentration was recorded near Gelendzhik.

In spring 2011, ammonium nitrogen concentrations in the surface waters showed a similar pattern to nitrate, being highest (typically around 0.015 to 0.025 mg/L) near the coast in the vicinity of Gelendzhik and Anapa. In the seaward part of the Marine Survey Area, concentrations were lower, ranging from 0.005 to 0.010 mg/L. Ammonium nitrogen concentrations were highest at depth, being 0.20 to 0.35 mg/L in deep waters.

Ammonium nitrogen content in the nearshore and offshore sections of the Marine Survey Area did not exceed the MAC of 2.9 mg/L for fisheries (Ref. 7.16).

Total and Organic Nitrogen

There is limited information available regarding total and organic nitrogen concentrations in the Black Sea. Literature values indicate that total nitrogen concentrations in the Russian sector of the Black Sea range from 89.6 to 681 µg/L with an average value of 263 µg/L in the open seas. Organic nitrogen concentrations range from 76 to 669 µg/L with an average value of 243 µg/L. The total nitrogen predominantly comprises organic nitrogen.

In autumn 2010, total nitrogen concentrations ranged from 0.05 to 1.32 mg/L with an average value of 0.14 mg/L. The majority of the total nitrogen was organic nitrogen. Organic nitrogen concentrations were 0.015 to 1.066 mg/L with an average value of 0.114 mg/L. Concentrations were highest in the northwest of the Marine Survey Area.

In spring 2011, total nitrogen concentrations in surface waters were typically 0.2 to 0.25 mg/L but were up to 0.4 mg/L in the northwest of the Marine Survey Area. Concentrations increased with depth, being 1.4 to 1.5 mg/L at 2,000 m depth. Organic nitrogen concentrations were typically 0.2 mg/L but were over 0.3 mg/L in the northwest and east of the Marine Survey Area. Concentrations increased with depth up to 1.33 mg/L at 2,000 m depth.

7.4.5.10 Sea Water Contamination

Previous surveys in the Russian Sector of the Black Sea have identified the presence of contaminants in the sea water, including several organochlorine pesticides, petroleum hydrocarbons, phenols, and anionic surfactants. Additionally, elevated concentrations of heavy metals were locally detected, including copper, cadmium, lead, mercury and zinc. Contaminant concentrations varied spatially, but were typically higher near the coast (Ref. 7.1, 7.3).

Additional marine surveys (Ref. 7.1) were undertaken within the Marine Survey Area in 2010 and 2011 to further assess recent water quality in the nearshore and offshore areas. The results are summarised in Table 7.20 and 7.21. The sampling locations are shown in Figure 7.3.

Table 7.20 Summary of Contaminants in Sea Water for Autumn (Ref. 7.1)

Parameter	Unit	MPC	Range	No. Detects
Oil Products	mg/L	0.05	0.006 – 0.18	6
Anionic Surfactants	mg/L	0.1	<0.025 – 0.043	7
Phenols	µg/L	1	<0.1 – 6.1	11
Organochlorine Pesticides	µg/L	0.01	<DL1	0
Arsenic	µg/L	10	0.43 – 3.26	23
Cadmium	µg/L	10	0.8 – 3.4	23
Chromium	mg/L	0.07	0.007 – 0.027	23
Copper	µg/L	5	1.7 – 10	23
Iron	mg/L	0.05	<0.02 – 0.072	8
Lead	µg/L	10	<2 – 15.6	19
Manganese	mg/L	0.05	<0.01 – 0.224	14
Mercury	µg/L	0.1	<0.016 – 0.03	2
Molybdenum	µg/L	1	<1 - 4	21
Nickel	µg/L	10	<5 – 5.1	1
Selenium	µg/L	2	<0.1	0
Zinc	µg/L	50	<0.2 – 39	18

Note –
1. The detection limit for the organochlorine pesticides varied between compounds:
α-hexachlorocyclohexane <0.0004 µg/L,
β-hexachlorocyclohexane <0.002 µg/L,
γ-hexachlorocyclohexane <0.0005 µg/L,
heptachlor <0.002 µg/L,
aldrin <0.01 µg/L,
4,4-dichlorodiphenyltrichloroethane (DDT) <0.003 µg/L,
4,4-dichlorodiphenyldichloroethylene (DDE) <0.002 µg/L,
4,4-dichlorodiphenyldichloroethane (DDD) <0.003 µg/L.
2. Background concentrations of some heavy metals (e.g. iron, manganese) in sea water in the deeper anaerobic waters would be anticipated to be higher than in the aerobic surface waters due to redox processes. For some heavy metals it is considered that exceedance of MACs set for fisheries is more significant in the surface waters than exceedance at depth in the anaerobic hydrosulphuric zone. Therefore, only MAC exceedances in the surface waters are presented in the above table; there may be additional exceedances in the deeper waters.

Table 7.21 Summary of Contaminants in Sea Water for Spring 2011 (Ref. 7.1)

Parameter	Unit	MPC	Range	No. Detects
Oil Products	mg/L	0.05	<0.004 – 0.03	9
Anionic Surfactants	mg/L	0.1	<0.025 – 0.113	8
Phenols	µg/L	1	<0.5 – 0.8	3
Organochlorine Pesticides	µg/L	0.01	<DL	0
Arsenic	µg/L	10	<0.5 - 1	13
Cadmium	µg/L	10	<5– 6.6	1
Chromium	mg/L	0.07	<0.02 – 0.042	27
Copper	µg/L	5	2.1 – 10	45
Iron	mg/L	0.05	<0.02 – 0.093	6
Lead	µg/L	10	18.3 – 37.9	45
Manganese	mg/L	0.05	<0.01 – 0.204	19
Mercury	µg/L	0.1	<0.016 – 0.06	19
Molybdenum	µg/L	1	<1 – 5	26
Nickel	µg/L	10	<5 – 5.2	2
Selenium	µg/L	2	<0.5 – 1.87	4
Zinc	µg/L	50	0.06 – 8	45

Note –
1. The detection limit for the organochlorine pesticides varied between compounds:
α-hexachlorocyclohexane <0.0004 µg/L,
β-hexachlorocyclohexane <0.002 µg/L,
γ-hexachlorocyclohexane <0.0005 µg/L,
heptachlor <0.002 µg/L,
aldrin <0.01 µg/L,
4,4-dichlorodiphenyltrichloroethane (DDT) <0.003 µg/L,
4,4-dichlorodiphenyldichloroethylene (DDE) <0.002 µg/L,
4,4-dichlorodiphenyldichloroethane (DDD) <0.003 µg/L.
2. Background concentrations of some heavy metals (e.g. iron, manganese) in sea water in the deeper anaerobic waters would be anticipated to be higher than in the aerobic surface waters due to redox processes. For some heavy metals it is considered that exceedance of MACs set for fisheries is more significant in the surface waters than exceedance at depth in the anaerobic hydrosulphuric zone. Therefore, only MAC exceedances in the surface waters are presented in the above table; there may be additional exceedances in the deeper waters.

Oil products were present in the majority of samples but have been detected at concentrations above MAC in only three samples in autumn 2010. Concentrations were highest near Gelendzhik (Figure 7.26). Oil products were detected but did not exceed the MAC in the coastal sample collected in summer 2011.

Anionic surfactants have been detected in the majority of the water samples. The only sample that exceeded the MAC for anionic surfactants was Station 14 at 1,000 m depth. Concentrations in the surface waters were generally low.

Phenols were detected in about half the water samples in 2010 but in a smaller proportion of samples in 2011. Concentrations were highest near Gelendzhik.

The single exceedance of the MAC for manganese in the surface waters was in a coastal station near Anapa. Manganese concentrations in the surface waters generally decreased with distance from the coast. Concentrations were higher, locally exceeding the MAC, at depth in the deep water area but this is likely to be due to natural processes. Iron exhibited a similar pattern.

Chromium concentrations were below MAC. Concentrations were highest near the coast and the in the seaward cyclonic rise; concentrations were lowest in the MBSC.

Figure 7.26 Spatial Distribution of Oil Product Concentrations in Surface Waters (Ref. 7.1)

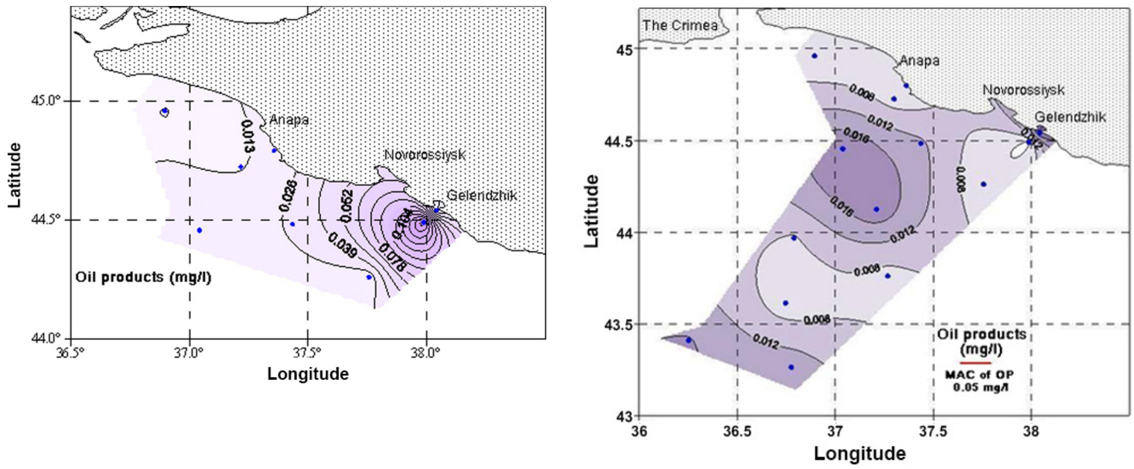

a) Autumn 2010

b) Spring 2011

Lead concentrations exceeded the MAC value in a significant proportion of the samples, including surface waters. Lead concentrations were typically highest near the coast (Figure 7.27). Lead concentrations on average are at or slightly above the MAC value.

Figure 7.27 Spatial Distribution of Lead Concentrations in Surface Waters (Ref. 7.1)

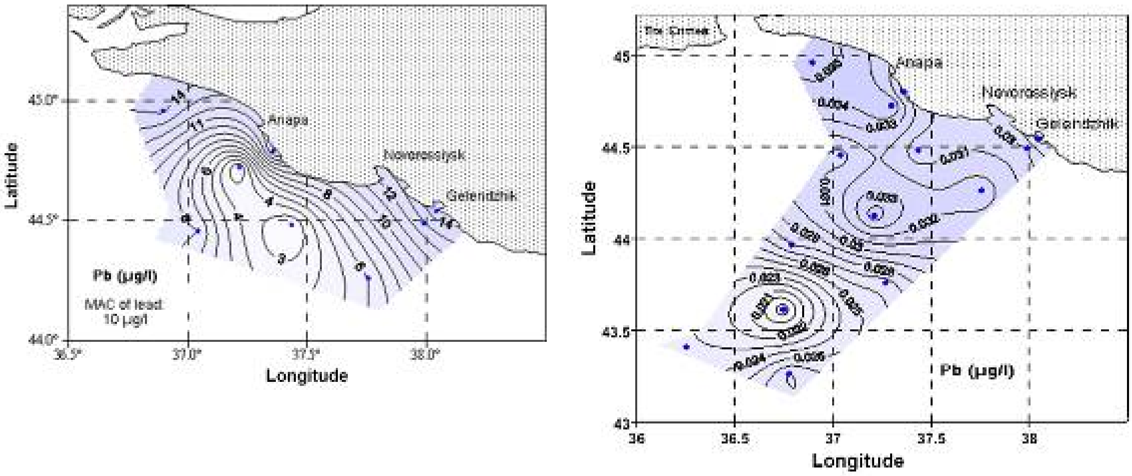

a) Autumn 2010

b) Spring 2011

Copper concentrations exceeded the MAC value in a large proportion of the samples, including surface waters. Copper concentrations on average are at or slightly above the MAC value. Concentrations are highest in the southeast of the Marine Survey Area (Figure 7.28). Generally the measured copper concentrations are similar to reported background concentrations in the Black Sea. Zinc concentrations were all below the MAC value but showed a similar distribution pattern to copper in the surface waters.

Figure 7.28 Spatial Distribution of Copper Concentrations in Surface Waters (Ref. 7.1)

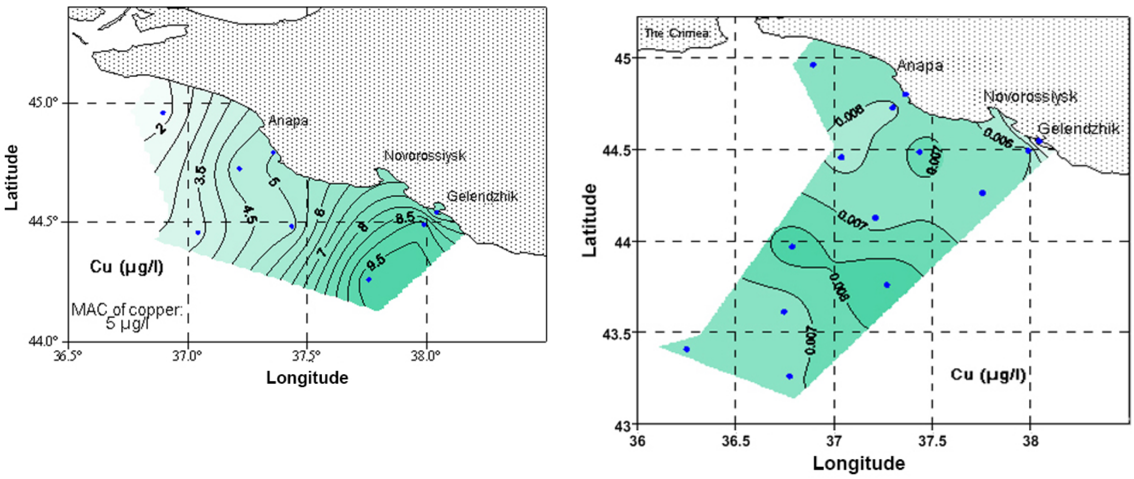

a) Autumn 2010

b) Spring 2011

Cadmium concentrations did not exceed the fisheries MAC and were in line with background concentrations in the Black Sea. Mercury concentrations did not exceed the fisheries MAC; concentrations were highest near the coast and in the area of cyclonic rise in the seaward area.

Nickel did not exceed the fishery MAC values in the autumn 2010 or spring 2011 surveys with concentrations typically being below detection limits except near the coast. However, in summer 2011, the concentration was 13.7 µg/L in the coastal sample, exceeding the MPC.

Concentrations of molybdenum were typically at or just above the MAC value. Concentrations were highest in the south and near Anapa. Generally the measured molybdenum concentrations were reported to be similar to background concentrations in the Black Sea.

Bacteriological testing was undertaken on two coastal samples collected in summer 2011. The results are consistent with relatively low levels of faecal contamination. Based on the limited testing, the waters meet the microbiological requirements of SanPiN 2.1.5.2582-10 (Ref. 7.17).

The eastern part of the Black Sea is less affected by eutrophication (increase in nutrients into the aquatic system) than the west due to the absence of major riverine inputs (Ref. 7.3).

The offshore Russian waters do not show evidence of significant pollution. Although some exceedances of fishery MACs by metals were measured, the majority of these can be attributed to natural background concentrations taking into account the natural chemical processes of the Black Sea. The coastal waters, particularly near Gelendzhik and Anapa, have elevated concentrations of contaminants present, including oil products, anionic surfactants, phenols and metals such as lead. Sources of contamination are likely to include port activities, runoff and discharges.

7.5 Geophysical Environment

7.5.1 Tectonic Setting and Geology

7.5.1.1 Tectonic Setting

The tectonic setting of the eastern Black Sea region is presented in Figure 7.29.

The Black Sea is a back-arc marginal extensional basin, which originated from the northward subduction of the Tethys Ocean beneath the southern margin of the Eurasian plate (Ref. 7.1).

The present day Black Sea basin was formed by the joining of two extensional basins, the Western Black Sea basin and the Eastern Black Sea basin, which have different tectonic histories and are different ages. The two basins are separated by the Mid-Black Sea high (Andrusov ridge and Archangelsky ridge). Further compressional tectonic processes led to the subsequent subsidence of the region (including western basin, eastern basin and separating ridge) to form the present day Black Sea basin (Ref. 7.1).

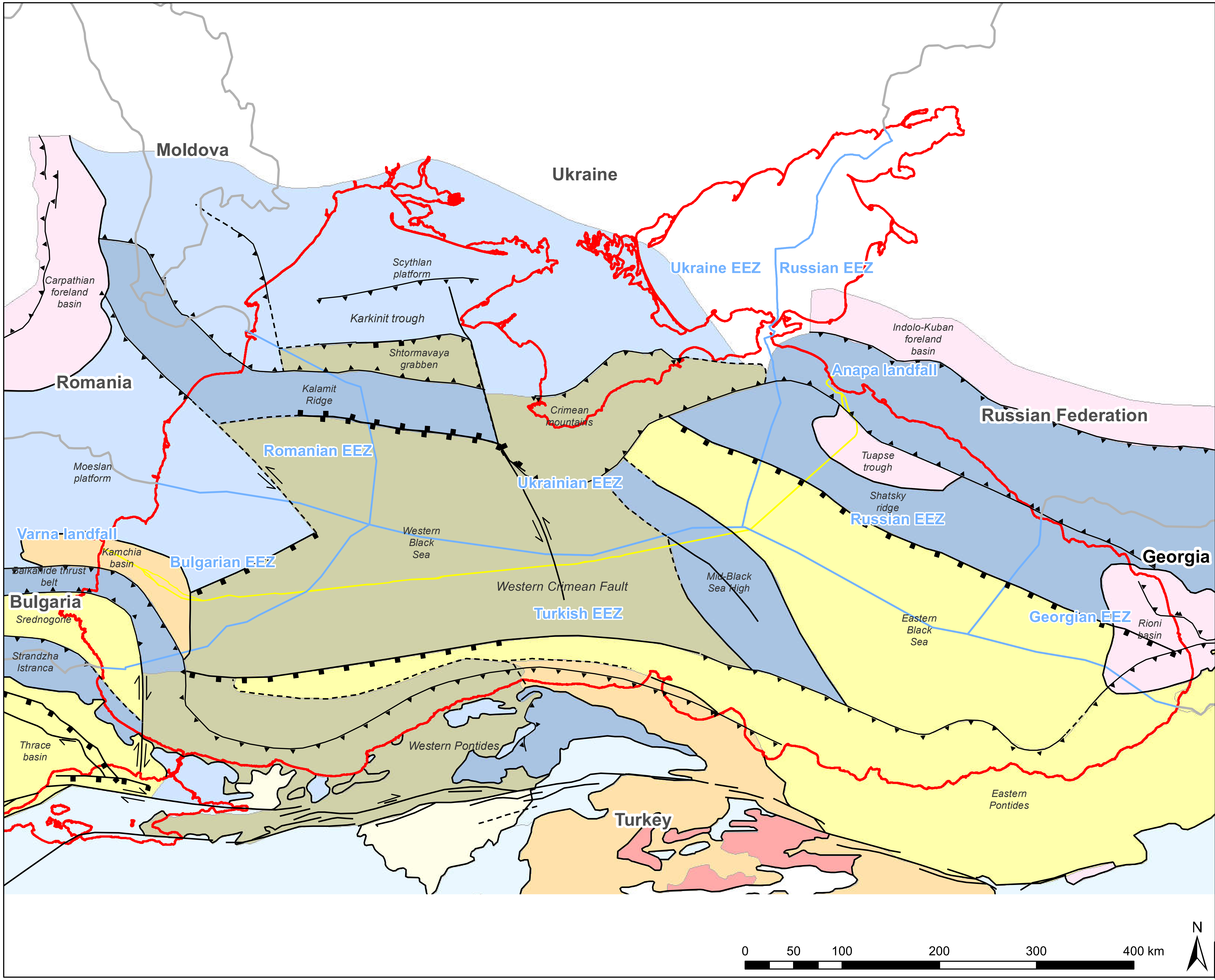

LEGEND

Russian Sector of South Stream Offshore Pipeline

Proposed offshore pipelines

Exclusive Economic Zone boundary

Country Boundaries

Black Sea

Fault Lines

Normal Fault

Reverse Fault

Tectonic contact (approx location)

Tectonic contact (known)

Strike-slip fault, showing relative movement

WCF Western Crimean Fault (approximate location)

Black Sea Tectonic Elements

Neogene post-tectonic sediments and piggy-back basins

Mid Eocene to Early Oligocene foreland basins

Late Cretaceous to Paleogene intra and back-arc basins and volcanic arcs

Late Cretaceous to Paleogene fore-arc basins

Aptian-Albian extensional basins and half grabens

Triassic to Early Jurassic extensional basins

Paleozoic to Triassic stable platform to continental margin

Subduction-accretion complex and post-collision volcanics

Metamorphic and igneous massifs

Projection: Lambert Conformal Conic

Revision Details	By Check	Check Date	Suffix

Purpose of Issue
For Information

Client
South Stream Offshore Pipeline ENERGISING EUROPE

Project Title
SOUTH STREAM OFFSHORE PIPELINE

Drawing Title
TECTONIC MAP OF BLACK SEA REGION

Drawn	Checked	Approved	Date
AH	IS	IS	29 May 2014

URS Internal Project No.	Scale @ A3
46369082	1:3,750,000

URS Infrastructure & Environment UK Limited
Scott House
Alencon Link, Basingstoke
Hampshire, RG21 7PP
Telephone (01256) 310200
Fax (01256) 310201
www.ursglobal.com

Drawing Number
Figure 7.29

Rev

Plot Date: 29 May 2014
File Name:I:\5004 - Information Systems\46369082_South_Stream\MXDs\Report Maps - Russia\Russian ESIA v2\Chapter 7 Geology\Figure 7-29 Tectonic Map of Black Sea Region.mxd

This page has been left intentionally blank

The Greater Caucasus is part of the Alpine-Himalayan orogenic system and is located between the Eurasian plate to the north and the African-Arabian plates to the south.

Global plate models and space geodetic measurements indicate that in the surrounding region, northward moving African and the Arabian plates collided with the Eurasian plate. From this collision, the Anatolian micro-plate moves westward with a rotation pole located approximately in the north of the Sinai Peninsula.

The Terrestrial Study Area is located in foothills, between the Greater Caucasus Main Range mountains and the Azov-Kuban lowland. Tectonically, the Terrestrial Study Area is part of the Greater Caucasus thrust belt, which extends east from the edge of the Tuapse trough (located in the Black Sea) inland to Indolo-Kuban foreland basin (Ref. 7.20). The north-western part of the Greater Caucasus' fold belt is a ridge composed of Mesozoic and Palaeogenic rocks. The landscape has been developed through the erosion of the mountain range following tectonic faulting and folding during the Neogene, approximately 23 to 2.6 million years ago (Ref. 7.1).

The Marine Study Area is located in the Eastern Black Sea Basin.

The south-western flank of the Greater Caucasus thrust belt extends along the narrow shelf and upper part of the Black Sea's continental shelf. Towards the north-west from Anapa, the Mesozoic and Palaeogenic rocks plunge sharply beneath the Oligocene to Quaternary sediments of the Kerch Strait.

The Tuapse depression (also known as the Tuapse Basin) was formed in the Oligocene by subduction beneath the Greater Caucasus. The depression is about 60 to 70 km wide, and is oriented northwest to southeast roughly parallel to the shore. The depression has a sharply asymmetric geometry, with a steep north-east slope and a gentle south-west slope.

The Shatsky Ridge is a massive raised crustal block that forms the north-eastern edge of the deep-water Eastern Black Sea depression. The Shatsky Ridge is oriented northwest to southeast and has very steep south-western and north-eastern slopes. The upper part of the elevation is covered by post-Maikopean deposits.

The Eastern Black Sea depression is the deepest part of the Marine Study Area. It is characterised by thick sedimentary sequences of Palaeogene and Holocene age. These sediments are underlain by Eocene chalk deposits over basement strata.

7.5.1.2 Terrestrial Geology

The underlying bedrock geology within the Terrestrial Study Area is characterised by terrigenous and carbonate Miocene and Pliocene rocks, including argillites and clays, conglomerates, limestones, dolomites, marls and sandstones (Ref. 7.1). Based on the geotechnical investigations, the majority of the near-surface strata in the Terrestrial Survey Area comprise marls interbedded with sandstone, limestones and clays (Ref. 7.21). These strata are more than 25 m thick in the Terrestrial Survey Area. The Miocene and Pliocene strata are underlain by folded Palaeozoic structures and Jurassic and Cretaceous monoclines. A map of the regional geology at the Study Area is presented in Figure 7.30.

The bedrock is exposed at the coast and locally in the valleys. The bedrock deposits are well to medium bedded (Ref. 7.22). The marl beds are up to 2 m thick. In the upper 5 m near the surface, the bedrock is weathered and has a low rock mass rating. At depth, the bedrock has a low to medium rock mass rating, with considerable lateral and vertical variation. At the shore, the bedrock bedding dips steeply towards the sea. The coastal ridge comprises an anticlinal structure; the folding is disrupted locally by faulting.

The bedrock deposits are overlain by a mantle of unconsolidated Quaternary deposits of variable thickness.

Overlying Quaternary deposits include a mantle of unconsolidated alluvial, colluvial, eluvial, fluvial, diluvial and coastal marine sediments of variable thickness ranging from a few metres to tens of metres. The general characteristics of Quaternary deposits encountered in the Terrestrial Survey Area are described below (Ref. 7.1):

- Alluvial deposits – Loose, unconsolidated (un-cemented) sediments, which have been eroded and/or reshaped by water and redeposited on land down gradient of their origin. Alluvial deposits are typically 1 to 5 m thick. Deposits are distributed along valley floors and are variable in composition (comprising sandy clay, limestones, marls and/or fragments of other types of weathered bedrock);
- Colluvial deposits – Loose unconsolidated variable sized sediments, ranging from silt to rock sized fragments. Deposits are typically located at the base of hill slopes, as a result of erosion and deposition by rain wash, sheetwash and/or slow downslope creep of sediments;
- Eluvial deposits – Soils derived from either the in-situ weathering of underlying bedrock or the weathering of bedrock combined with limited movement or accumulation of the soils due to gravitational creep on gently inclined slopes;
- Fluvial deposits – Fluvial soils are typically located on alluvial floodplains, river fans and valleys. They form on alluvial sediments and can be mixed in with flood surge deposits. Deposits include loam, silts and sandy clays to clayey sands;
- Diluvial (flood) deposits – Encountered mainly on the slopes of hills and at the base of coastal cliffs. Deposits comprise loose accumulation of angular rock fragments in a matrix of clay and sand, and typically range between 1 to 5 m thick; and
- Coastal Marine Sediments – Includes sandy beaches, and sand, gravel and boulders.

Soils are typically formed through the erosion and re-deposition of underlying bedrock deposits. The predominant soil forming bedrock material is weathered marl. Soils covering higher slopes and ridges are typically formed by the weathering or re-deposition of calcareous argillites and interbedded sandstones and siltstones. Soils encountered within river valley systems typically form from weathered calcareous marls, interbedded limestones, siltstones and shales. Deposits in the valley bottoms comprise variable gravel and sand deposits with occasional layers of clays and loam material interbedded in the coarser-grained material (Ref. 7.23).

The characteristics and distribution of soils across the Terrestrial Survey Area are described in further detail in **Chapter 8 Soils, Groundwater and Surface Water**.

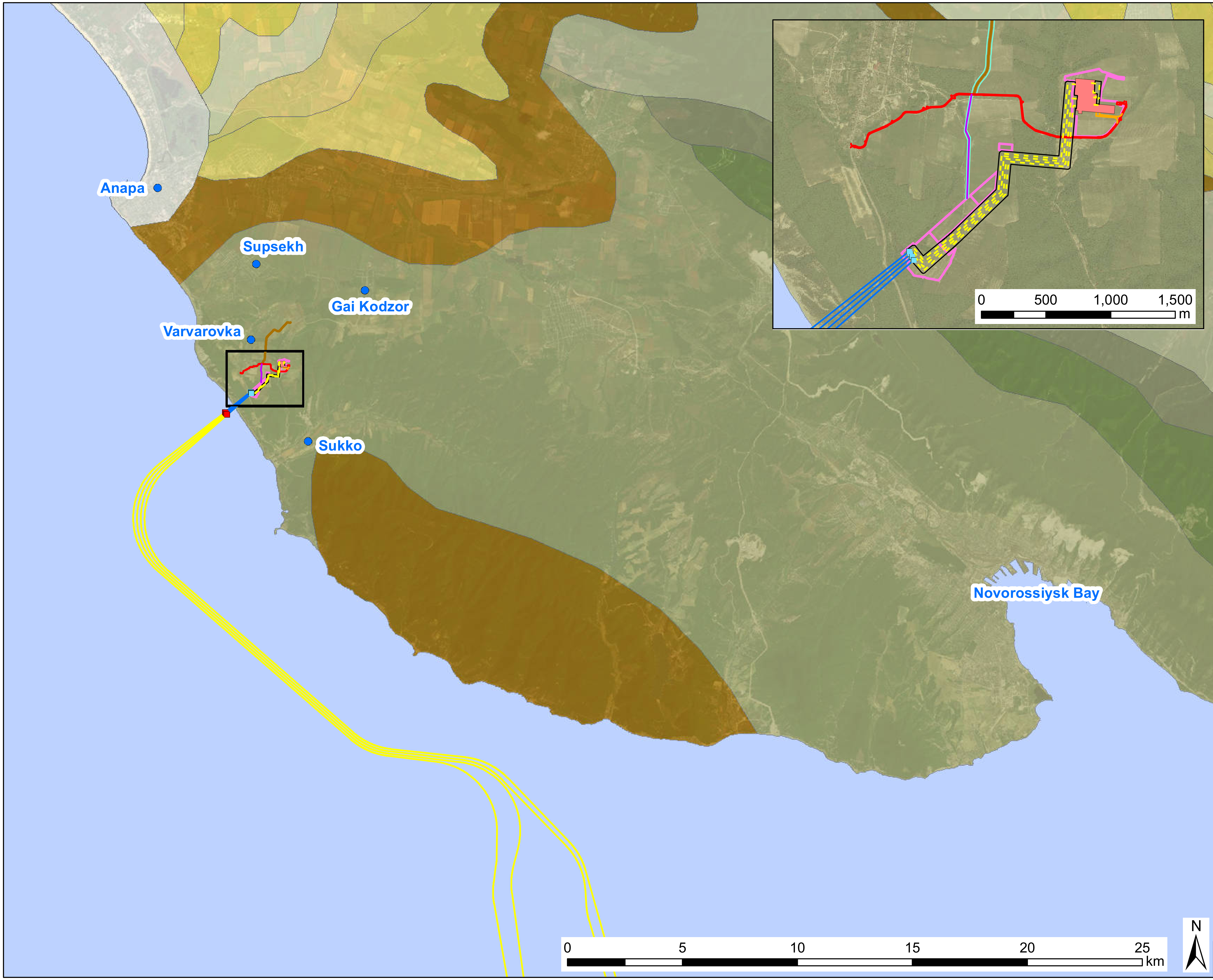

LEGEND

- Russian Settlements

Geology

- Middle-quaternary deposits
- Pliocene deposits
- Akchagly stage deposits
- Cimmerian stage deposits
- Upper Miocene and Lower Pliocene deposits
- Oligocene and Miocene deposits
- Lower section (Polenian section of Volga) deposits
- Cenomanian, Turonian stage and Senonian stage deposits
- Senonian (Konyanian, Santonian, Campanianand Maastrichtian) stage deposits
- Turonian stage deposits
- Aptian and Albian stage deposits

Russian Sector of South Stream Offshore Pipeline

- Proposed landfall section pipelines
- Landfall facilities
- Proposed microtunnels
- Proposed offshore pipelines
- Right-of-Way
- Microtunnel exit pit
- Microtunnel entry shaft
- Temporary construction area for road construction
- Construction sites

Roads

- Permanent access road to be constructed by SSTTBV
- Temporary access road constructed by SSTTBV
- Varvarovka bypass road (used by Project during construction only)
- Permanent access road to be constructed by Gazprom Invest

Projection: Lambert Conformal Conic

Revision Details	By / Check	Check Date	Suffix

Purpose of Issue
For Information

Client
South Stream Offshore Pipeline ENERGISING EUROPE

Project Title
SOUTH STREAM OFFSHORE PIPELINE

Drawing Title
GEOLOGICAL MAP OF THE LANDFALL SECTION OF THE PROJECT AREA

Drawn	Checked	Approved	Date
AH	IS	IS	19 Mar 2014

URS Internal Project No.	Scale @ A3
46369082	1:150,000

URS Infrastructure & Environment UK Limited
Scott House
Alençon Link, Basingstoke
Hampshire, RG21 7PP
Telephone (01256) 310200
Fax (01256) 310201
www.ursglobal.com

Drawing Number
Figure 7.30
Rev

Plot Date: 19 Mar 2014
File Name:I:\5004 - Information Systems\46369082_South_Stream\MXDs\Report Maps - Russia\Russian ESIA v2\Chapter 7 Geology\Figure 7-30 Geological Map of the Landfall Section of the Project Area.mxd

This page has been left intentionally blank

7.5.1.3 Marine Geology

The geology in the nearshore and offshore sections of the Marine Study Area comprise both Upper Cretaceous and Palaeogene Flysch deposits. Upper Cretaceous flysch deposits comprise coarsely stratified bituminous marls inter-bedded with the bands of quartz-glauconite sandstones. The uppermost sequence of Cretaceous flysch deposits are typically dark clays, separated by sandstones and dense dark marls. Palaeogene flysch deposits comprise dense clays, dark coloured hard metamorphosed marls with some inter-bedded sandstone bands.

During the Neogene stage of Alpine orogeny the flysch deposits of both the Upper Cretaceous and Palaeogene were subject to intensive deformation and folding associated with this period of thrusting and faulting.

The marine sediments that overlie the bedrock vary in thickness from absent to several metres thick. The marine sediments are discussed further in Section 7.5.5.

7.5.2 Seismicity and Geohazards

The tectonic structure of the Black Sea basin is complex and the collision zone between the African and Eurasian plates, as well as movement around the various microplates, has created a zone which is prone to earthquakes. Significant earthquakes have affected several countries, including Russia, on the eastern side of the Black Sea tectonic basin.

The Greater Caucasus is a zone with active compression where thrust and strike-slip faulting associated with on-going earthquake activity has continued to the present time (Ref. 7.25). A seismically active zone is known in the Anapa region where the Crimean and Caucasus structures meet. This is manifested as a seismic belt from the southern foot of the Crimea to the Anapa region. In 1966, the Anapa earthquake (magnitude 5.8) occurred in this belt.

Seismic activity in the region typically has a potential to cause earthquakes of magnitude 5 to 6 on the Richter Scale (Ref. 7.1). Recent earthquakes in the area include a 4.9 magnitude earthquake centred in Varenikovskaya (located approximately 32 km northeast of Anapa) in 2012 and a 4.4 magnitude earthquake centred at Anapa in 2011.

Seismic studies (Ref. 7.5, 7.29, 7.30, 7.31, 7.32, 7.33, and 7.34) have been undertaken along the Pipeline route.

The Pipeline route crosses the southern branch of the Marfovsky Fault (Figure 7.31). This fault is active (Ref. 7.22). The fault is not a single lineament but instead comprises a fracture zone with northern and southern branches. The fault zone is approximately 200 m wide. The fault is well defined due to a distinct tectonic scarp. Current displacement values are estimated to be 0.2 m vertically and 1 m horizontally (Ref. 7.22). Slow (creep) fault displacement is estimated to be at a rate of 0.2 to 0.35 mm per year (Ref. 7.22).

As described in **Chapter 5 Project Description**, the fault will be crossed using traditional open-cut techniques. However, to minimise the effect of potential displacement from seismic activity, each pipeline will be laid in an enlarged trench backfilled with loose sand rather than the previously excavated soils. The combination of the wider trench and backfilling with loose sand allows the pipelines to move in a lateral direction. This reduces the risk of movement on the Marfovsky Fault affecting pipeline integrity.

The pipeline route also crosses the Shingarsky Fault (Figure 7.32). This fault was mapped using geophysical survey methods (Ref. 7.21). The Shingarsky Fault comprises a fracture zone up to 50 m wide of weak and weathered rock. Based on local geomorphology and the overlying superficial deposits, this fault is considered to be inactive (Ref. 7.5). The Shingar River is aligned with the Shingarsky Fault; the weathered fracture zone of the fault is likely to have allowed preferential erosion along the line of the fault during flood events. The microtunnel route crosses the Shingarsky Fault.

The West Utrish Fault is a large regional tectonic fault associated with the structural zoning of the North West Caucasus (Ref. 7.22). It is inferred to have an east-west strike. The West Utrish Fault has not been identified within the Project Area (Ref. 7.22); it is interpreted to be parallel to the coast (probably on seaward side) and to be inactive in the Project Area.

Additional fracture zones (interpreted to be potential faults) have also been interpreted (Ref. 7.22, 7.27) from the seismic survey data and geohazard mapping. These may reflect conjugate faulting or jointing associated with past activity of the Shingarsky Fault.

Four fissure zones have been mapped along the coastal ridge (Ref. 7.22); these are shown on Figure 7.31. The fissure zones are up to 80 m wide. The fissure zones have been preferentially weathered and have a topographical expression. The fissure zones may have formed through local tectonic or gravity-induced ground movements. These may relate to the deep-seated rotational failure planes mapped along the coast or to conjugate jointing associated with past activity of the Shingarsky Fault.

Although the abyssal plain is predominantly flat / to gently inclined, hill and ravine features are locally present. Hills are typically formed by mud volcano activity and may be 1 to 30 m high, with basal diameters of 600 to 1,000 m wide. Mud volcanoes are formed by the expulsion of mud, rock fragments and fluids (especially methane) from depth. Recent turbidite flows occur in the vicinity of the mud volcanoes. No large mud volcanoes have been identified along the Pipeline route (Ref. 7.36). Ravines are typically associated with tectonic faults, none of which are considered to be active (Ref. 7.28). The ravines are generally asymmetric in shape, with one relatively steep slope (typically 10 to 20 m deep) and one comparatively flatter slope; although some symmetrically shaped gently inclined ravines are also encountered. Ravines are typically between 500 to 1,000 m in length (minimum of 200 and maximum of 4,500 m).

Natural gas seepage associated with the degradation of organic rich material may be encountered on the abyssal plain. In addition, features associated with natural gas seepages include blow outs of shallow gas reservoirs and gas plumes (Ref. 7.1).

The Russian continental slope is currently tectonically active, with fault movement impacting slope stability, sediment distribution and earthquakes. Tectonic activity reduces away from the coast from the Caucasus Mountains to the Tuapse depression (Ref. 7.5).

The north eastern Black Sea seismic source zone is characterized by low to moderate seismicity with the majority of events having a magnitude lower than 5 (Ref. 7.26, 7.30). The largest event recorded occurred in 1905 with a magnitude of MW 6.6 and focal depth of 38 km. The epicentre was in the offshore Southern Black Sea at more than 300 km from the Anapa landfall. The event was associated with a tsunami.

No significant seismic events have been recorded within the Shatsky Ridge. Very rare earthquakes may be associated with small movements over rejuvenated faults penetrating the Quaternary layer. Faults occur in the Maikopean (Upper Palaeogene – Lower Neogene) clays on the shelf of the Kerch-Taman deflection and in the Tuapse deflection. These faults are associated with clay diapers and mud volcanoes. The faulting is predominantly oriented northwest-southeast.

Several of the earthquakes in the Black Sea region appear to have been associated with tsunami waves along the coast (Ref. 7.26).

Within the Marine Study Area, seismic studies (Ref. 7.5, 7.30, 7.31, 7.32, 7.33, 7.34, and 7.35) indicate that:

- Major active tectonic faulting does not cross the offshore pipeline route (Ref. 7.26, 7.30);
- Active faults were not observed on any of the sub-bottom profiles conducted along the pipeline routes (Ref. 7.29);
- No faults considered dangerous to pipeline integrity have been identified (Ref. 7.26) along the pipeline route in the marine Project Area;
- Sediment deformation associated with tectonic movement is most likely to impact very soft superficial clay deposits on the shelf and continental slopes; and
- Limited slope failure involving 2 to 3 m thick layers of sediment and movement of superficial sediments on the continental slope are anticipated as a result of an earthquake of with a return period of 1 in 475 years. Shallow failures of <2 to 3 m thick have been predicted for an earthquake of this recurrence period.

7.5.3 Terrestrial Geomorphology

The landscape and geomorphology of the Terrestrial Survey Area often dictates the vegetation cover. There are two distinct landscape terrains and associated vegetation cover:

- Plain (gently sloping plateau) and hilly terrain covered by a complex of arid woodlands; and
- Hilly submontane terrain, covered by mixed oak, pine, juniper forests and arid woodlands.

A map of the local geomorphology of the Terrestrial Survey Area is presented in Figure 7.32.

This page has been intentionally left blank

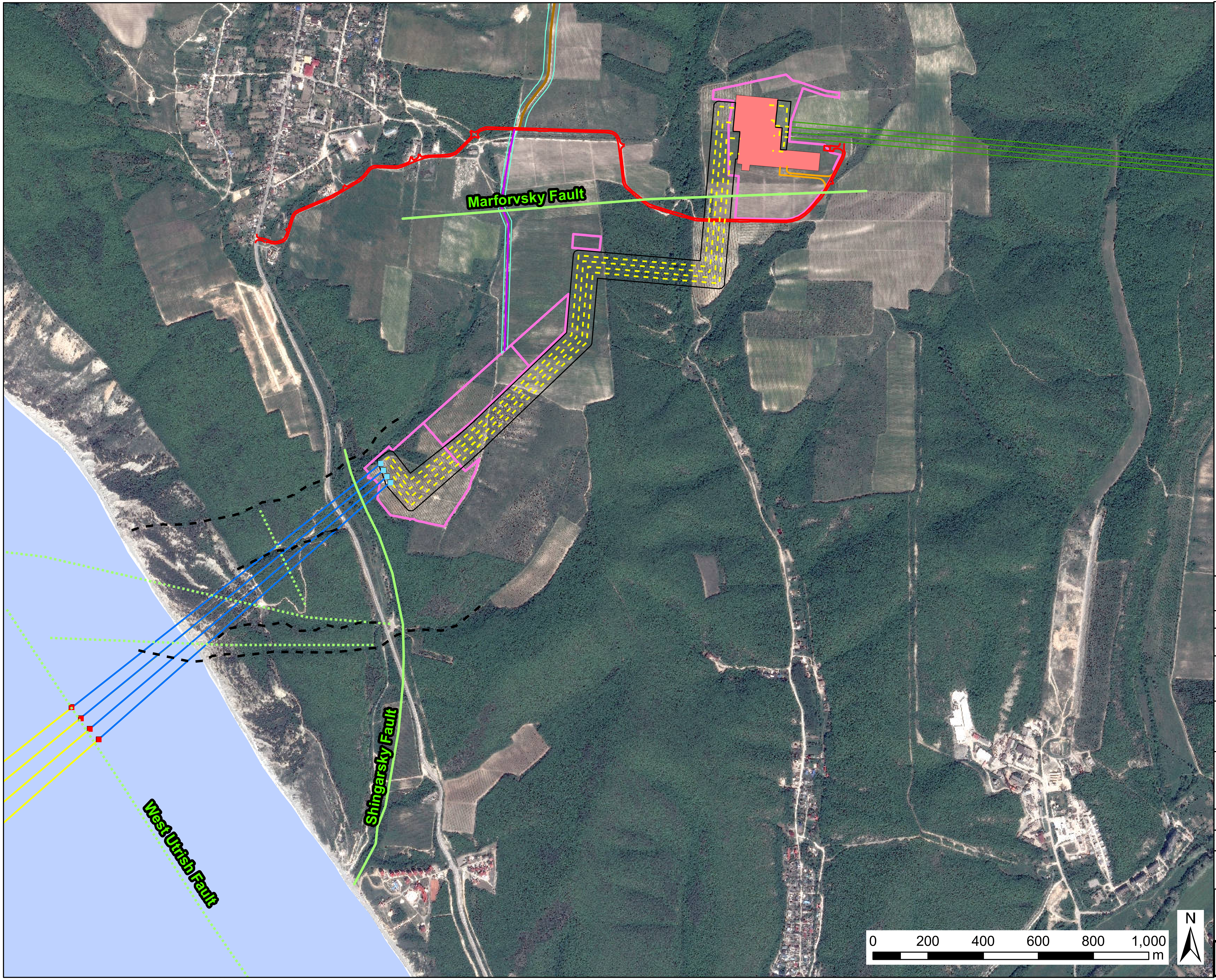

LEGEND

Indicative Fault and Fissure Lines

- Fault
- Possible Fault
- Fissure Zone

Russian Sector of South Stream Offshore Pipeline

- Proposed landfall section pipelines
- Landfall facilities
- Proposed microtunnels
- Proposed offshore pipelines
- Right-of-Way
- Temporary construction area for road construction
- Construction sites
- Microtunnel entry shaft
- Microtunnel exit pit
- Permanent access road to be constructed by SSTTBV
- Temporary access road constructed by SSTTBV
- Varvarovka bypass road (used by Project during construction only)

United Gas Supply System

- United Gas Supply System pipelines
- Permanent access road to be constructed by Gazprom Invest

Projection: Lambert Conformal Conic

Revision Details	By / Check	Check Date	Suffix

Purpose of Issue: For Information

Client: South Stream Offshore Pipeline — South Stream ENERGISING EUROPE

Project Title: SOUTH STREAM OFFSHORE PIPELINE

Drawing Title: MAPPED FAULTS IN TERRESTRIAL LANDFALL SECTION

Drawn	Checked	Approved	Date
AH	IS	IS	04 Mar 2014

URS Internal Project No.	Scale @ A3
46369082	1:12,500

URS Infrastructure & Environment UK Limited
Scott House
Alençon Link, Basingstoke
Hampshire, RG21 7PP
Telephone (01256) 310200
Fax (01256) 310201
www.ursglobal.com

Drawing Number: Figure 7.31

Rev:

Plot Date: 04 Mar 2014
File Name:I:\5004 - Information Systems\46369082_South_Stream\MXDs\Report Maps - Russia\Russian ESIA v2\Chapter 7 Geology\Figure 7-31 Mapped Faults in Terrestrial Landfall Section.mxd

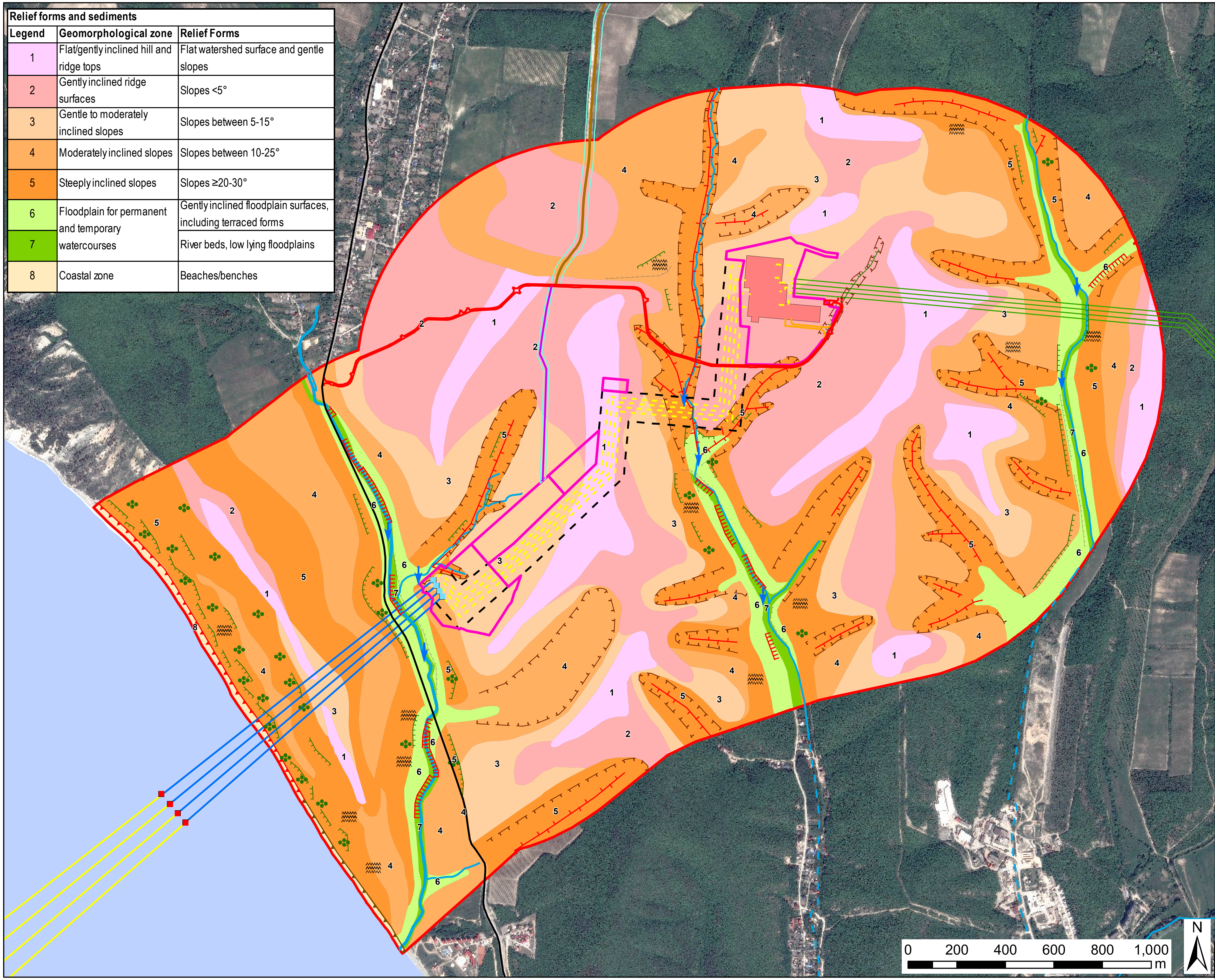

Relief forms and sediments

Legend	Geomorphological zone	Relief Forms
1	Flat/gently inclined hill and ridge tops	Flat watershed surface and gentle slopes
2	Gently inclined ridge surfaces	Slopes <5°
3	Gentle to moderately inclined slopes	Slopes between 5-15°
4	Moderately inclined slopes	Slopes between 10-25°
5	Steeply inclined slopes	Slopes ≥20-30°
6	Floodplain for permanent and temporary watercourses	Gently inclined floodplain surfaces, including terraced forms
7		River beds, low lying floodplains
8	Coastal zone	Beaches/benches

LEGEND

Geomorphological features and associated geohazards

Lateral Erosion of rivers and streams
Gully (linear) erosion
Abrasion of cemented sedimentary rocks
Abrasion of unconsolidated sediments
Landslides
Mobile talus and rockfalls
Mudflows

Other symbols

Scarp
Man-made mudflow mitigation measures (ditches, dams, water - diversion canals etc.)
Edge of small erosion forms (gullies and hollows)
Study Area
Main roads
Rivers
Inferred watercourses

Russian Sector of South Stream Offshore Pipeline

Proposed landfall section pipelines
Landfall facilities
Proposed microtunnels
Proposed offshore pipelines
Construction corridor
Temporary construction area for road construction
Construction sites
Microtunnel entry shaft
Microtunnel exit pit
Permanent access road to be constructed by SSTTBV
Temporary access road constructed by SSTTBV
Varvarovka bypass road (used by Project during construction only)

United Gas Supply System

United Gas Supply System pipelines
Permanent access road to be constructed by Gazprom Invest

Projection: Lambert Conformal Conic

Purpose of Issue: For Information

Client: South Stream Offshore Pipeline / South Stream ENERGISING EUROPE

Project Title: SOUTH STREAM OFFSHORE PIPELINE

Drawing Title: GEOMORPHOLOGICAL MAP OF THE TERRESTRIAL SURVEY AREA

Drawn	Checked	Approved	Date
AH	IS	IS	04 Mar 2014

URS Internal Project No.	Scale @ A3
46369082	1:15,000

URS Infrastructure & Environment UK Limited
Scott House
Alençon Link, Basingstoke
Hampshire, RG21 7PP
Telephone (01256) 310200
Fax (01256) 310201
www.ursglobal.com

Drawing Number: Figure 7.32

Rev:

Plot Date: 04 Mar 2014
File Name:I:\5004 - Information Systems\46369082_South_Stream\MXDs\Report Maps - Russia\Russian ESIA v2\Chapter 7 Geology\Figure 7-32 Geomorphological Map of the terrestrial survey area.mxd

An example of the gently rolling hills encountered in the Terrestrial Survey Area showing a combination of agricultural fields (vineyards) and woodlands is presented below in Figure 7.33. The ecological habitats are described in **Chapter 11 Terrestrial Ecology**.

Figure 7.33 Typical Undulating Landscape of Terrestrial Landfall Section (Ref. 7.1)

The landfall facilities will be located approximately 1.4 km inland north-east of a steep coastal cliff (approximately 150 m high where crossed by the Pipeline route), on a high level gently sloping 'plateau'. The surface of the plateau is typically gently undulating; however, in places the plateau has been eroded by fluvial processes to form steeply sloped river valleys, up to 150 m deep. Erosion features include hollows, incisions and gullies, which are often steeply sided and are up to 5 to 10 m deep (Ref. 7.1).

7.5.3.1 Fluvial Geomorphology

The fluvial erosion features are typically formed by a process of surface washout and flooding by the ephemeral[7] watercourses. This causes soil sediments and underlying rock to be removed and transported down gradient to form landslide and talus (debris) slope deposits (Figure 7.34).

[7] An ephemeral waterbody is a wetland, spring, stream, river, pond or lake that only exists for a short period following rainfall or snowmelt.

The spring-summer period is characterised by large storms, which often lead to further soil erosion and subsequent aggradation and accumulation of sediments on lower slopes.

Figure 7.34 Erosion Features Associated with the Watercourse in the Graphova Gap (Ref 7.1)

Valley and water channel features associated with ephemeral watercourses and their tributary gullies are also present across the Terrestrial Survey Area. Further details on the watercourses and groundwater within the Terrestrial Survey Area are provided in **Chapter 8 Soil, Groundwater and Surface Water.**

Watercourses in the Terrestrial Survey Area include the Shingar River and an unnamed tributary of the Sukko River (Graphova Gap). Both rivers flow approximately north to south crossing the Project Area, with the route of the proposed pipeline crossing them at approximately right angles. The Pipeline will cross the Graphova Gap by open-cut methods and will be microtunnelled beneath the Shingar River.

In the vicinity of where the proposed pipeline route crosses the Shingar River, the river valley is asymmetrical in shape, and the base of the valley is approximately 55 to 65 m wide. The slope on the eastern side of the valley is approximately 15 to 25°, 30 to 50 m in length and forested. The western side of the valley has been altered due to the construction of the coastal access road. The slope is stepped, with the road constructed on a cut and fill bench approximately 13 to 15 m wide. The western slope is very steep in places (up to 25 to 35°), largely treeless and is subject to slope erosional processes. The Shingar River is typically 1.5 to 2.5 m wide in the vicinity of the pipeline crossing and is located approximately 1.0 to 2.0 m below the adjacent floodplain terrace at the base of the river valley (Ref. 7.1).

Approximately 1.5 km east of the Shingar River, the pipeline route crosses the unnamed tributary of the Sukko River at the Graphova Gap. At this location, the Graphova Gap is asymmetrical in shape, and the base of the valley is approximately 80 to 100 m wide. Valley slopes are 30 to 40 m high and steeply sloped at 20 to 30°. In general, the slopes of the valley are forested; however, there are localised areas of slope that are devoid of vegetation (due to removal associated with economic activity within the valley) that have exposed bedrock and associated erosion processes in the valley sides. On the lower slopes of the valley and associated floodplain are several man-made embankment and ditch features (typically <3.0 m wide and 0.5 to 1.3 m deep) constructed as protection measures to help control storm water flow into valley of the unnamed tributary (Ref. 7.1).

The steep scarp slopes along the Graphova Gap and the Shingar River are subject to fluvial erosion. Erosional scour of 3 m can be expected as well as undercutting and collapse of the banks (Ref. 7.22).

Russia's Black Sea coastal region is known to experience periodic mudflows. The sudden formation of mudflow and mudrock flows is possible in the valleys of the Shingar River and the Graphova Gap and their tributary gullies. Retrospective analysis and reports from locals indicate that mudflows occur once every several (5 to 7) years, each time causing large damage (Ref. 7.5). Mudflows are typically triggered by intense rainfall events or prolonged rain.

7.5.3.2 Coastal Morphology

The coastal cliff is approximately 150 m high in the landfall area of the pipeline crossing and generally convex to a stepped-in profile. The average steepness of the slope is 15° to 25°; however, in places the slope can increase to 40° to 70° (Ref. 7.22). The lower 30 to 50 m of the cliff is typically covered by a talus apron of eroded and abraded loose cliff sediments, with active cliff erosion and rockfall processes having been observed to a height of 120 to 140 m above sea level (Ref. 7.1). Vegetation within the coastal zone is limited to sparse plant cover on the cliffs, rock outcrops and scree slopes associated with the coastal cliffs. At the shore, the beach deposits comprise varied and often poorly sorted sediments ranging from boulders and pebbles to sands and silts. The width of the beach at the foot of the cliff is generally 5 to 15 m wide.

Erosional processes associated with the coastal cliff zone include landsliding and slumping of the coastal cliff and erosion of interbeds of softer sediments exposed in the cliff face (Figure 7.35). Erosion processes along the coastal cliff typically occur as a result of abrasion and weakening of the cliff face from wave action, gravity slumping or tectonic processes (earthquakes or movement along fault planes).

The relatively narrow beach provides limited protection to the base of the cliffs against direct wave action. Wave attack also assists in the removal of material at the toe of the cliffs resulting in periodic landsliding and slumping events (Figure 7.35). In the Terrestrial Survey Area, cliff recession rates are typically 3 to 10 cm per year and the average shoreline recession is calculated to be 41.6 m per century. The microtunnelling approach to the shore crossing (**Chapter 5 Project Description**) mitigates the risks associated with coastal erosion.

Figure 7.35 Examples of Typical Coastal Abrasion Features Associated with Coastal Cliff Landsliding and Erosion of Softer Sediments on the Cliff Face (Ref. 7.1)

There are large-scale rotational slump features along the coast (Ref. 7.22), where material is moving downhill under gravity. These are up to 160 m long and 700 m wide, with hanging walls of up to 15 m. These are regarded as active features. Their rotational failure planes are potentially deep-seated.

A relatively recent landslip has occurred approximately 2 km northwest of the Project Area (Ref. 7.22). This feature has collapsed into the sea causing a local inflection of the coastline. The landslip is about 500 m wide. The toe of the slope extends 60 m into the sea. This landslip is assumed to have failed in a rotational manner. The failure plane may extend below sea level.

Within the coastal area of the Abrau Peninsula located to the south of the Terrestrial Study Area are four landslides, inferred to be earthquake induced, with areas of approximately 3 to 4 km^2 (Ref. 7.1). The heads of the earthquake induced landslides are located on land but the features extend a further 2.0 to 2.5 km out to sea across the coastal shelf.

7.5.4 Marine Geomorphology

The geometry of the sea floor in the Russian Sector of the Black Sea has been mapped using a multi-beam echosounder (SSC FSUGE Yuzhmorgeologiya, 1996-1997). The bathymetry data has been used to assess the marine geomorphology (Ref. 7.5).

From east to west the route of the pipeline crosses three main geomorphological zones through the Russian Sector of the Black Sea: the continental shelf, the eastern continental slope and the abyssal plain. The geomorphological zones are shown in Figure 7.36.

The geomorphology of each zone is discussed in the following sections:

Figure 7.36 Geomorphological Zones of Russian Sector of the Black Sea (Ref. 7.5)

7.5.4.1 Continental Shelf

The Russian continental shelf is gently inclined towards the west at 0.4° and is subdivided into two zones:

- Coastal slope - extending from coastline to 50 m below sea level (mbsl); and
- Coastal platform - extending from 50 mbsl to 100 mbsl.

Sediment cover on the Russian Shelf is typically between 5 to 12 m thick and overlays folded bedrock of carbonate flysch.

The western extent of the Russian continental shelf is bound by a major fault scarp which crosses the Black Sea between Anapa and Gelendzhik, which marks the start of the Continental slope.

Evidence of landslides on the continental shelf has been identified near the Utrish Cape. Elsewhere on the shelf, limited evidence of landsliding has been found. Mudslides in response to earthquakes are anticipated in the base of the continental shelf. Sensitive deposits include the weak silts found close to the brow of the shelf.

7.5.4.2 Continental Slope

Beyond 100 m water depth, the continental slope starts dipping steeply to the west towards the abyssal plain. The transition from the continental shelf to the continental slope is marked by a distinct escarpment.

The shape of the continental slope off Anapa is controlled by bedrock, comprised primarily of the Mesozoic and Neogene Flysch which is also observed along the present coast. Bedrock is at or close to the surface in parallel ridges aligned along the slope. The presence of bedrock at or near the sea floor is the main reason why the continental slope is steep (Ref. 7.5).

In general, the gradient of the continental slope decreases towards the base of the slope (at 1,900 m depth). Gradients can exceed 30° at the shelf break and the continental slope typically varies from 27° at the top to 5° at the bottom.

The geomorphology of the continental slope is characterised by highly dissected dendritic drainage patterns of ridges and canyons. This morphology is the result of cycles of erosion, which caused retreat of the slope and the development of a random network of valleys (Ref. 7.5). The channels are partially filled with mud flow deposits.

The Anapa Canyon is the predominant geomorphic feature on the continental slope in the Study Area (Ref. 7.26). The Anapa Canyon cuts through sediments from the Pleistocene Kuban River delta. The main canyon corresponds with the sediment transport path from the Sea of Azov to the Black Sea and is a relic feature of the estuaries of the Don and Kuban rivers. As the Kuban fan slopes southeast towards the abyssal plain, the toe of the continental slope is found at a progressively lower elevation moving towards the southeast. The canyon itself is an integral part of the submarine delta formed from the Kuban and Don Rivers. The canyon runs parallel to the Russian Black Sea coast from a depth of 200 m to approximately 1,500 m. A further two stable canyons have been identified running down the continental slope and merging with the Anapa canyon at its mouth. The northern slope of the Anapa canyon is steep and itself incised by smaller canyons. The floor of the canyon is further incised by a trough. The canyon is shown in Figure 7.37. The interpreted geomorphology where the Pipeline route crosses the canyon is shown in Figure 7.38.

The upper slope is shown in Figure 7.39. The gullied terrain has rugged topography. The gullies are dendritic (Figure 7.40). The sidescan sonar images (Figure 7.41) suggest the present of coarse sediment in the upslope part of the dendritic gullies (Ref. 7.36). Locally bedrock is exposed in the gully walls (Figure 7.42). Gully system heads form a characteristic 'cauliflower' shape (Ref. 7.36). Upslope, most gullies gradually shallow and die out just below the continental shelf edge. However, some terminate in a distinct headwall scarp that suggests that gullies can propagate upslope by headward erosion (Ref. 7.36).

Downslope, the broad valleys have steep downslope gradients (8 to 10^0) but relatively smooth floors. The valley flows are characterised by sediment waves oriented across the slope. There are frequent large boulders (Figure 7.43) covered only by a thin intermittent sediment drape (Ref. 7.29).

Small carbonate mounds related to fluid seepage can be identified at a few locations along the Russian shelf break at depths between 110 and 140 m (Ref. 7.36); a small number are in relatively close proximity to the Pipeline route (Figure 7.44). These carbonate mounds are usually associated with gas seeps. Gas seeps have been documented in the Black Sea. Some of these seeps are associated with flare reaching up to 500 m from the sea floor, although the majority are between 50 and 130 m high (Ref. 7.36). The majority of gas seeps occur along the shelf break and are often associated with faulting. The principal biogeochemical process forming the concretionary carbonates at the seeps is the sulphate-dependent anaerobic oxidation of methane. This can create reef structures several metres in height. These structures release methane bubbles.

The lower Russian continental slope (Figure 7.45), extending from 1,500 m to about 2,000 m, is generally relatively smooth with a decreasing gradient. The exception to this smooth slope is a marked incision where the Anapa Canyon cuts across the slope, creating a series of scarps at about 1,650 m water depth.

Figure 7.37 Schematic Diagram of Anapa Submarine Canyon (Ref. 7.28)

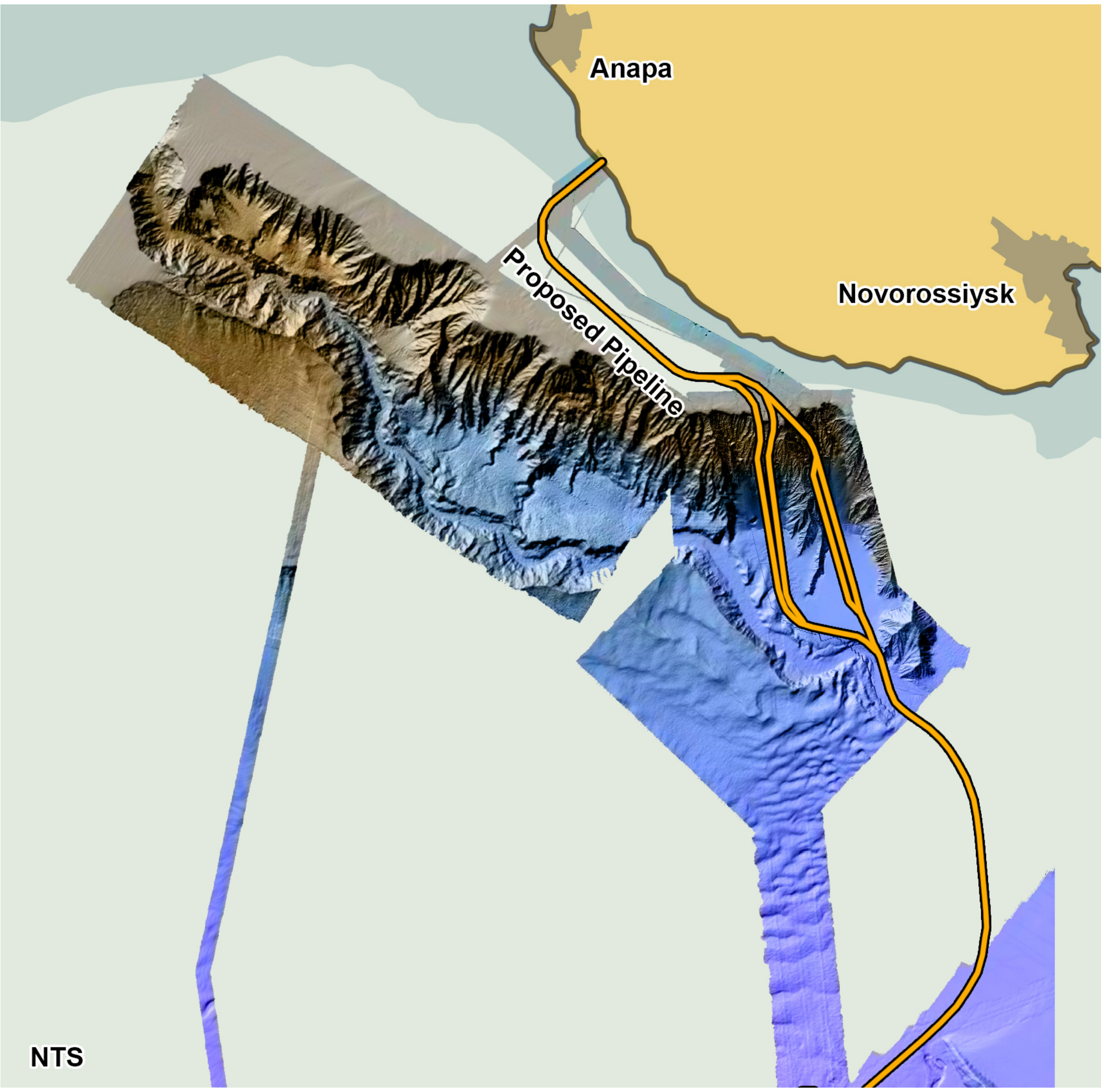

Figure 7.38 Summary Interpretation of Geomorphological Features on Upper Russian Slope (Ref. 7.36)

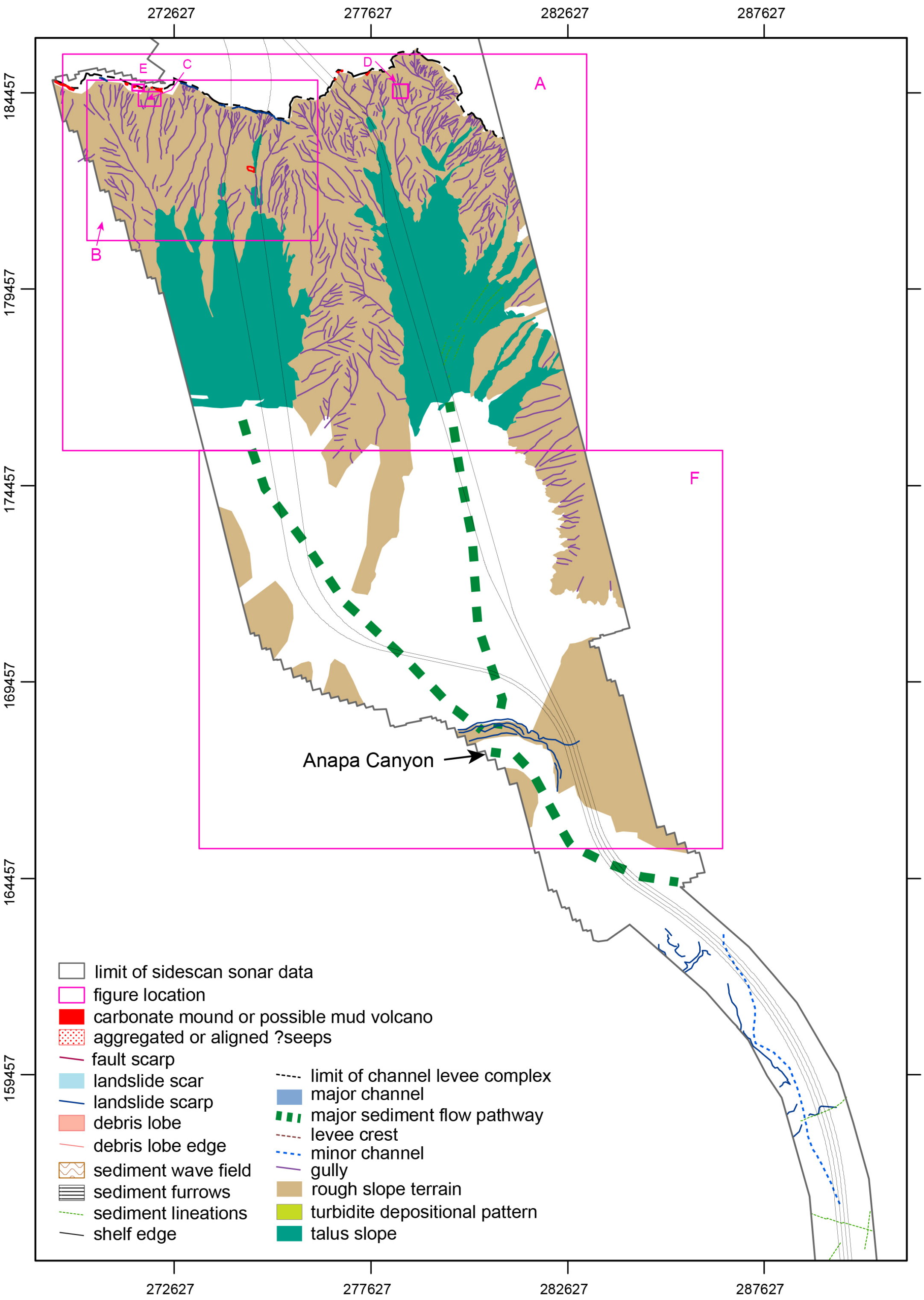

Figure 7.39 3D Representation of the Upper Russian Slope (Location A) (Ref. 7.36)

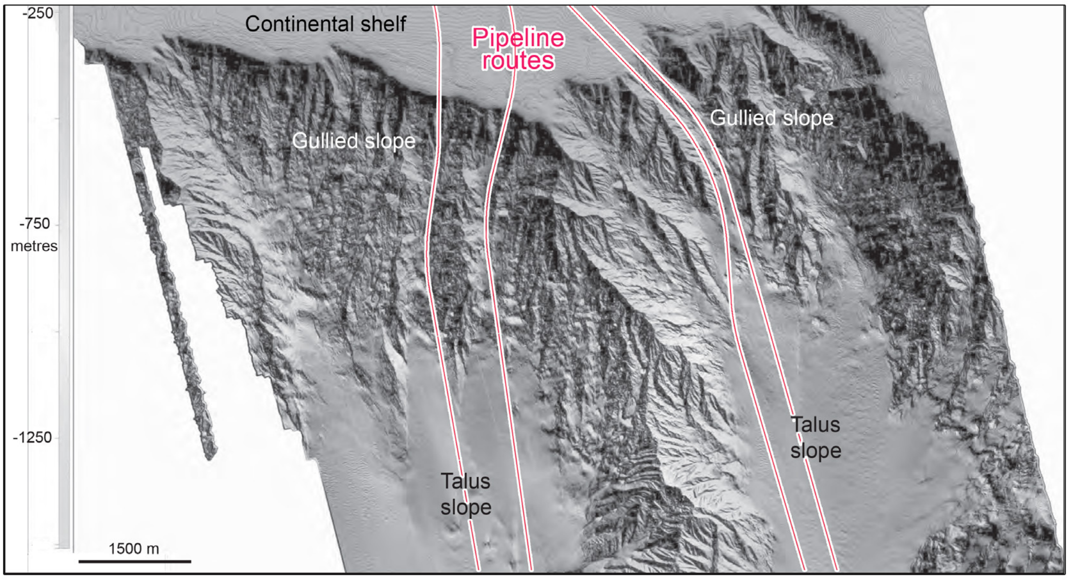

Figure 7.40 Sidescan Sonar Image of Dendritic Gully Systems on Upper Russian Slope (Location B) (Ref. 7.36)

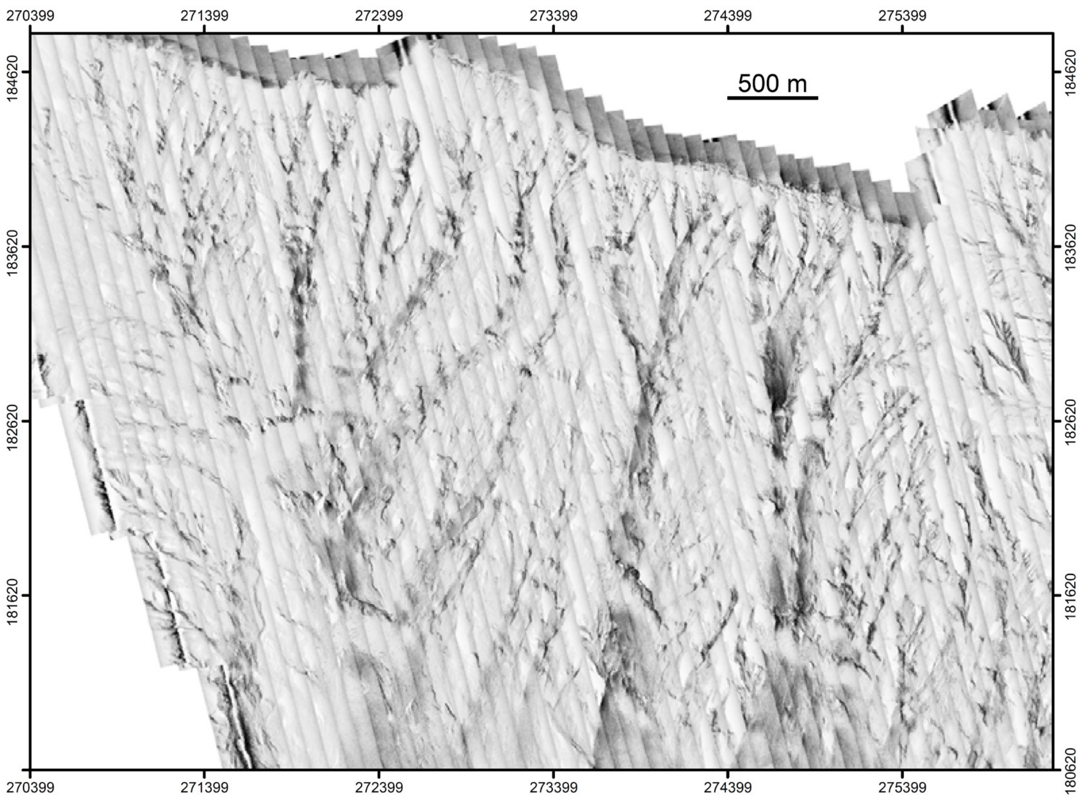

Figure 7.41 Sidescan Sonar Image of Upslope Part of Dendritic Gully System (Location C) (Ref. 7.36)

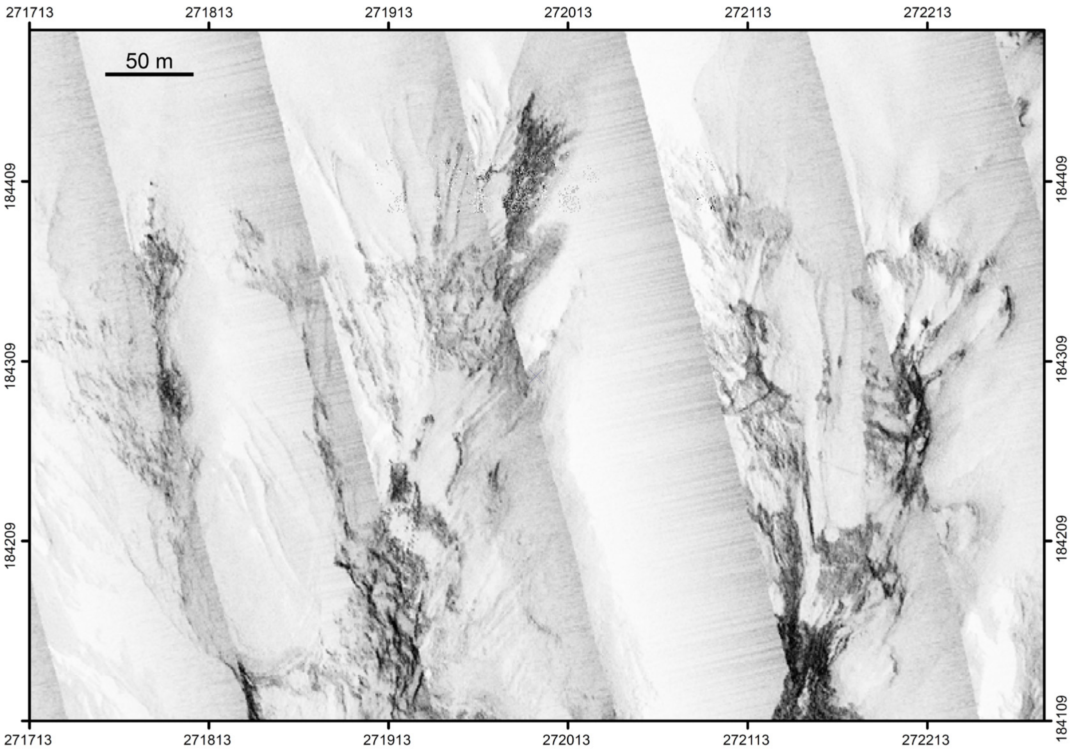

Figure 7.42 Sidescan Sonar Image of Outcropping Bedrock on Gully Walls (Location D) (Ref. 7.36)

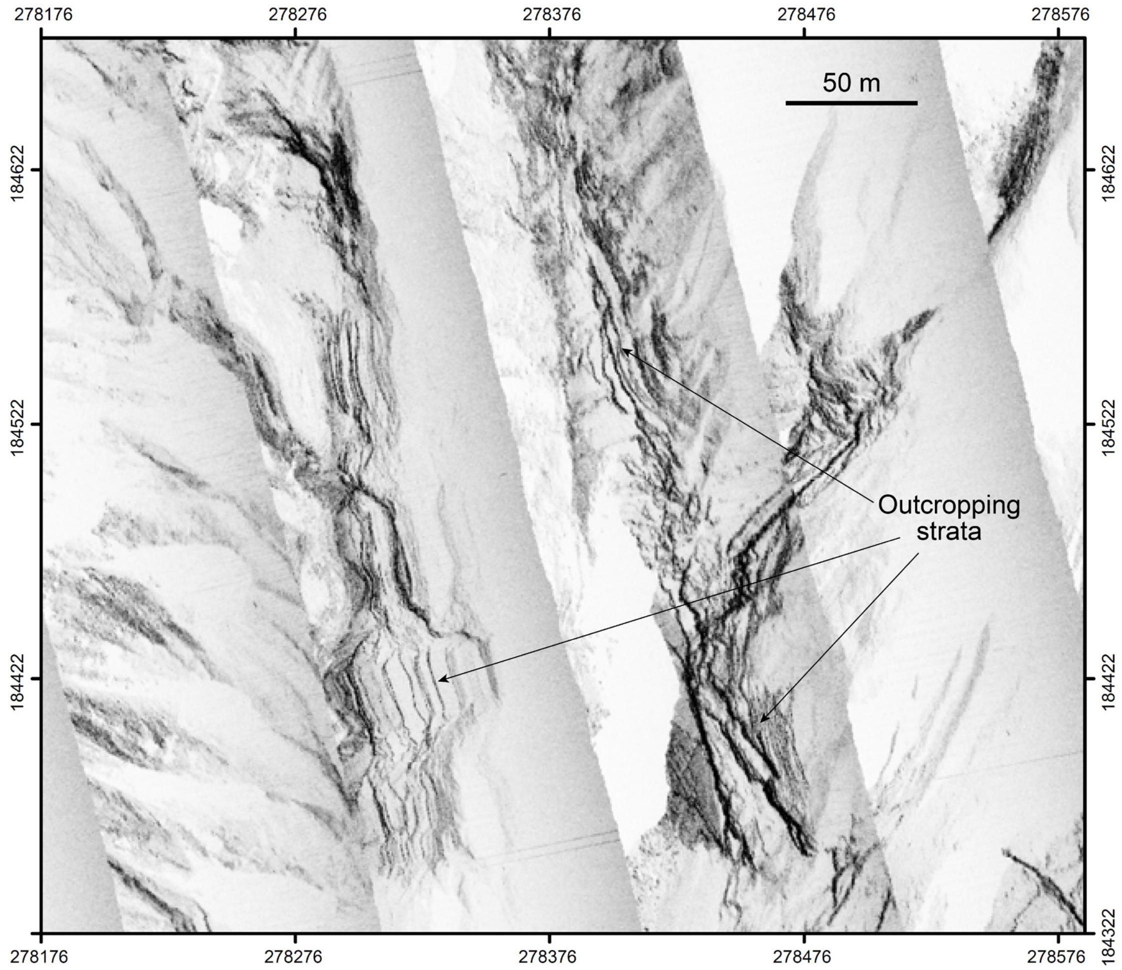

Figure 7.43 ROV Survey Images of Boulders on Upper Russian Slope (Ref. 7.36)

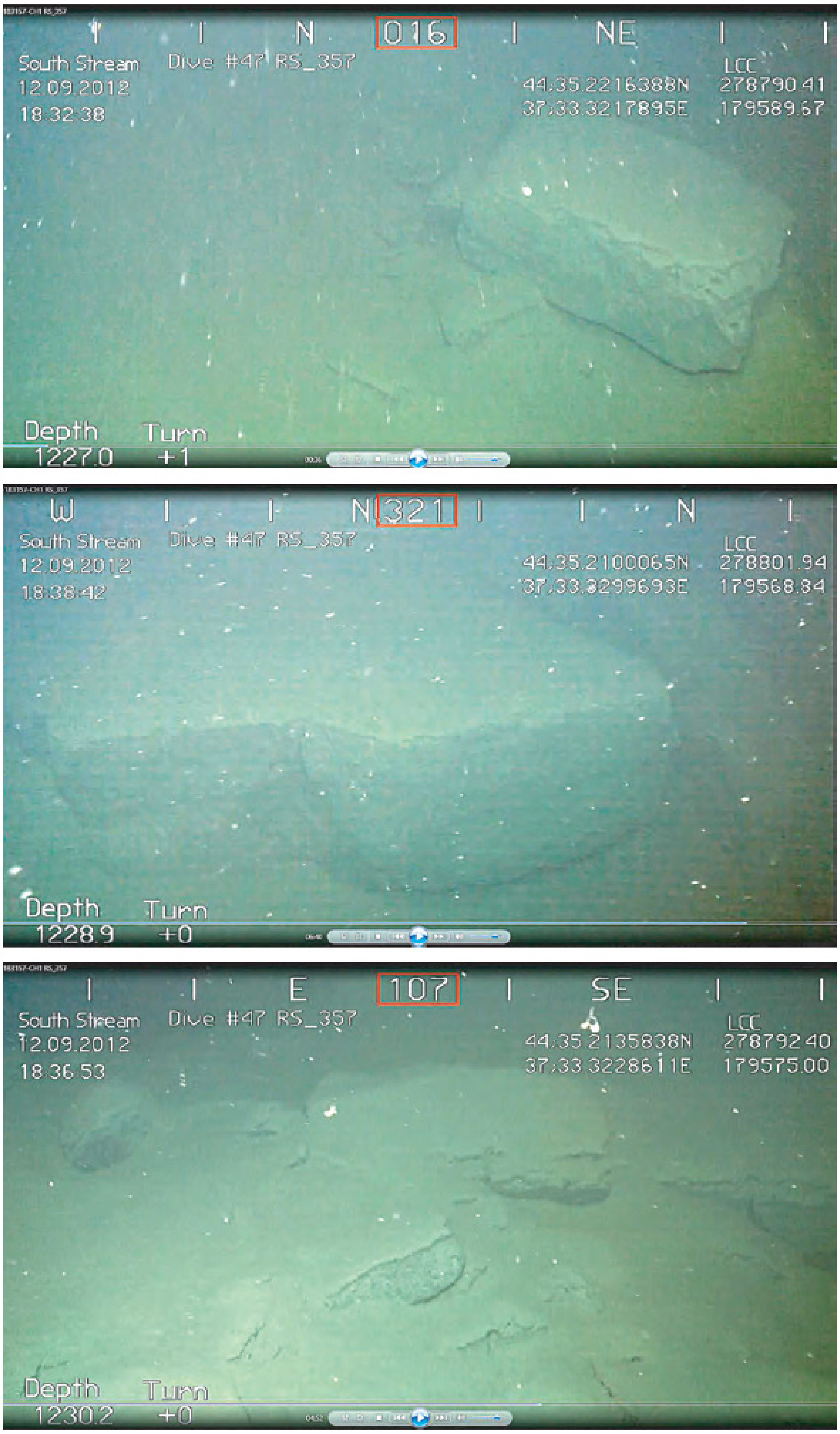

Figure 7.44 Sidescan Sonar Image of Small Carbonate Mounds near Shelf Break (Location E) (Ref. 7.36)

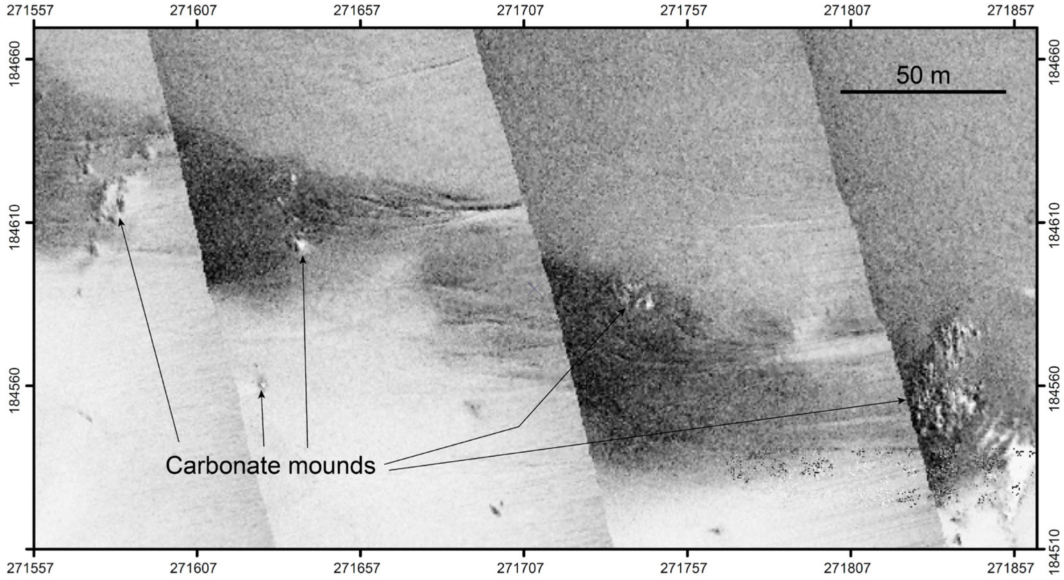

Figure 7.45 Overview of Sidescan Sonar Data for Lower Russian Slope (Location F) (Ref. 7.36)

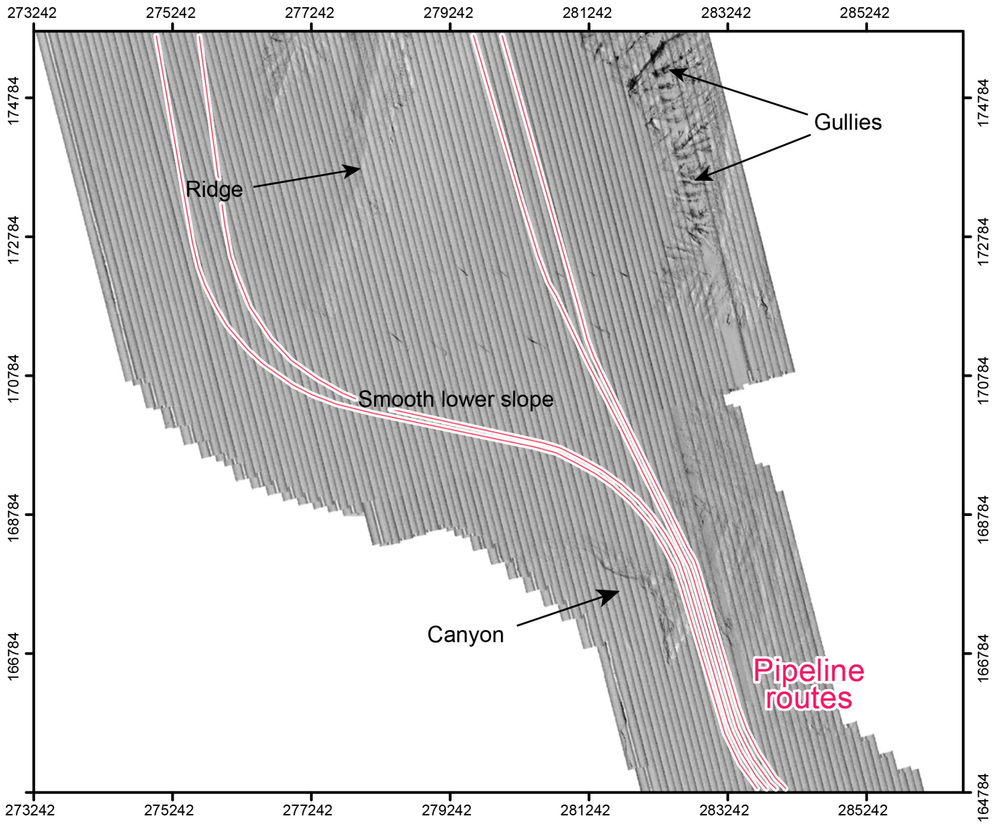

The Anapa Canyon and associated channel is covered by soft sediment, suggesting it is not an active conduit for turbidity currents at the present time. The sedimentary drape is about 1 to 2 m thick, suggesting limited turbidity current activity during the last few thousand years.

The Anapa Canyon appears to continue as a stream of fine sediment extending to the abyssal plain. The regional data shows the channel extends beyond the limits of the continental slope and that sediments from the canyon affect the morphology of the Holocene portion of the Kuban Delta. Recent sediment may be creeping slowly under gravity down the slope in this area of the continental rise.

Downslope from the Anapa Canyon, the slope is characterised by landslide scars and depositional detritus lobes. These are all low relief features with slide scarps typically only a few metres high (Ref. 7.36). Figure 7.46 shows a landslide scarp on the lower Russian slope. This scarp is 2 to 4 m high and may represent a palaeocoastal feature. Figure 7.47 shows debris lobe features on the lower Russian slope. The lobe edges exhibit typical frond-like patterns.

Figure 7.46 Sidescan Sonar Image of Landslide Scarp on Lower Russian Slope (Ref. 7.36)

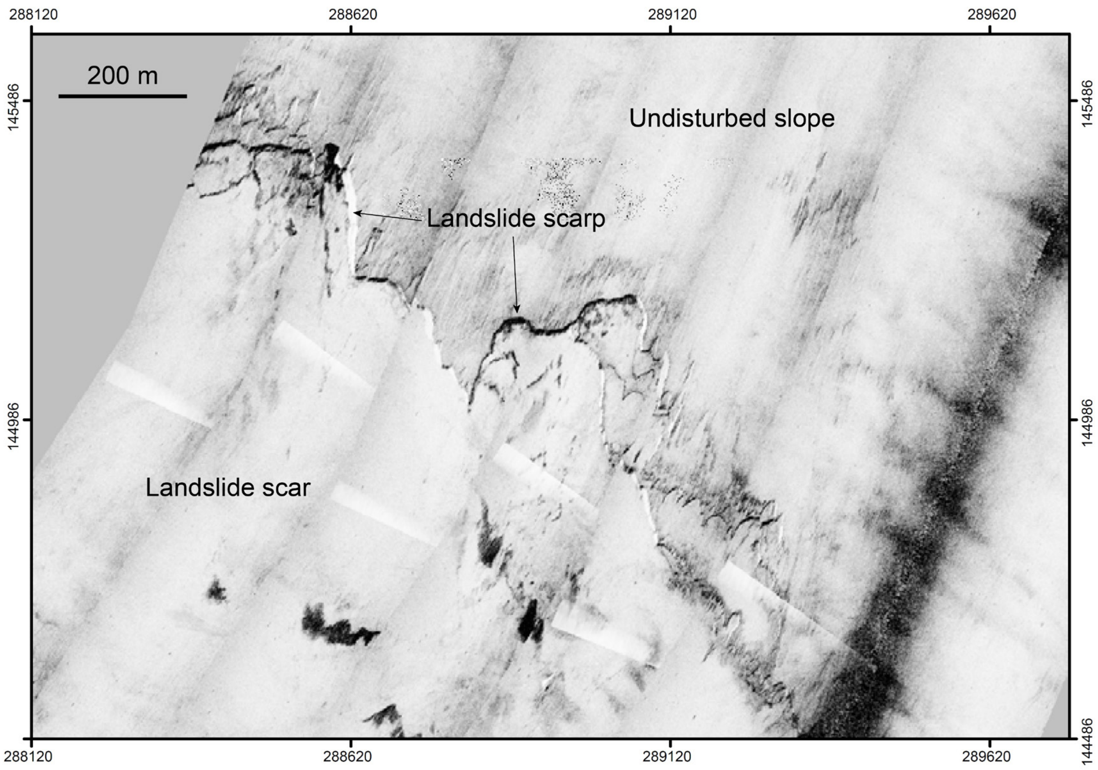

The seabed in the continental slope area is generally characterised by unstable sediments and is often subject to dynamic processes, including gravity flows of sediment towards the abyssal plain (e.g. submarine slumps and associated "turbidite" flows). Instability of the seabed sediment is often triggered by seismic activity and, to a lesser extent, by the sedimentation process itself.

Figure 7.47 Sidescan Sonar Image of Debris Lobes on Lower Russian Slope (Ref. 7.36)

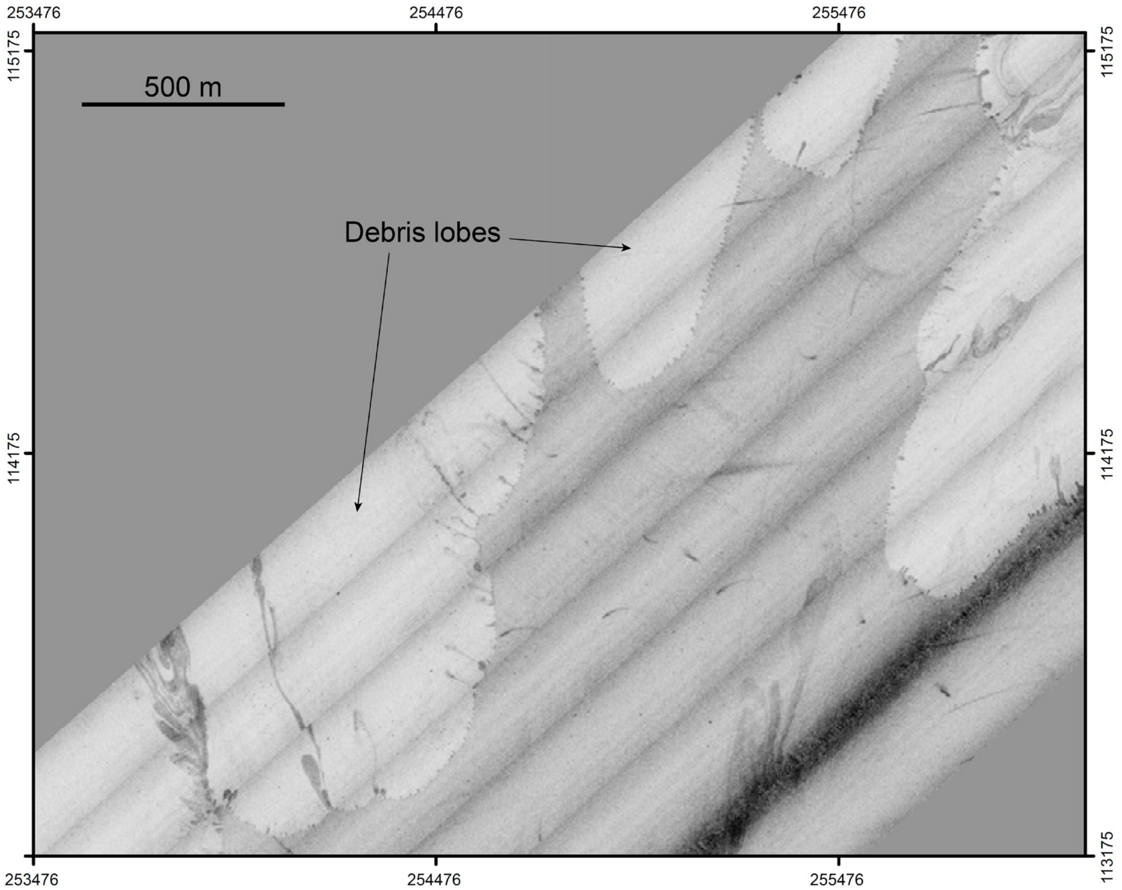

Sediment cover typically comprises very soft clays with some shells, overlaying an unconformity of debris flow deposits and layers of stiff clays and fine sands. The thickness of sediments on the slope is variable, from no sediments present to >20 m of sediment cover. The lower part of the continental slope was denuded in the Pleistocene. There are locally outcrops of basement rocks.

The Anapa canyon has been identified as a key engineering constraint on the continental slope. As described in **Chapter 4 Analysis of Alternatives**, in order to spread the risk associated with the seabed instability on the continental slope, the pipeline route is split such that two pipelines are to be laid down in each of the two stable canyons, with the four pipelines converging again at the mouth of the Anapa canyon.

Landslide activity is most intense in the upper part of the continental slope due to the steeper slope angle. As described in **Chapter 4 Analysis of Alternatives**, the alignment of the pipeline route has been selected following geohazard mapping; the pipeline route is designed to utilise areas with comparatively stable submarine topography as far as is possible.

The pipeline crossing relative to the Anapa Canyon is illustrated in Figures 7.48 and 7.49.

Figure 7.48 Anapa Canyon Crossing

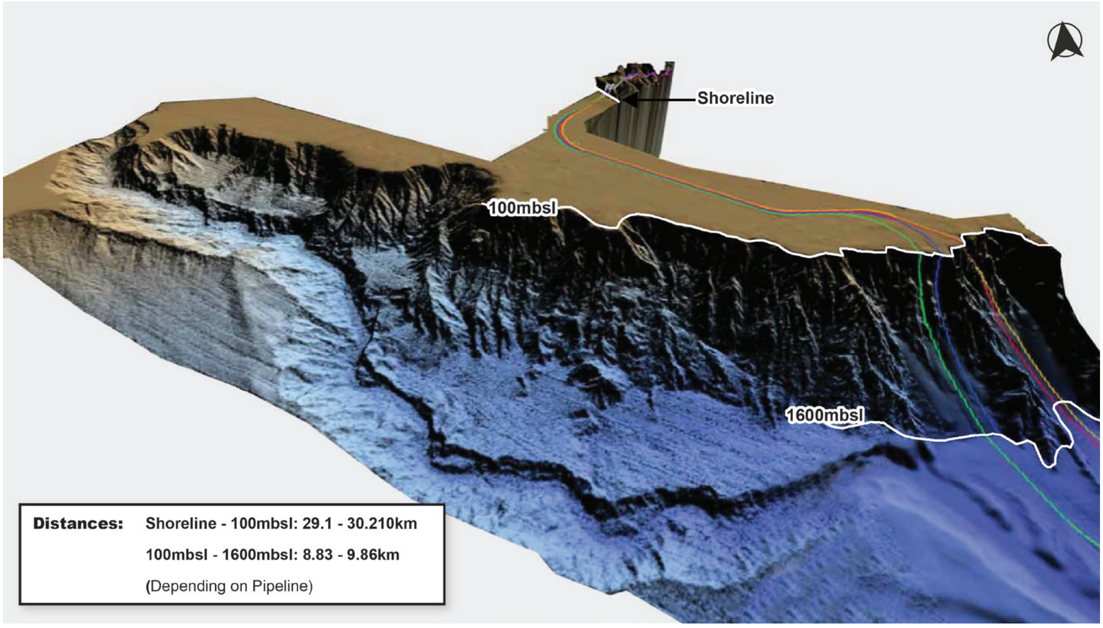

Figure 7.49 Continental Slope Crossing

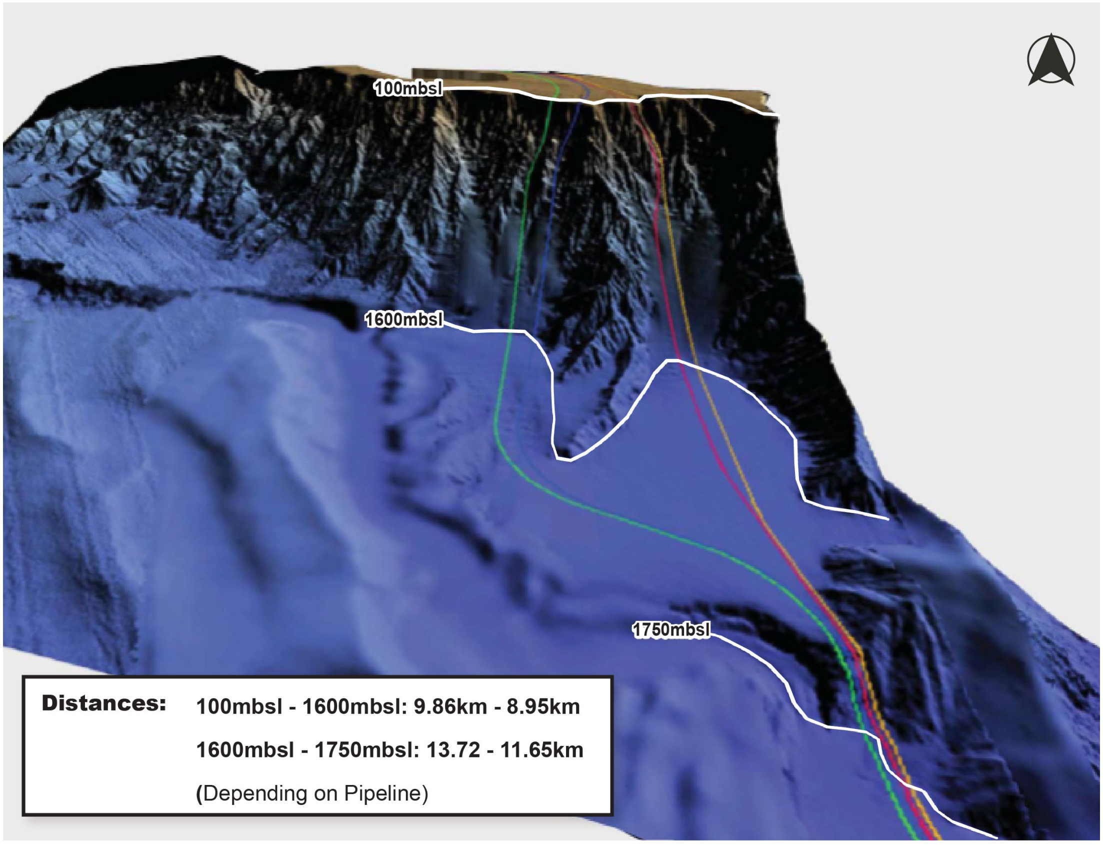

7.5.4.3 Abyssal Plain

The abyssal plain lies at the base of the continental slope and gently slopes to the west to a maximum depth of approximately 2,200 m. From the base of the continental slope, the pipeline route extends across the abyssal plain towards the border of the Russian EEZ with the Turkish EEZ. There is no clear slope break marking the boundary between the lower continental slope and the abyssal plain.

Figure 7.50 shows the typical conditions on the abyssal plain. The sea floor is essentially smooth and almost featureless across the entire area. There are lineations, predominantly trending west northwest approximately parallel to the contours. The pattern of lineations suggests that they are related to the inflow of dense saline water from the Mediterranean into the Black Sea (Ref. 7.36). These features have negligible bathymetric expression, suggesting that they are relatively old features buried by later sedimentation (Ref. 7.36). The lack of topographic relief on the lineations suggests that the process that created them is not currently active (Ref. 7.36). These lineations are associated with irregular marks, which are interpreted to be tool marks due to objects such as trees carried in bottom currents gouging the sea floor.

Figure 7.50 Sidescan Sonar Image of Abyssal Plain Showing Lineations and Tool Marks (Ref. 7.36)

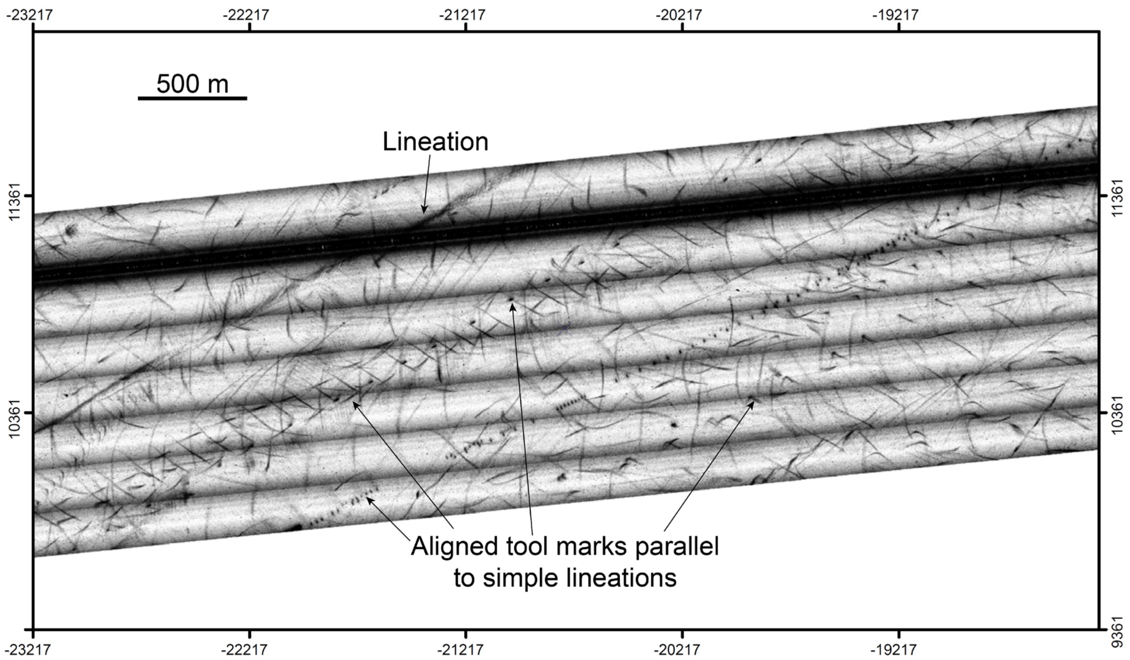

The seabed within the abyssal plain is typically characterised by horizontal layers of carbonate rich silt and / or clay sized sediments.

7.5.5 Marine Sediments

This section presents a description of the sediment transport processes associated with the marine environment and the characteristics of sediments encountered in the nearshore and offshore sections of the Marine Study Area. Further discussion of sediments in the context of marine ecological receptors are presented in **Chapter 12 Marine Ecology**.

7.5.5.1 Sediment Transport

The main sedimentary processes in the Black Sea are associated with the deep-sea fans located off the major rivers, with downslope sediment transport by turbidity currents through canyon systems, with landslides on the continental margins and with the development of mud volcanoes.

Sediment transport processes within the Black Sea are presented below in Figure 7.51. In the offshore section of the Marine Study Area, a north westward drift is evident, while in the nearshore section of the Marine Study Area, the drift is easterly. In the Marine Study Area (nearshore section), littoral drift of eroded sediment occurs in a south-easterly direction with a net drift rate of 19,000 m^3/year (Ref. 7.1).

The majority of the seabed's surface is formed by Quaternary sediments. Due to the absence of major rivers in the coastal area, there is currently minor mass sediment transportation onto the shelf (Ref. 7.26). The main sources of sediment for the Anapa shelf are the Don and Kuban Rivers, which currently discharge through the Kerch Strait from the Sea of Azov (Figure 7.51). Secondary sources are the small rivers flowing from the southern slopes of the Greater Caucasus. Autumn and spring river surges may initiate submarine debris flows locally. High point sources of sediment can be introduced locally onto the shelf by large collapses of the coastal hills (Ref. 7.26). Additionally, a significant proportion of the sediment is of biogenic origin, forming within the marine environment.

The coastal processes where the pipeline route crosses the shore are predominantly represented by abrasion, sometimes complicated with rock falls and rock slides (Ref. 7.1). There is an accumulative relief zone in the coastal waters up to about 30 m water depth (Ref. 7.1) where wave activity transports sediments as is evidenced by the development of ripple marks.

The shelf in the Study Area comprises an abrasion-aggradation plain. Sediment transport at the shelf break and on the continental slope is predominantly due to mass wasting, including landsliding and density currents. On the Russian margin sediment transport via turbidity currents and debris flows was common during the last glacial period, but has been much reduced during the last 9,000 years (Ref. 7.36). Sediment creep has also been observed on the continental slope (Ref. 7.1).

Figure 7.51 Sediment Transport Processes within the Black Sea (Ref. 7.42)

Sediment drift system in the coastal zone
Suspended matter flows in the off shore zone

1 Rioni Depression Zone
2 East Caucasian Zone (Mzimta River - Kodori River)
3 West Caucasian Zone (Kudepsta River - Anapa)
4 Taman - Kerch Zone (Anapa - Feodosia)
5 South Crimean Zone (Feodosia - Balaklava)

Route of Proposed Pipeline

The MBSC may not have the capacity to initiate sediment motion on the seabed, but will influence a) the fallout patterns of fine suspended sediments entering the area and b) the residual trajectory of sediment suspended in the nearshore area by wave action.

Mud flows along the sea bed are characteristic of the south-eastern part of the Marine Study Area. They are common on the continental slope and the abyssal plain. These mud flows are fastest close to the sea bed, with maximum values of around 3 m/s but more typical values are less than 0.15 m/s.

Seismicity in the region is directly related to sediment transport processes:

- At the shelf break, deposits that have slowly accumulated over time can be 'shocked' into motion as sediment-gravity flows (liquefaction). Slumps occur, some on a very large scale, which may turn into turbidity currents which, through long periods of activity, carve the canyons that are found on the steep slope areas. This is an important process by which, over geological time, shelf sediments are transferred to abyssal depths;
- Fault movement below deep recent sedimentary deposits can cause bed surface features such as fault-aligned ridges, and mud volcanoes (faults triggering gas release). Faults also often control the alignment of major features (canyons, scarp slopes); and
- Fault movements can cause tsunamis, which produce sediment transport in littoral zones.

7.5.5.2 Sediment Composition

Typically the sediments of the Marine Survey Area (nearshore section) comprise a mix of stones, gravels and sands. The sands typically have a bulk density of 1.6 to 2.0 g/cm^3 and a porosity of 23 to 25% (Ref. 7.1). Bedrock outcrops locally in the shallow waters. Additional sediment type data were collected during the 2013 marine survey (Ref. 7.8). Photographs of the sea bed taken during the survey are presented in Figure 7.52. Table 7.22 presents the sediment type of sampling locations based on the classification proposed by Folk (Ref. 7.41), which groups sediment grains into mud, sand and gravel on the basis of their diameter. The relative proportion of the sediment grains in the three categories is then used to describe the sediment.

Coastal sample locations were dominated by rock and sand deposits. Continental shelf locations dominated by mud with a limited number of samples containing sand and gravel grains. The continental slope samples were all classified as mud.

In the fans of the Kuban and Don Rivers on the continental slope, contemporary and Upper Holocene (Nymph) sands are also occasionally encountered.

Figure 7.52 Photographs of Seabed Sediments in Coastal Waters (Ref. 7.8)

a) Photograph at N 44⁰48.559' E 37⁰21.435'. Water depth 10.1 m

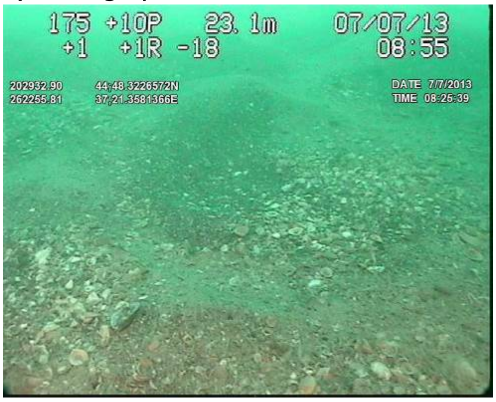

b) Photograph at N 44⁰48.322' E 37⁰21.358'. Water depth 23.1 m

c) Photograph at N 44⁰48.146' E 37⁰21.080'. Water depth 33.7 m

Table 7.22 Sediment Type Groupings[8] of 2013 Marine Survey Sediment Type Data (Ref. 7.8)

Sediment Type	No. of Samples	Depth Range (m)	Average Depth (m)
Coastal (72 samples in water depth 0-25 m)			
Rock	46	3.7 – 19.7	10.4
Gravelly Sand	4	20.5 – 21.7	20.95
Sandy Gravel	4	21.7 – 22.2	22
Muddy Sandy Gravel	3	24.5 – 24.7	24.6
Gravel	14	19.4 – 26.7	23.8
Muddy Gravel	1	16.9	16.9
Continental Shelf (112 samples in water depth 33-113 m)			
Sandy Mud	12	33.2 – 68.6	56.3
Mud	82	50.6 – 110.8	71.2
Slightly Gravelly Sandy Mud	10	68.9 – 113.1	86.7
Slightly Gravelly Mud	4	89.7 – 91.1	90.4
Gravelly Mud	3	53.2 – 56	54.8
Muddy Gravel	1	52.9	52.9
Continental Slope (16 samples in water depth > 364 m)			
Mud	16	364.8 – 572.9	485.5

There are clays and clay loams in the lower strata of the Quaternary section, which locally intersect with the shelf's brow and the upper part of the continental slope, and also the lower part of the shelf.

The reported thickness of the clay and silt sediments in the Caucasian shelf reaches 10 m. In the Taman zone of the shelf the silts are 20 m or more thick. The clays are grey and dark-grey, silty and calciferous. The bulk density ranges from is 1.39 to 2.02 g/cm^3. The porosity is

[8] Based on Folk Classification (Ref. 7.41).

typically around 65% and the natural moisture content of the shelf muds ranges from 31 to 117% (Ref. 7.1). The typical composition of the clay sediments is summarised in Table 7.23.

Table 7.23 Typical Composition of Clay Sediments on Continental Shelf (Ref. 7.1)

Parameter	Category	Typical Proportion (%)
Grain Size (mm)	0.005 – 0.010	56 - 65
	0.01 – 0.05	29 - 36
	>0.05	3 – 8
Grain Type	Clays	52.4
	Quartz and Feldspars	8.5
	Rock Fragments	14.4
	Organic Material	2.3
	Authigenic Calcite	6.7
	Sulphides	20.5
Clay Minerals	Illite	63 - 69
	Chlorite and Kaolinite	25 - 29
	Montmorillonite	6 – 10

Within the continental slope and abyssal plain unconsolidated water-saturated organic silts dominate. The thickness of the sediments on the slope is variable from no sediments present to several metres of sediment cover. The thickness of these sediments penetrated by the sampling is 6 m. The sediments in the deep abyssal plain typically have a high rate of sedimentation in the eastern Black Sea of between 0.2 – 0.4 m per thousand years (Ref. 7.5).

The variations in sea level over the history of the Black Sea (Section 7.4.4) are reflected in the marine sediment profile on the continental slope and abyssal plain (Ref. 7.36). In summary the most recent pelagic sediment layers in the Black Sea can be divided into:

- Unit I, the upper horizon approximately 30 cm thick, is a micro-laminated sediment, rich in plankton derived carbonates (coccoliths), with relatively low levels of organic carbon. This unit was deposited in oxygen depleted bottom waters;

- Unit II sediment (ca. 30 to 70 cm below the surface) is a micro-laminated sapropel[9] deposited under anoxic marine conditions between approximately 2,700 and 7 to7,700 years ago in waters deeper than 200 m. The onset of Unit II is characterized by the occurrence of thinly laminated layers rich in aragonite crystals and by a sharp increase in Total Organic Carbon;
- Transitional unit, marking the transition from lacustrine to marine conditions. This unit varies across the basin; and
- Unit III sediment, below approximately 70 cm, is older than 7,000 years and was deposited when the Black Sea was an oxic freshwater lake, and are characterised by mix of organic-poor clays and silts. Unit III sediments have organic contents <1%.

Above Unit I sediments lies a discrete proto-white lamina layer (about 2 cm thick), and above this lies a discrete benthic flocculant layer, also known as flocs or as the "fluff layer", also about two cm thick. The flocculant layer has been observed to be largely composed of lithogenic material derived from the surrounding rivers (47%), carbonates derived from coccoliths (31%) with the remains of diatom and silicoflagellete blooms (7%) and particulate organic carbon, e.g. faecal pellets (6%). The proto-white laminae layer is composed of coccoliths (46%), lithogenic material (33%), the remains of diatom and silicoflagellate blooms (4%) and particulate organic carbon (7%). On the abyssal plain, the most recent flocs form black, mat-like aggregations form black, mat-like aggregations, sometimes with an outer lighter-coloured rim, that collect in subtle bathymetric lows (Ref. 7.36).

The transition from the continental slope to the abyssal plain is typically characterised by a smooth transition in sediment geology, with the sediments of the abyssal plain being characterised by a higher mineral composition.

The surface horizon of the silts (Unit I) alternates between terrigenous aleuropelite silts with a thickness up to 5 to 7 cm and coccolith-sapropel pairs with a thickness ranging from 1 to 3 mm up to 2 to 3 cm (Ref. 7.1). These are also known as "turbidite" deposits. The layer of sapropel silt contains up to 20% organic carbon. The turbidite deposits are green-grey and dark grey and range from indistinctly stratified to finely layered. The sediment is viscous at the surface and soft plastic at depth. There is a characteristic hydrogen sulphide odour.

The silts often include inclusions of hydrotroilite, coccolith ooze, sapropel, and shell and plant detritus. The latter are usually sulphidised with micro-crystals of pyrite. Gas is present as bubbles and is also evident through sediment bulking. Again, there is a characteristic hydrogen sulphide odour. The typical composition of the silts is summarised in Table 7.24.

The majority of the deep water sediments are clays and silts. There is a regular compacting process of the silts with depth in the sediment profile. In the depth interval 0 to 0.1 m from the seabed, the silts are viscous and viscous-plastic; with depth the sediments are compacted, gradually becoming soft-plastic (Ref. 7.1).

---

[9] Sapropel (organic-rich sediment) is produced when high levels of surface water productivity deposit organic matter into oxygen depleted bottom waters where the organic matter cannot be consumed.

Table 7.24 Typical Composition of Silt Sediments on Continental Slope (Ref. 7.1)

Parameter	Category	Average Proportion (%)
Grain Size (mm)	0.005 – 0.010	45
	0.01 – 0.05	55
	>0.05	0.38
Grain Type	Clays	13
	Quartz and Feldspars	34
	Rock Fragments	6
	Organic Materials	14
	Secondary Minerals (mica, terrigenous calcite, glauconite, chlorite, epidote-zoisite, amphiboles, pyroxenes)	10
	Accessory Minerals (garnet, tourmaline, sphene, apatite, zircon etc.)	0.2
	Authigenic Calcite	3
	Sulphides	19

The organic-rich sapropel and coccolith horizons are described as micro-layered jelly-like viscous sediments. Carbonate concentrations range between 1 and 57%. Organic matter content ranges from 4 to 36%.

The geotechnical properties of the silt depend on the degree of compaction, which, in turn, is related to the depth of the sediments. Sediment density increases with depth in the sediment profile. The viscosity coefficient of the sediments also decreases with depth. The bulk density of the abyssal plain deposits ranges from about 1.3 g/cm^3 at the sea bed to about 1.5 g/cm^3 at 50 cm depth. Moisture content also varies with lithology and depth. The natural moisture content of the abyssal plain sediments ranges from about 350% at the sea bed to about 125% at 50 cm depth. Sapropel sediments often have particularly high moisture contents, often exceeding 400% and sometimes reaching 550 to 600%.

Gas saturation of the sediments predominantly occurs in the silt deposits. Sources of gases may be migration flow of hydrocarbons from deeper parts of the section (particularly in the Taman Shelf), the gas draining from gas hydrate formations, or the build-up of diagenetic gases due to an excess of organic matter along buried palaeo shore lines (particularly along the shelf between Novorossiysk Bay to Sochi). Carbonate mounds, which are likely to be associated with gas seeps, have been locally identified near the shelf break.

Gas hydrates are commonly present in water depths below about 620 m although occasionally they have been identified in shallower waters (Ref. 7.36).

The concentration of gases (primarily methane) in the sediments is variable, ranging from 0.0107 to 7.1169 cm^3/kg with a typical local background value of 0.0285 cm^3/kg. With depth, the gas content rises by a factor of 1.5 to 2.5 but concentrations can be locally anomalously high, with concentrations being orders of magnitude higher than typical background values.

7.5.5.3 Sediment Quality

A known feature of the Black Sea basin is the presence of hydrogen sulphide (H_2S). The widespread presence of H_2S at depths over around 100 m is controlled by the redox environment. The shelf sediments are typically oxidised whereas the slope sediments are typically poorly reductive (Eh values -100 to +50 mV) but locally poorly oxidising (Eh values +50 to +300 mV); the latter are thought to be due to the influence of landslides and sediment wash. The sediments on the abyssal plain and in the fan of the Kuban and Don Rivers are highly reducing (Eh <-300 mV).

Contemporary Black Sea sediments together with their significant content of organic matter are characterised by high values of concentrations of sulphur and its reduced forms. The main form of accumulation of reduced sulphur in these sediments is pyrite (FeS_2). Pyrite is formed in the process of the sediments' diagenesis from hydrotroilite ($FeS \bullet H_2O$) under its reaction with molecular sulphur.

In deep-water sediments, around 90% of the aggregate amount of reduced sulphur is present in the form of pyrite, which sometimes forms microconcretions (Ref. 7.1). In the silts on the continental slope, where there is an intense sulphate reduction process, there is an upper layer with a significant amount of hydrotroilite and free hydrogen sulphide. The latter's content in the slopes' silts reaches 100 mg/kg, while in deep-water sediments it is usually 3 to 5 mg/L. In the majority of sediments, the molecular-sulphur content is 200 to 300 mg/kg, or 6 to 8% of the aggregate content of sulphur compounds.

The pH of the continental slope sediments ranges from 6.98 to 8.12 with an average value of 7.54. The pH of the abyssal plain sediments is relatively even, ranging from 7.43 to 7.77 with an average value of 7.57.

Previous surveys in the area have identified the presence of contaminants in the marine sediments. Contaminants previously identified include petroleum hydrocarbons, phenols, anionic surfactants and heavy metals. Concentrations were typically highest near the coast, particularly in the vicinity of the main towns.

In addition, some heavy metals (e.g. iron, manganese) are naturally present in relatively high concentrations in the marine sediments in deep waters owing to the prevailing redox environment.

The level of sea bed pollution depends on many factors. These are mainly the lithological type of the deposit, particle sizes, the depth of the sea, the properties of the polluting substances (pollutants) and the level of their arrival from the coast, hydrological conditions, the system of currents, etc.

For the Caucasian coast of the Black Sea, which has a narrow shelf, pollutants in suspension are carried beyond the shelf, to the foot of the slope, where, as a rule, their greatest concentrations occur. In the shallow water of the coastal zone the highest concentration of terrigenous material is found. In this zone there is a greater degree of disturbance of sediment and a greater amount of oxidation taking place. This results in a more intensive self-purification of the sediment; these factors become weaker with distance from the shore.

Sediment sampling was undertaken in the 2010, 2011 and 2013 surveys (Ref. 7.1, 7.8) to assess concentrations of potential pollutants; the results are summarised in Table 7.25 (2010 and 2011 samples), Table 7.26 (2013 grab samples) and Table 7.27 (2013 sediment cores). In the absence of appropriate Russian standards for the assessment of marine sediments, international standards for contaminated sediments (target values of the "Dutch List") (Ref. 7.18) were used to benchmark the quality of marine sediments. The values selected are referred to here as adopted marine sediment standards (AMSS).

Elevated phenol concentrations were identified in the majority of the samples. Concentrations of phenol were typically higher in the deep water samples compared with those from the nearshore environment. The elevated phenols may be derived from anthropogenic sources or may also be associated with natural organic matter in the sediment.

Anionic surfactants were detected in every sediment sample. Concentrations were typically higher in the deep water samples compared with those from the nearshore environment; concentrations were observed to rise with distance from the shore. The anionic surfactants are likely to be derived from anthropogenic sources.

Petroleum concentrations did not exceed the AMSS in the coastal sediment samples. Petroleum concentrations exceeded the AMSS in three out of six samples from the continental shelf and in two out of eight deep water samples. The elevated concentrations of petroleum may be derived from anthropogenic sources or may also be associated with natural organic matter in the sediment or natural hydrocarbons (oil and gas) beneath the Black Sea.

Whilst heavy metals have been detected in the marine sediments and locally exceed the AMSS, the results should be reviewed in the context of the natural geochemical setting. Organic silts and clays in reducing conditions might be expected to naturally have some heavy metals present - e.g. iron is naturally present in the form of pyrite and troilite. The sediment quality data should be viewed in this context. Metal concentrations were typically higher in the shelf and deep water samples than in the coastal samples. This is likely to reflect the change in sediment lithology and redox environment with increasing water depth and distance from the shore.

Table 7.25 Summary of Contaminants in Marine Sediments for 2010-2011 (Ref. 7.1, 7.18)

Parameter	AMSS	Shallow Water Coastal Area		Continental Shelf		Deep Water (Continental Slope and Abyssal Plain)	
		Measured Range	No. Exceeding AMSS	Measured Range	No. Exceeding AMSS	Measured Range	No. Exceeding AMSS
		(mg/kg)	(out of 15)	(mg/kg)	(out of 6)	(mg/kg)	(out of 8)
Phenol	0.05	0.05 – 0.40	14	0.01 – 0.37	5	0.40 – 0.68	8
Anionic Surfactants	NA	0.2 – 2.9	-	3.9 – 16.0	-	2.7 – 19.2	-
Petroleum Products	50	0.010 – 0.209	0	18 - 108	3	12 - 407	2
Arsenic	29	0.36 – 0.64	0	2.3 – 3.5	0	1.3 – 5.6	0
Cadmium	0.8	0.12 – 0.48	0	0.05 – 0.22	0	0.02 – 0.661	0
Chromium	100	5.24 – 8.75	0	5.5 – 21.11	0	8.75 – 20.7	0
Copper	35	3.26 – 8.56	0	5.73 – 34.15	0	12.9 – 50.8	6
Iron	NA	3.1 – 13.1	-	3.09 – 18.4	-	13.79 – 26.76	-
Lead	85	0.95 – 19.8	0	8.05 – 24.6	0	5.7 – 23.6	0
Manganese	NA	0.11 – 0.23	-	0.83 – 0.37	-	0.435 – 0.662	-
Mercury	0.3	0.007 – 0.037	0	0.014 – 0.087	0	0.017 – 0.084	0
Molybdenum	10	<0.001	0	0.001 – 0.008	0	0.001 – 0.007	0

Continued...

Parameter	AMSS	Shallow Water Coastal Area		Continental Shelf		Deep Water (Continental Slope and Abyssal Plain)	
		Measured Range	No. Exceeding AMSS	Measured Range	No. Exceeding AMSS	Measured Range	No. Exceeding AMSS
		(mg/kg)	(out of 15)	(mg/kg)	(out of 6)	(mg/kg)	(out of 8)
Nickel	35	1.3 – 9.0	0	0.95 – 31.48	0	13.7 – 38.3	2
Selenium	NA	<0.1	-	<0.1	-	<0.1	-
Zinc	140	12.9 – 28.1	0	16.4 – 75.4	0	26.9 – 69.5	0

Complete.

Copper concentrations exceeded the AMSS in six out of eight deep water samples. Nickel concentrations exceeded the AMSS in two out of eight deep water samples. Although these samples had concentrations that were elevated above the AMSS, the measured concentrations are within the typical range for Black Sea sediments and thus do not necessarily indicate anthropogenic pollution. Heavy metal concentrations were typically higher in the Gelendzhik / Anapa region of the shelf and slope than in the rest of the Marine Survey Area.

Table 7.26 Summary of Contaminants in Marine Sediments from 2013 Grab Samples (Ref. 7.8, 7.18)

Parameter	AMSS (mg/kg)	Shallow Water Coastal Area		Continental Shelf		Deep Water (Continental Slope)	
		Measured Range	No. Exceeding AMSS	Measure d Range	No. Exceeding AMSS	Measured Range	No. Exceeding AMSS
		(mg/kg)	(out of 14)	(mg/kg)	(out of 25)	(mg/kg)	(out of 4)
Aluminium	NA	450 – 1300	NA	3600 – 8300	NA	6900 – 9300	NA
Arsenic	29	5– 17	0	2.6 – 6.4	0	3.6 – 4.6	0
Cadmium	0.8	0.038 – 0.096	0	0.058 – 0.2	0	0.13- 0.33	0

Continued...

Parameter	AMSS (mg/kg)	Shallow Water Coastal Area		Continental Shelf		Deep Water (Continental Slope)	
		Measured Range	No. Exceeding AMSS	Measure d Range	No. Exceeding AMSS	Measured Range	No. Exceeding AMSS
		(mg/kg)	(out of 14)	(mg/kg)	(out of 25)	(mg/kg)	(out of 4)
Chromium	100	2.2 – 4.1	0	4.5 – 8.3	0	6.5 – 8.1	0
Copper	35	2.4 – 7.7	0	4.9 – 27	0	18 - 33	0
Lead	85	1.8 – 5	0	6.6 – 26	0	8.1 – 27	0
Mercury	0.3	0.004 – 0.015	0	0.017 – 0.062	0	0.028 – 0.055	0
Nickel	35	2.3 – 9.9	0	7.3 – 21	0	18 – 22	0
Selenium	NA	<0.5	-	<0.5	-	<0.5	-
Zinc	140	14 – 42	0	29 – 99	0	46 - 70	0
Petroleum Products	50	<5 – 5.5	0	<5 – 110	6	<5 – 42	0
Total PCB (Sum 7)(µg/kg)	20 (µg/kg)	0.11 – 0.91	0	0.25 – 3.8	0	0.73 – 3.5	0
BETX (µg/kg)	NA	<10	-	<10	-	<10	-
Total PAH (Sum 10) (µg/kg)	1000 (µg/kg)	1.68 – 21.37	0	1.3 – 340.92	0	84.39 – 239.12	0

Complete.

From the 2013 sediment analyses petroleum products were the only parameter to exceed the AMSS in the grab samples (Ref. 7.8). The AMSS was exceeded at 6 out of 25 locations on the continental shelf with no exceedances from coastal or continental slope samples.

Similar to the 2010 and 2011 surveys, parameter concentrations increased with increasing water depth with the highest concentrations recorded in the continental shelf and continental slope samples with the exception of arsenic, which showed the highest concentration in coastal samples.

Table 7.27 Summary of Contaminants in Marine Sediments from 2013 Core Samples (Ref. 7.8, 7.18)

Parameter	AMSS	Shallow Water Coastal Area		Continental Shelf	
		Measured Range	No. Exceeding AMSS	Measured Range	No. Exceeding AMSS
		(mg/kg)	(out of 6)	(mg/kg)	(out of 8)
Aluminium	NA	640 – 990	NA	5000 – 9100	NA
Arsenic	29	11– 28	0	3.5 – 5.6	0
Cadmium	0.8	0.035 – 0.055	0	0.12 – 0.16	0
Chromium	100	2.9 – 3.4	0	6 – 7.4	0
Copper	35	2.6 – 11	0	16 – 26	0
Lead	85	2.8 – 4.7	0	8.3 – 21	0
Mercury	0.3	0.004 – 0.07	0	0.032 – 0.057	0
Nickel	35	4.5 – 9.7	0	16 – 22	0
Selenium	NA	<0.5	-	<0.5	-
Zinc	140	22 – 41	0	42 – 64	0
Petroleum Products	50	<5 – 150	1	<5 – 54	1
Total PCB (Sum 7)(µg/kg)	20(µg/kg)	0.12 – 0.2	0	0.17 – 1.74	0
BETX (µg/kg)	NA	<10	-	<10	-
Total PAH (Sum 10) (µg/kg)	1000(µg/kg)	1.24 – 11.58	0	18.47 – 146.58	0

Concentrations of petroleum products were again the only parameter to exceed the AMSS in the core samples from proposed areas of dredging and seabed intervention. Exceedances occurred in 1 of 6 samples from the coastal samples in the proposed dredging area (location 17, top half of core = 150 mg/kg) and 1 of 8 samples from the seabed intervention areas on the continental shelf (location 38, top half of core = 54 mg/kg).

7.6 Conclusion

This chapter has provided a description of the physical and geophysical environment associated with the Project. Further, detailed baseline studies have been undertaken as part of each of the assessments contained within Chapters 8 to 18 which follow.

References

Number	Reference
Ref. 7.1	Giprospetzgas (2011), Complex engineering surveys at the phase “design documentation” within the framework of the “South Stream” gas pipeline marine sector project implementation. Technical documentation Volume 5: Environmental survey and archaeological studies. Part 1 Environmental survey, The Russian sector. Book 3: Technical report.
Ref. 7.2	Institute of Ocean Sciences, RAS, (2011), Southern Branch (Gelendzhik City) - Hydrological Environmental Database
Ref. 7.3	The Black Sea Commission “State of the Environment Report 2001-2006/7” Chapter 7. Available from http://www.blacksea-commission.org/_publ-SOE2009-CH7.asp [Accessed on 1 Nov2012]
Ref. 7.4	Giprospetzgas (2011), Complex engineering surveys at the phase “design documentation” within the framework of the “South Stream” gas pipeline marine sector project implementation. Technical Documentation Volume 6. Engineering survey. Part 3 - Metocean survey. Third stage. Book 2
Ref. 7.5	Intecsea Worley Parsons Group (2010), Feasibility Study for Construction of South Stream Gas Pipeline. Volume 9: Route Evaluation, Part 2 Geohazard Assessment Report, Archive No 6976.101.003.11.14.09.02-1.
Ref. 7.6	Intecsea Worley Parsons Group (2013), South Stream Offshore Pipeline FEED Metocean Design Parameters Report 10-00050-10-GE-REP-0020-0004, 22-Feb-13, Rev B1.
Ref. 7.7	Peter Gaz (2013), South Stream (Russian Sector). Volume 5 – Engineering and environmental studies and archaeological investigations. Part 1 Engineering and Environmental Studies. Book 5 Landfall Section near Anapa. Technical Report. 6976.101.004.21.14.05.01.05/1.
Ref. 7.8	Giprospetzgas (2013), Technical report on environmental survey on sites of underwater hydraulic engineer works in nearshore part of the Russian sector of the Black Sea within the framework of the “South Stream” gas pipeline marine sector project implementation. SST PER-REP-203477.
Ref. 7.9	All Union State Standard GOST 17.1.5.05-85 Nature Protection. Hydrosphere. General Requirements for surface and sea waters, ice and atmospheric precipitation sampling.
Ref. 7.10	International Finance Corporation (IFC) (2007), Environmental, Health, and Safety Guidelines for Electric Power Transmission and Distribution. World Bank Group.
Ref. 7.11	International Commission on Non-Ionizing Radiation Protection (ICNIRP) (2010), Guidelines for Limiting Exposure to Time-varying Electric, Magnetic, and Electromagnetic Fields. Published in: Health Physics 99(6):818-836.

Number	Reference
Ref. 7.12	Russian Standard (1984), SanPiN 2971-84 Sanitary Standards and Rules for Public Protection against the Impact of an Electrical Field Created by Overhead Power Lines with an Alternating Power of Industrial Frequency.
Ref. 7.13	Russian Standard (2007), GN 2.1.8/2.2.4.2262-07. 2.1.8. Physical factors of the environment. 2.2.4. Physical factors of production environment. Maximum permissible levels of magnetic fields at 50 Hz in residential and public buildings and residential areas.
Ref. 7.14	Russian Standard (2008), MU 2.6.1.2398-08. Methodological guidelines. Radiation monitoring and sanitary epidemiological assessment of land plots for construction of houses, buildings and public facilities and industrial projects with regard to radiation safety. Approved by the Chief Medical Officer of the Russian Federation, G.G. Onishchenko, on July 2, 2008.
Ref. 7.15	Russian Standard (2009), SanPiN 2.6.1.2523-09 Radiation safety standards NRB-99/2009. Approved by the Decision of Chief State Medical Officer of the Russian Federation No. 47 of July 7, 2009.
Ref. 7.16	Order of the Federal Fisheries Agency No. 20 dated 18.01.2010, on approving the standards for Water Quality in Fishing Water Bodies, including Standards for maximum permissible concentrations of Harmful Substances in the Water of Fishing Water Bodies.
Ref. 7.17	Russian Standard SanPiN 2.1.5.2582-10 on Sanitary and epidemiological requirements for protection of sea coastal waters against pollution in areas of water use of the population.
Ref. 7.18	Ministry of Environmental Protection and Spatial Development of the Netherlands (2000), Circular on target values and intervention values for soil remediation.
Ref. 7.19	Krasnodar Regional Centre for Hydrometeorology and Environmental Monitoring: Anapa WMO, Weather Station ID 37001, located at latitude 44° 53’ North and longitude 037° 17’ East, at an elevation of 6 metres above sea level (masl).
Ref. 7.20	A.G. Robinson (1997), Chapter 1: Introduction: tectonic elements of the Black sea Region, in A.G. Robinson (editor) Regional and petroleum geology of the black Sea and surrounding region. AAPG Memoir 68, page 1-6. Enclosure 1. Tectonic elements, Black Sea region (map accompanying Chapter 1).
Ref. 7.21	Giprospetzgas (2013), Complex engineering surveys at the phase “design documentation” within the framework of the “South Stream” gas pipeline marine sector project implementation. Technical documentation Volume 18: Integrated Survey. The Russian sector.
Ref. 7.22	Intecsea Worley Parsons Group (2013), Anapa Geohazard Summary. Memorandum 10-00050-TN-0033. Rev. B.

Number	Reference
Ref. 7.23	M.N. Petrushina (2000), Landscape structure of the southern Abrau peninsula /Nature of the Abrau Peninsula (landscapes, vegetation and animal populations). Moscow. Geography Faculty of Moscow State University, p. 15-25.
Ref. 7.24	Afanasenkov, Nikishin and Obukhov (2007) Geological Structure and Hydrocarbon Potential of the Eastern Black Sea.
Ref. 7.25	Geological Map of the Russian Platform and Adjacent Regions (1965), 16 Sheets, 1:1,500,000. Sheet 15.
Ref. 7.26	Intecsea Worley Parsons Group (2013), South Stream Offshore Pipeline FEED Pipeline Geohazard Summary Report 10-00050-10-SS-REP-0050-0003, 19-April-13, Rev B1.
Ref. 7.27	Intecsea Worley Parsons Group (2013), South Stream Offshore Pipeline FEED Pipeline Geohazard Impact Assessment Report 10-00050-10-MX-REP-0060-0013, 19-April-13, Rev 0.
Ref. 7.28	Intecsea Worley Parsons Group (2013), South Stream Offshore Pipeline FEED Pipeline Geohazard Study Review Report 10-00050-10-GE-REP-00520-0002, 27-Feb-13, Rev 0.
Ref. 7.29	Intecsea Worley Parsons Group (2013), South Stream Offshore Pipeline FEED - Seismic Study Review Report. Ref. 10-00050-10-GE-0020-0003.
Ref. 7.30	Peter Gaz (2011), Seismic Hazard Assessment of the Offshore Section of South Stream Gas Pipeline Route across the Black Sea.
Ref. 7.31	D'Appolonia (2011), Report Seismicity Study, Anapa Approach, Project No. 11-157, Doc. No. 11-157-H2, Rev. 0, April.
Ref. 7.32	D'Appolonia (2011), Report Seismicity Study, Full Route, Project No. 11-157, Doc. No. 11- 157-H3, Rev. 0, June.
Ref. 7.33	D'Appolonia (2012), Probabilistic Fault Displacement Hazard Assessment (PFDHA) Phase I, Project No. 11-157, Doc. No. 11-157-H11, Rev. 0, April.
Ref. 7.34	DAppolonia (2012), Final Probabilistic Seismic Hazard Assessment, Full Route, Project No. 11-157, Doc. No. 11-157-H10, Rev. 0, March.
Ref. 7.35	http://hycom.org. Black Sea Metocean data from the Hycom dataset.
Ref. 7.36	Seascape Consultants Ltd (2013), The Recent History of the Black Sea including Interpretation of Newly Acquired Seabed Survey Data for the South Stream Offshore Pipeline Project. Report to South Stream Transport BV. Ref. 2013/08.
Ref. 7.37	The Black Sea Commission: http://www.blacksea-commission.org/_publ-BSAtlas.asp [Accessed on 10 Oct 2012].

Number	Reference
Ref. 7.38	Ryabinin E., Zilberstein, O., Seifert, W. (1996), Storm surges. World Meteorological Organisation, WMO/TD No. 779.
Ref. 7.39	N. N. Valchev et al. (2012), Past and recent trends in the western Black Sea storminess, Nat. Hazards Earth Syst. Sci., 12, 961–977, 2012.
Ref. 7.40	Port summary data for Novorossiysk. Obtained from http://www.worldportsource.com/ports/portCall on 19/09/2013
Ref. 7.41	Folk, R.L., (1954), The distinction between grain size and mineral composition in sedimentary rock nomenclature. Journal of Geology 62 (4), 344-359
Ref. 7.42	International Action for Sustainability of the Mediterranean and Black Sea Environment (IASON) Project (2006), Available from: http://www.iasonnet.gr/library/final_deliverables/IASON_515234_D4-2.pdf?bcsi_scan_AB11CAA0E2721250=0&bcsi_scan_filename=IASON_515234_D4-2.pdf [Accessed on 12/09/2012].